5-2020

Protection Against Atherosclerosis by A Non-native Pentameric CRP that Shares its Ligand Recognition Functions with an Evolutionarily Distant CRP

Asmita Pathak
East Tennessee State University

Protection Against Atherosclerosis by A Non-native Pentameric CRP that Shares its Ligand Recognition Functions with an Evolutionarily Distant CRP

A dissertation

presented to

the faculty of the Department of Biomedical Sciences

East Tennessee State University

In partial fulfillment

of the requirements for the degree

Doctor of Philosophy in Biomedical Sciences

---

by

Asmita Pathak

May 2020

Dr. Douglas Thewke, Ph.D., Chair

Dr. Cecilia A. McIntosh, Ph.D.

Dr Chuanfu Li, MD

Dr. Krishna Singh, Ph.D.

Dr. Valentin Yakubenko, Ph.D.

Keywords: C-reactive protein, Inflammation, Atherosclerosis, Evolution, *Limulus Polyphemus*, Ligand-recognition functions, Gene Expression, STAT3

ABSTRACT

Protection against atherosclerosis by a non-native pentameric CRP that shares its ligand recognition functions with an evolutionarily distant CRP

by

Asmita Pathak

C-reactive protein (CRP) is an acute phase protein of the innate immune system that has been evolutionarily conserved. Human CRP is known to exist in two different pentameric conformations; native CRP and non-native CRP that possess differential ligand recognition functions. The structure of CRP evolved from arthropods to humans, in terms of subunit composition, disulfide bonds, and glycosylation pattern. Along with change in structure, the gene expression pattern of CRP also evolved from a constitutive protein in lower invertebrates to an acute phase protein in humans. The objective of this study was to determine the function of a non-native pentameric CRP, that binds to atherogenic LDL, in atherosclerosis and compare the ligand recognition functions of human pentameric CRP with an evolutionary distant CRP for understanding the evolution of the structure of CRP. Additionally, *in vitro* reporter gene assays were used to gain further insight into the regulation of human CRP gene expression by an IL-6 inducible transcription factor, STAT3. We observed that CRP, in its non-native pentameric conformation, binds to atherogenic LDL and slows the progression of atherosclerosis in a site-specific manner in high fat diet fed $LDLR^{-/-}$ mice. Further, we observed that the ligand recognition function of CRP from an evolutionary conserved species, *Limulus polyphemus,* is different than that of native pentameric human CRP, but overlaps that of non-native pentameric human CRP. Lastly, we screened the proximal 300 bp region of the CRP promoter and identified

a novel STAT3 binding site at position -134 located upstream of the previously identified, transcriptionally active STAT3 site at -108. In conclusion, non-native pentameric human CRP is an atheroprotective molecule whose ligand recognition functions exhibit similarity with CRP from an evolutionarily distant species. IL-6 mediated transcriptional regulation of human CRP is modulated, in part, by STAT3 binding to two distinct positions on the CRP promoter.

DEDICATION

This manuscript is dedicated to my father Ajay Kumar Pathak and mother Archana Pathak. My parents have been the pillars of strength throughout my life. They have supported me through thick and thin. Even though miles apart, they are always there when I need them. They have provided me with the guidance through important and difficult decisions of life, instill the patience in me when I have been worn out and strengthened me when I was willing to give up. I thank them deeply from my heart to never give up on me and make me who I am today.

ACKNOWLEDGEMENTS

I would like to express my deepest gratitude to my mentors Dr. Douglas Thewke and Dr. Alok Agrawal. Their constant guidance, love towards science and vigor in sharing knowledge shaped me into a researcher that I became in all these years. Through their guidance, advice, encouragement, and support, I have been able to reach this stage of my career. I will forever be grateful to them.

I would also like to thank my thesis advisory committee members Dr. Cecilia A. McIntosh, Dr. Krishna Singh, Dr. Chaunfu Li, and Dr. Valentin Yakubenko for all the advice and encouragement they provided. I am thankful to Dr. Mitchell Robinson, Dr. Gregory Ordway, and Dr. Lana Cook for their guidance in the Biomedical Science program. I am also grateful to all the faculty of the Biomedical Sciences Graduate program who have contributed to my education. Without the support of my lab members, Dr. Sanjay K. Singh and Donald Neba Ngwa, my journey wouldn't have been so delightful. Along with helping me, they also added a cheerful environment to the lab.

I would also like to thank my brother Vatsalya Pathak, my grandmother Satya Sharma for all the love and support that she has been showering on me from overseas and my other extended family members Dr. Rajesh Sharma and Dr. Ashish Pathak for not only providing me guidance in both personal and academic matters but for also providing a home away from home to me. Last, but not the least, I am so grateful to all my friends, in India and in US as without their support this journey wouldn't have been so smooth for me.

TABLE OF CONTENTS

.

LIST OF TABLES

Table Page

LIST OF FIGURES

ABBREVIATIONS

Aβ	Amyloid β peptide 1-42
Ac-LDL	Acetylated low-density lipoprotein
Ca^{2+}	Calcium ions
C/EBP	CCAAT/enhancer-binding protein
CRP	C-reactive protein
CRP-I	PCh-binding Limulus CRP
CRP-II	PEt-binding Limulus CRP
EMSA	Electrophoretic Mobility Gel Shift Assay
E-LDL	Enzymatically modified low-density lipoprotein
HDL	High density lipoprotein
HFD	High fat diet
IL-6	Interleukin 6
IL-1β	Interleukin 1β
LDL	Low density lipoprotein
Luc	Luciferase
Mut	Mutant
NF-κB	Nuclear Factor-kappaB
ORO	Oil Red O

Ox-LDL	Oxidized low-density lipoprotein
PAGE	Polyacrylamide gel electrophoresis
PCh	Phosphocholine
PEt	Phosphoethanolamine
SAP	Serum Amyloid P
SDS	Sodium dodecyl sulfate
SLE	Systemic Lupus Erythematosus
STAT	Signal transducer and activator of transcription
TBS-Ca	TBS, pH 7.2, containing 0.1% gelatin, 0.02% Tween 20 and 2 mM $CaCl_2$
TBS-EDTA	TBS, pH 7.2, containing 0.1% gelatin, 0.02% Tween 20 and 5 mM EDTA
WT	Wild-type

CHAPTER 1

INTRODUCTION

C-reactive protein (CRP) is an acute phase protein of the human innate immune response system that has been conserved during evolution. CRP was named so because it was discovered to precipitate the C-polysaccharide of the pneumococcal cell wall (1). CRP belongs to the phylogenetically conserved family of pentraxins and it falls in the category of short pentraxins along with serum amyloid P (2). The primary ligand-binding specificity of CRP is for phosphocholine (PCh)-containing substances, and this PCh-binding property of CRP is calcium dependent (3). CRP pentamer has a recognition face, that contains binding sites for PCh and calcium ions (Ca^{2+}), and an effector face that lies opposite to the recognition face (4,5).

Structure of CRP

Human CRP is a pentamer composed of five identical non-covalently linked subunits (Fig 1.1). Each subunit has a molecular weight of approximately 23 kDa and is composed of 206 amino acids. The five subunits of pentameric CRP are symmetrically arranged around a central pore, with every subunit folded into two antiparallel β sheets forming a flattened jelly-roll topology. Each subunit has a binding site for PCh, the primary ligand for CRP, and Ca^{2+}. The PCh-binding site lies on the recognition face of the CRP pentamer and it is made up of two bound Ca^{2+} along with a hydrophobic pocket formed by three critical amino acids, Phe^{66}, Thr^{76}, and Glu^{81}. The phosphate group of PCh interacts with the two Ca^{2+} while the choline moiety of PCh interacts with Phe^{66} (3 methyl groups of choline) and Glu^{81} (positively charged nitrogen atom of choline). Thr^{76} indirectly participates in forming the PCh-binding site by creating an appropriately sized hydrophobic pocket for PCh to fit (6-8).

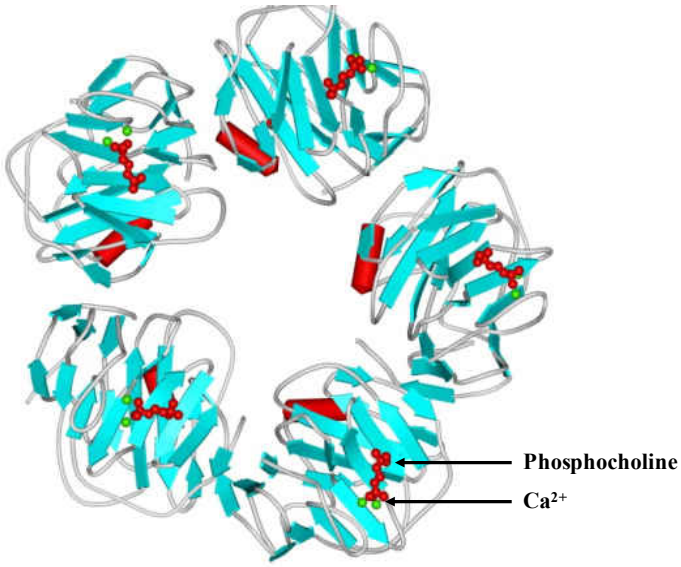

Figure 1.1: Crystal structure of CRP complexed with PCh in the presence of Ca^{2+}. The PCh moiety is represented in red while the Ca^{2+} are represented in green (Shrive AK, et al., 1996, Nature Struct. Biol. 3:346: used with permission).

At the PCh-binding pocket, CRP also binds to phosphoethanolamine (PEt)-containing substances, cholesterol, and histones (9,10). The face opposite to the recognition face, is the effector face of the CRP pentamer. The effector face interacts with C1q, the classical complement pathway protein, and Fcγ receptors via a cleft that extends from the center of each subunit to the central pore. The amino acids critical for forming the C1q binding site on CRP are Asp^{112} and Tyr^{175} (4,11-12). A slight conformational change is required in the CRP pentamer for optimal binding of C1q to ligand-complexed CRP and the ligand to which CRP is complexed determines the conformational change (13).

Functions of CRP

CRP is a key component of the inflammatory response in humans and its association with various disease pathologies such as atherosclerosis, pneumococcal infection, rheumatoid arthritis, systemic lupus erythematosus (SLE), and cancer has been studied. It has been shown to bind to substances containing exposed PCh-groups such as bacterial pneumococcal C-polysaccharide, low-density lipoprotein (LDL), and apoptotic or damaged cells (14-16). Ligand-complexed CRP activates the classical complement pathway via binding to C1q. This ligand-bound CRP-C1q complex mediates the clearance of pathogens and cellular debris (4,11). In addition to activation of complement, it also induces phagocytosis via indirect interaction with Fcγ receptors on macrophages (12).

CRP has been shown to exist in two pentameric structural conformations: native and non-native. Native pentameric CRP, at physiological pH, recognizes and binds to molecules with exposed PCh-groups while non-native pentameric CRP recognizes and binds to immobilized proteins exhibiting malformed or misfolded proteins in addition to binding to molecules with exposed PCh-groups and this interaction occurs in conditions resembling inflammatory states (17).

CRP has been shown to be protective against bacterial infection (*Streptococcus pneumoniae*) where, in its native pentameric conformation it binds to the exposed PCh-groups on the bacteria and then this ligand-complexed CRP binds to C1q and activates the classical complement pathway mediating pathogen clearance. In this way, native CRP is protective against early stages of pneumococcal infection (18-20). Non-native pentameric CRP, on the other hand, binds to immobilized Factor-H along with binding to exposed PCh-groups on the bacteria. Due to this dual functionality of non-native pentameric CRP, it is protective against

both early and late stages of pneumococcal infection (21-22). In addition to protection against *Streptococcus pneumoniae*, CRP has been shown to increase survival of mice injected with *Salmonella typhimurium* (23).

The association of CRP with chronic inflammatory conditions such as atherosclerosis, has been described in light of its increased serum levels (24). CRP has been shown to bind to modified or atherogenic forms of LDL along with its co-localization with macrophages and modified LDL at atherosclerotic lesions (25). In a study using a mouse model with human like hypercholesterolemia, CRP has been shown to slow down the progression of atherosclerosis (26). In a mouse model of SLE, human CRP was shown to prevent and reverse nephritis (27). Also, CRP has been shown to protect myeloma cells from chemotherapy-induced apoptosis (28).

Significance of Serum CRP levels

CRP is an acute phase plasma protein in humans, concentration of which increases in acute, chronic and some non-inflammatory conditions (29, 30). The serum concentration of CRP, in a healthy individual, is 0.8-3 mg/L but, following the onset of an inflammatory state the concentration of CRP increases rapidly (Fig. 1.2). This increase in serum concentration ranges from 1-3 mg/L to several hundred and thousand-fold higher (31). Following the resolution of inflammation, there is an equally rapid decrease in CRP concentration down to basal levels (32). Therefore, for diagnosis of various acute and chronic inflammatory diseases, serum CRP levels are used as a marker of inflammation.

Elevation of CRP concentration above baseline levels was recommended by the American Heart Association to be used as a predictor for cardiovascular diseases such as atherosclerosis (24). Due to variations in the serum CRP levels in healthy population, it is not

clear whether we can use elevated CRP levels as an independent risk factor for prediction, diagnosis, and pathogenesis of any inflammatory disease (33,34).

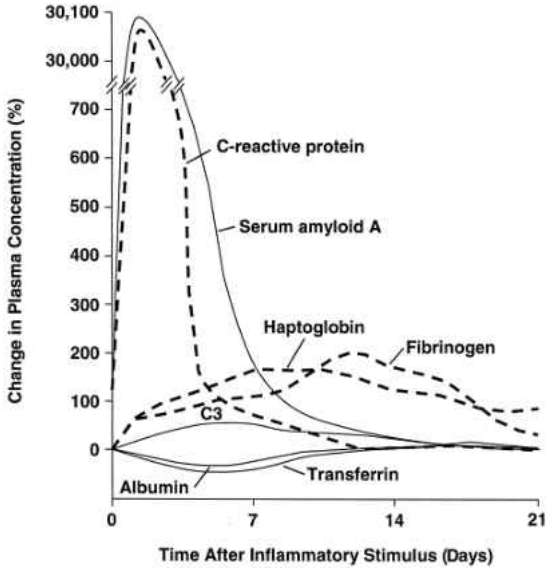

Figure 1.2. Percent change in plasma concentrations of various acute phase proteins following an inflammatory stimulus (Gabay C, et al., 1999, N. Engl. J. Med. 340, 448-54: used with permission).

CRP and Atherosclerosis

Atherosclerosis is a chronic inflammatory disease that is initiated by the retention of lipids along the arterial lining with subsequent modification of LDL. Modified LDLs, often characterized as atherogenic LDL, are engulfed by macrophages, which then transform into lipid-loaded foam cells. Foam cells are pro-inflammatory and initiate the process of lesion formation (35). The generation of extracellular acidic environment, lipid retention, lipoprotein modification, and conversion of macrophages into LDL-loaded foam cells are the hallmarks of

such localized inflammatory atherosclerotic lesions. The development of an acidic extracellular milieu may be due to macrophage activation, hypoxia, lactate generation and proton generation (36-41).

CRP has been implicated in the pathogenesis of atherosclerosis, yet its function remains undefined. Human CRP, apart from being present in the circulation, is also deposited in the extracellular matrix of localized inflammatory sites such as atherosclerotic plaques in both humans and animal models (42-45). Previous studies have examined the binding of native pentameric CRP to two atherogenic forms of LDL: enzymatically modified LDL (E-LDL) and oxidized LDL (ox-LDL). CRP binds to E-LDL at physiological pH in a Ca^{2+}-dependent and PCh-inhibitable manner. This binding is dramatically increased in the presence of acidic pH (39,41). CRP does not bind to ox-LDL at physiological pH but gains the ability to bind to ox-LDL at acidic pH. Acidic pH does not monomerize CRP, and the change in the binding is reversible on pH neutralization. This binding of CRP to ox-LDL is not Ca^{2+}-dependent, indicating that acidic pH causes a conformational alteration of the CRP pentamer, and exposes a functional site in CRP that is buried at physiological pH. Along with structural studies of CRP at acidic pH, these results suggested that inter-subunit interactions were involved in the acidic pH induced 'loosening' of the CRP pentamer (46).

In studies using animal models of atherosclerosis, native human CRP has not been shown to have an effect on the initiation and progression of atherosclerosis (47-50). However, *in vitro* studies have shown that CRP, in its alternate structural conformation, has the ability to bind to modified atherogenic LDL, such as ox-LDL. CRP has also been shown to prevent macrophage foam cell formation *in vitro*. Because the presence of an acidic environment is a hallmark of atherosclerotic lesions, the absence of such inflammatory environment in these rodent models of

atherosclerosis might explain the ineffectiveness of human CRP as the CRP administered to these animals might not have undergone the low pH-induced structural modification that is required for it to bind ox-LDL and prevent ox- LDL induced foam cell formation (51). In this dissertation, in specific aim 1, the anti-atherosclerotic function of CRP in its non-native pentameric structural conformation will be investigated.

Rationale and Hypothesis

Acidic pH transforms native pentameric CRP pentamer into a 'loosened' pentamer confirmation and exposes the hidden ox-LDL binding site that was previously buried. As the pH of the atherosclerotic lesion in animal models may not be acidic, to test the role of CRP in atherogenesis it is essential to have a modified CRP that can bind to ox-LDL at physiological pH. We hypothesize that site-directed mutagenesis of the amino acids involved in the inter-subunit interactions will result in a 'loosened' pentamer that can bind to ox-LDL at physiological pH. Such mutant CRP, created by site-directed mutagenesis, that displays the ability to bind to ox-LDL at physiological pH can either prevent or delay the initiation and progression of atherosclerosis.

Evolutionary Conservation of CRP

CRP is an evolutionarily conserved protein as, across the animal phyla, it has been found in every organism where its presence has been sought (52) (Fig 1.3).The American horseshoe crab *Limulus Polyphemus*, an arthropod, has been considered to be a living fossil as it diverged approximately 300-500 million years ago and is the best characterized invertebrate source of pentraxin proteins. In the hemolymph of *Limulus Polyphemus*, hemocyanin is the predominant protein followed by pentraxins as the second most abundant protein. Amongst the pentraxins CRP, SAP-like pentraxin, and limulin are present in the hemolymph of these animals (53). Three

subunits of *Limulus* CRP have been established based on the amino acid sequence, disulfide bonds and sites of glycosylation, that have been shown to exist in equimolar amounts (54).

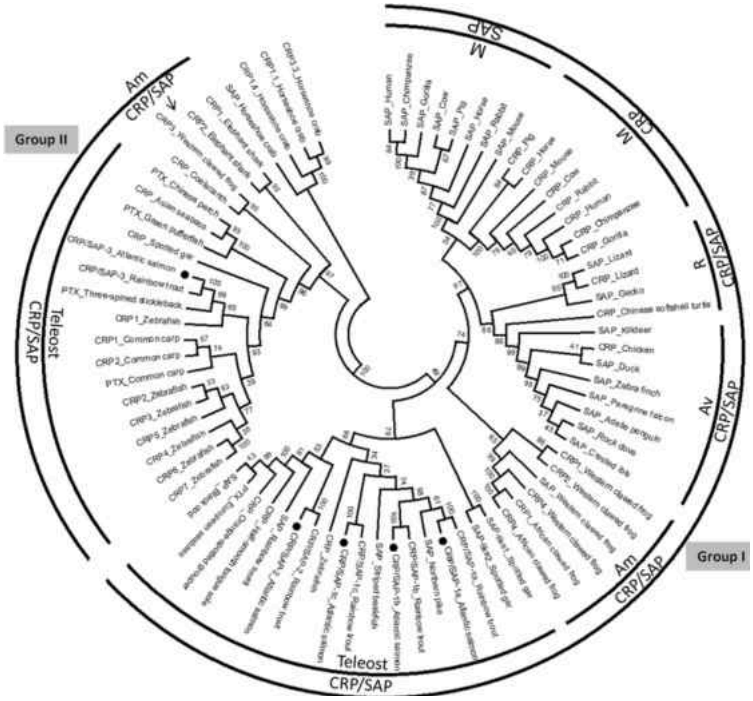

Figure 1.3. Phylogenetic tree of CRP (Lee PT, et al., 2017, Fish Shellfish Immunol. 65, 42-51: used with permission).

During evolution, the structure of CRP changed. Unlike human CRP, which is a pentamer, *Limulus* CRP is a stack of two hexamers composed of six identical subunits (~12 subunits) (54) although the region in human CRP that is critical for PCh-binding and Ca^{2+} ion binding show sequence identity with *Limulus* CRP (55). Human CRP, in its native pentameric conformation, binds to molecules and cells that have exposed PCh residues in a Ca^{2+}-dependent manner. Human CRP, in its alternate or non-native pentameric conformation recognizes an, as

yet, undefined pattern on immobilized, aggregated and conformationally altered proteins. The alternate structural conformation of CRP is achieved in response to inflammatory conditions characterized by acidic pH and oxidative stress (17). As opposed to human CRP, *Limulus* CRP is a glycoprotein. Published literature suggests that there are three distinct pentraxin species in *Limulus* depending upon its PCh, PEt, and sialic acid binding properties: CRP, SAP-like protein, and limulin respectively (54-59). Not much is known about the functions and the structure-function relationships of *Limulus* CRP. Specific aim 2 of this dissertation is designed to explore the functions of *Limulus* CRP.

Rationale and Hypothesis

These invertebrates lack an adaptive immune system, therefore humoral components such as the pentraxins are implicated in non-specific host defense and innate immunity that has been evolutionarily conserved. The discovery of *Limulus* CRP and its study provides important insights in the evolution of pentraxins and subsequent divergence of function in comparison to human CRP, over the period of time. The differences in the overall structure and glycosylation states between invertebrate and vertebrate CRP indicate that the functions of CRP are also specific. The evolutionary conservation of CRP from invertebrates to humans and its high circulating concentration in an ancient invertebrate provides insight into the importance of CRP and its biological functions. We hypothesize that, unlike human CRP, *Limulus* CRP does not require a structural change to recognize and bind to pathogenic and toxic proteins formed due to harsh environments where these arthropods live.

Regulation of CRP gene expression

Like its structure, the level of CRP gene expression also changed during evolution. In lower invertebrates such as the American horseshoe crab *Limulus polyphemus,* CRP is a constitutively expressed protein and is present in the hemolymph at all times at high concentration. In mice, CRP gene is expressed at a very low level. In rats, CRP is a minor acute phase protein. In humans, CRP is the prototypic acute phase protein whose serum level increases several folds in response to inflammatory conditions. CRP serves as a non-specific biomarker of inflammation and its serum concentration is often measured to monitor the resolution of inflammation. Currently, experiments are underway in several laboratories to understand the mechanism of human CRP gene expression in hepatocytes (32, 40, 60-62).

Human CRP is a hepatic protein that is encoded by a single gene located on the short arm of chromosome 1(62). Several hepatic cell lines such Hep3B, HepG2, and Huh7 are used to study CRP gene expression as the availability of primary human hepatocytes is limited. Various cytokines such as interleukin 6 (IL-6), interleukin 1β (IL-1β), TNFα, TGFβ, and IL-17 regulate CRP gene expression via activation of specific transcription factors (63-67). Hep3B is the most commonly use cell line model to study CRP gene expression and the cytokines that majorly regulate gene expression in these cell lines are IL-6 and IL-1β (68). IL-6 increases CRP transcription through activation of transcription factors CCAAT/enhancer-binding protein β (C/EBPβ) and signal transducer and activator of transcription 3 (STAT3) (69-72). IL-1β is insufficient by itself to activate CRP gene expression, however, when acting synergistically with IL-6, it enhances the effects of IL-6 by activating the transcription factor nuclear factor-kappa B (NF-κB) (73-75). Apart from these cytokine-activated transcription factors, CRP gene expression is regulated by constitutively expressed transcription factors such as HNF-1, HNF-3, C/EBPδ,

RBP-Jκ, and Oct-1 (76-81).

It has been shown that the proximal 157 bp region of the CRP promoter at the 5' flanking region is sufficient for the synergy between IL-6 and IL-1β and this region of the CRP promoter contains binding sites for multiple transcription factors including cytokine-activated transcription factors and constitutively expressed transcription factors. Previous studies have identified the binding sites at which these transcription factors bind and induce and regulate CRP gene expression (64,75,82) (Fig 1.4).

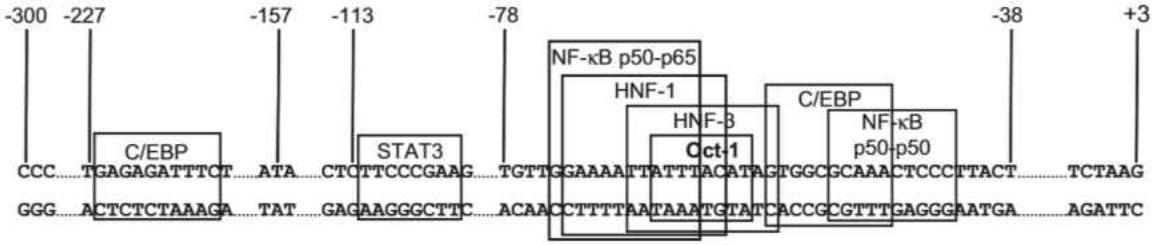

Figure 1.4. The -300 to +3 region of the proximal promoter region of the CRP gene is shown. The binding sites of various transcription factors on the promoter are boxed (adapted from Prem Prakash Singh et al., 2007, J Immunol. 178, 7302-09).

STAT3 is a major transcription factor activated by IL-6. STAT3 binds to specific response elements in the promoter regions containing $TT(N)_4AA$ or $TT(N)_5AA$ motifs. A functional, STAT3-binding site, centered at position -108 on the CRP promoter has been previously identified when searched within the first 157 bp region of the promoter (83). However, the data suggest that this STAT3 site is not the only site through which IL-6 activated STAT3 works. STAT3 induces its effect by binding to both $TT(N)_4AA$ and $TT(N)_5AA$

sequences in the promoter. In specific aim 3 of this dissertation, we will identify putative STAT3-binding sites in the 300 bp region of proximal CRP promoter and elucidate the role of STAT3 in CRP gene expression.

Rationale and hypothesis

Previously, it has been reported that, in response to IL-6, the induction of CRP gene expression driven by the first 300 bp region is higher than when driven by only 157 bp of the promoter. We hypothesize that there are more STAT3-binding sites (besides the one present at position -108) on the CRP promoter, likely to be located within the -157 to -300 bp region that might participate in inducing and regulating CRP gene expression.

For better understanding the role of CRP in light of its structure-function relationship, we had three major questions. The first question entailed to the function of a structurally altered pentameric CRP (non-native CRP) in the initiation and progression of atherosclerosis, whose ligand recognition function differs from native CRP. For the second question, we wanted to learn if this structure-dependent ligand recognition function of human CRP diverged during evolution by using CRP from an evolutionarily distant species, *Limulus polyphemus.* And lastly, for the third question, we wanted to better understand the transcriptional regulation of CRP gene expression by studying the function of an IL-6 inducible transcription factor, STAT3. These questions were addressed through different projects that are stated in the specific aims below.

Specific Aims

1. Determine the atheroprotective ability of human CRP in a murine model of atherosclerosis.
    a. Identification of a CRP mutant created by site-directed mutagenesis which binds to immobilized ox-LDL at physiological pH.
    b. Determine the effects of the CRP mutant capable of binding to ox-LDL on the development of atherosclerosis employing LDL receptor knockout mouse model of atherosclerosis.
        - The findings are presented in Chapter 2
2. Purification and characterization of CRP from the hemolymph of *Limulus Polyphemus.*
    a. Purification of PCh-binding and PEt-binding protein.
    b. Deglycosylation of PCh-binding and PEt-binding proteins.
    c. Define ligand-binding properties of native and deglycosylated PCh-binding and PEt-binding proteins.
        - The findings are presented in Chapter 3
3. Investigating the role of transcription factor STAT3 in human CRP expression in hepatic cells.
    a. Screening for STAT3-binding sites in the first 300 bp region on the CRP promoter.
    b. Confirm the binding of STAT3 to the putative STAT3-binding sites identified.
    c. Determine if any of the putative STAT3-binding sites are transcriptionally active.
        - The findings are presented in Chapter 4

CHAPTER 2

CRP is an atheroprotective molecule

Running title: Atheroprotective nature of a non-native pentameric CRP

Asmita Pathak[1], Sanjay K Singh[1], Douglas Thewke[1], and Alok Agrawal[1*]

[1]Department of Biomedical Sciences, James H. Quillen College of Medicine, East Tennessee State University, Johnson City, TN, USA

Number of words: 7701

Number of figures: 5

Number of tables: 1

[*] Correspondence should be addressed to: AA (agrawal@etsu.edu)

Abstract

Objective- C-reactive protein (CRP) is a pentameric, acute phase protein that exists in three structural conformations: native pentameric, non-native pentameric, and monomeric. *In vitro,* native CRP does not bind to oxidized LDL, however, non-native CRP binds to oxidized LDL as it has been proposed that CRP changes its structure at sites of inflammation. *In vivo*, native CRP is neither pro-atherosclerotic nor atheroprotective and we hypothesize that this ineffectiveness of native CRP is due to an inappropriate inflammatory microenvironment in the arterial wall that stalls CRP from changing its structure.

Methods and Results- In the current study, we evaluated the impact of a mutant CRP F66A/T76Y/E81A CRP, that is capable of binding to oxidized LDL at physiological pH, on the development of atherosclerosis. $LDLR^{-/-}$ mice were fed on a high fat diet for 10 weeks and administered with and without F66A/T76Y/E81A CRP. We found that administration of F66A/T76Y/E81A CRP significantly reduced the extent of atherosclerotic lesion in the whole aorta and slowed the progression of atherosclerosis, but it did not show an effect on the development and progression of atherosclerosis in the aortic root. F66A/T76Y/E81A CRP was found to be localized in the atherosclerotic lesion in the aorta. Also, F66A/T76Y/E81A mutant CRP administration did not alter the plasmid lipid levels.

Conclusion- F66A/T76Y/E81A CRP showed a site-specific atheroprotective effect via dwindling atherosclerotic lesion development and progression in the aorta. Overall, the data indicates that CRP is an atheroprotective molecule and such mutant CRP might represent as a novel therapeutic tool for the treatment of atherosclerosis.

Abbreviations:

ApoE$^{-/-}$	Apolipoprotein E knockout
ApoB$^{100/100}$ LDLR$^{-/-}$	Apolipoprotein / low density lipoprotein receptor knockout
Ca^{2+}	Calcium-ions
CRP	C-reactive protein
DI	Distilled water
E-LDL	Enzymatically modified low density lipoprotein
HDL	High density lipoprotein
HFD	High fat diet
LDL	Low density lipoprotein
LDLR$^{-/-}$	Low density lipoprotein receptor knockout
mCRP	Monomeric C-reactive protein
mut CRP	F66A/T76Y/E81A mutant CRP
Ox-LDL	Oxidized low density lipoprotein
ORO	Oil Red O
PCh	Phosphocholine
TBS-Ca	TBS, pH 7.2, containing 0.1% gelatin, 0.02% Tween 20 and 2 mM $CaCl_2$
WT	Wild-type

Introduction

Atherosclerosis, an inflammatory disease of the heart, is caused by the dysfunction of the endothelial wall leading to infiltration, deposition and subsequent modification of low-density lipoprotein (LDL) along arterial lining (1-3). LDL, modified either by oxidation [oxidized LDL (ox-LDL)], acetylation [acetylated LDL] or enzymatic modification [enzymatically modified LDL (E-LDL)], is recognized and engulfed by macrophages to form foam cells. Modification of LDL and formation of foam cells via macrophages are the two primary events marking the hallmark of the development of atherosclerosis (3-5). Modified LDL has also been shown to induce the expression of chemokines, pro-inflammatory cytokines, and other mediators of inflammation at sites of atherosclerotic lesions. The pH in atherosclerotic lesions has also been shown to be acidic due to proton and/or lactate generation, hypoxia, and activated macrophages (6-10).

C-reactive protein (CRP) is an acute phase protein of hepatic origin. Structurally, it is a pentamer of identical subunits, in which each subunit contains a phosphocholine (PCh)-binding site and calcium ion (Ca^{2+})- binding site. It binds to PCh and PCh-containing ligands in a Ca^{2+}-dependent manner and Glu^{81}, Phe^{66} and Thr^{76} are critical for this interaction. In a normal physiological environment, CRP exists as native pentameric CRP, but upon exposure to a localized pathological and inflammatory environment, it changes its structure to a non-native pentameric state (11-17). This structural change of CRP from its native to non-native pentameric state upon sensing of an inflammatory environment is reversible. Native CRP has been shown to bind to E-LDL but not to ox-LDL. Its binding to ox-LDL is dependent on the presence of an inflammatory microenvironment since CRP is able to change its native pentameric structure to a non-native pentameric structure at acidic pH (18-23). In addition to this binding capability, it has

also been found to co-localize with LDL and macrophages in atherosclerotic lesions in both human and experimental animals, further suggesting a function in atherosclerosis (24-28).

Previously, native CRP has been investigated for its role in the development of atherosclerosis using several different murine models of atherosclerosis such as ApoE $^{-/-}$ (Apolipoprotein E knockout), LDLR $^{-/-}$ (LDL receptor knockout), and ApoB $^{100/100}$ LDLR $^{-/-}$ (Apolipoprotein B$^{100/100}$/. LDL receptor knockout). The conclusion of the studies was that CRP was neither pro-atherogenic nor anti-atherosclerotic (29-32). One possible explanation for the observed lack of effect of native CRP on atherosclerosis in these studies is that the mouse models do not possess a suitable acidic microenvironment to induce native CRP to undergo structural change to its non-native structural conformation.

In the present study, we examined the effect of F66A/T76Y/E81A mutant CRP (mut CRP) on the development of atherosclerosis in LDLR$^{-/-}$ mice fed on a high fat diet (HFD). We hypothesize that administration of this mut CRP, that binds to ox-LDL under physiological conditions, would display beneficial effects on atherosclerosis in mice. In this study, we tested this hypothesis by comparing the extent of atherosclerosis in HFD fed LDLR$^{-/-}$ mice, injected with and without mut CRP. We found that administration of mut CRP significantly reduced the *en face* atherosclerotic lesion area and slowed the progression of the disease in the whole aorta, but, had no effect on the development of atherosclerosis in the aortic root. Overall, the data indicate that administration of mut CRP does exibhit an atheroprotective effect in mice and it further suggests that CRP in humans is a part of anti-atherosclerotic mechanism.

Methods

Construction, Expression and Purification of mut CRP (F66A/T76Y/E81A Mutant CRP)

The construction of mut CRP has been described earlier (33). Briefly, a clone of F66A/T76Y/E81A stably transfected in CHO cells was used for cell culture. Cells were cultured in SFM media supplemented with 1% FBS and 1% Penicillin-Streptomycin stock and grown. Media, containing mut CRP, was collected and centrifuged at 10,000 rpm for 10 minutes and mut CRP was purified from cell culture supernatants by a Ca^{2+}-dependent affinity chromatography on a Phosphoethanolamine-conjugated Sepharose column followed by gel filtration chromatography on a Superose 12 column, as described previously (33).

Ox-LDL Binding Assay

Binding activity of mut CRP for ox-LDL at physiological pH was evaluated by an ELISA- based binding assay. Briefly, microtiter wells were coated with ox-LDL (10 µg/ml diluted in 1X TBS) and incubated overnight at 4 °C. Wells were blocked with 0.5% gelatin for 45 minutes followed by addition of purified CRP [Wild type (WT) and mut CRP], diluted in buffer containing 1X TBS, 0.1% gelatin, 0.02% Tween 20, and 2 mM $CaCl_2$ (TBS-Ca, pH 7.2). Wells were incubated with CRP for 2 h at 37 °C. Following CRP incubation, wells were washed with TBS-Ca and rabbit anti-CRP antibody (Sigma, cat# C3527-1VL; diluted 1/1000 in TBS-Ca), was added (100 µl /well, 1 h at 37 °C) to detect bound CRP. HRP-conjugated donkey anti-rabbit IgG (GE Healthcare, cat# GENA934), diluted in TBS-Ca, was used (100 µl /well, 1 h at 37 °C) as the secondary antibody. Color was developed using ABTS as the substrate, and the absorbance was read at 405 nm in a microtiter plate reader (Molecular Devices).

Animal Procedures

Eight-week-old male LDLR$^{-/-}$ mice in the C57BL/6 background (#002207, Jackson Laboratory, Bar Harbor, ME, USA) were placed on a HFD consisting of 21% fat and 0.2% cholesterol (TD.88137; Envigo) for 10 weeks. After 1 week of HFD, mice were given injections of mut CRP (50 μg/injection) every other day via alternating intra-venous (IV) and intra-peritoneal (IP) routes for upto 9 weeks as depicted in (Fig 2.1). Control mice were injected with an equivalent volume of vehicle (TBS). The dosage of mut CRP to be injected into mice was decided on the basis of its rate of clearance, as previously performed pharmacokinetic studies demonstrated the rate of clearance of mut CRP *in vivo* to be approximately 15-20 hours (33). At two weeks intervals, groups (n=6) of mice were fasted overnight, anesthetized and anti-coagulated blood samples were obtained by cardiac puncture prior to cardiac perfusion with ice-cold neutral buffered 10% formalin induced (Sigma, cat # HT-501128). Hearts and aortas were cleared of adventitial fat and excised. Aortas were saved in 10% formalin at 4^0 C and heart tissue was embedded in OCT medium and stored at -80 °C as done previously (34). All mice were housed in a pathogen-free, temperature- and humidity-controlled room in the Animal Research Facility at East Tennessee State University. All mice studies were approved by and conducted in accordance with the guidelines administered by the Institutional Animal Care and Usage Committee of East Tennessee State University and in conformity with the Public Health Service Policy on Humane Care and Use of Laboratory Animals.

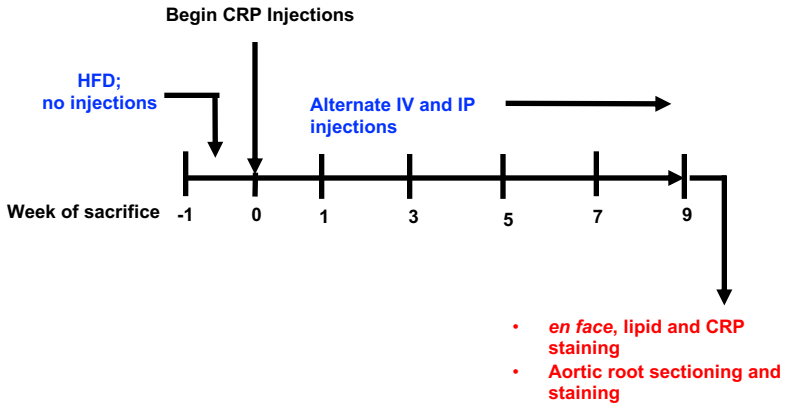

Figure 2.1: A schematic representation of the protocol used during the study.

Analysis of Atherosclerosis

Atherosclerotic lesions throughout the thoracoabdominal aorta were evaluated in formalin-fixed aortae opened longitudinally (*en face*) and stained with 0.5% Sudan IV, as described previously (34). The extent of the total aortic lumen stained positive with Sudan IV was quantified in digital images using Image J (35). For evaluation of atherosclerosis in the aortic root , cross-section (8-µm) of frozen OCT-embedded heart tissue were collected on microscope slides starting at the first appearance of the aortic valve leaflets until the disappearance (~ 48-72 sections per mouse). Every other cross-section spanning the entire aortic root were stained with Oil-red O (ORO) for lipids and counterstained with hematoxylin. Digital photomicrographs were acquired with an Olympus BX41 microscope equipped with a CCD color camera (QImaging) and the area staining positive for ORO was quantified using the Image J software as previously described (34). All measurements were performed independently in a blind fashion.

Immunostaining

Formalin-fixed, Sudan IV stained aortae were first washed with water for 30 minutes followed by alcohol dehydration through a series of graded alcohol washes. Aortae were washed first with 70% alcohol for 30 minutes followed by 80% alcohol for 30 minutes, and then 95% alcohol for 30 minutes. Post-dehydration, aortae were washed twice with xylene with each xylene wash lasting for 30 minutes (36). Aortae were then washed with 1X PBS for 5 minutes and immunostaining for mut CRP was performed using Vectastain ABC Elite kit (Vector laboratories, cat # PK-6100) and manufacturer's instructions were followed. Bound CRP was detected with rabbit anti-CRP (Sigma, 10 μg/ml /aorta). Biotinylated goat-anti rabbit IgG was used as the secondary antibody. Color was developed using two different peroxidase substrates: Brown colored reaction produced by DAB (Vector laboratories, ImmPACT DAB, cat # SK-4105) and blue colored reaction produced by TMB (Vector laboratories, cat # SK-4400). Manufacturer's instructions were followed.

Measurement of Lipids in the Plasma of LDLR$^{-/-}$ mice

Plasma was collected from whole blood via cardiac puncture at the time of sacrifice using EDTA as an anti-coagulant. Plasma lipid levels [HDL (high density lipoprotein) and LDL/VLDL] were analyzed using Cholesterol Assay Kit- HDL and LDL/VLDL (abcam; cat # ab65390). Lipid levels were measured in the pooled plasma samples at every given week point and manufacturer's instructions were followed.

Data Analysis

For atherosclerosis samples, data were analyzed using non-parametric test (Mann-Whitney test) using Graphpad Prism software. $p \leq 0.05$ was considered statistically significant. For plasma lipid analysis, data is represented as mean $\pm$ standard deviation and unpaired student t-test was used to analyze statistically significant differences. $p \leq 0.05$ was considered statistically significant.

Results

F66A/T76Y/E81A Mutant CRP Binds to ox-LDL at Physiological pH

As shown previously (33), the overall structure of mut CRP was pentameric and the mutation did not affect the stability of the protein *in vivo.* Additionally, mut CRP was found to circulate freely in the mouse serum. The binding activity of mut CRP and WT CRP for ox-LDL at physiological pH was assessed and mutant CRP bound to ox-LDL in a dose dependent manner at physiological pH (pH 7.2). As expected, WT CRP did not bind to ox-LDL at physiological pH (Fig 2.2).

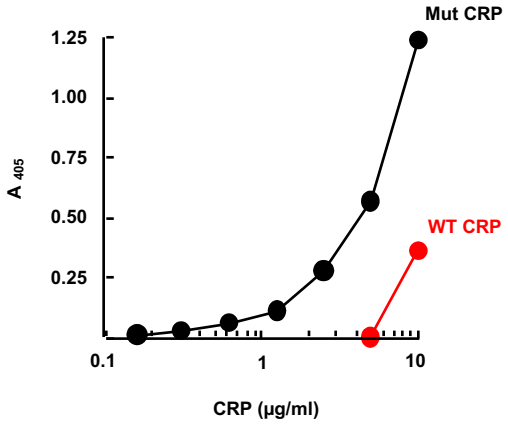

Figure 2.2: F66A/T76Y/E81A mutant CRP binds to ox-LDL at physiological pH unlike WT CRP. Microtiter wells were coated with ox-LDL. WT CRP (red) and mut CRP (black) diluted in TBS-Ca were then added to the wells in increasing concentration. Bound CRP was detected by using rabbit anti-CRP antibody and HRP-conjugated donkey anti-rabbit IgG.

This result show that mut CRP has the ability to recognize and bind to ox-LDL *in vitro*, in the absence of an acidic environment. Furthermore, this binding is PCh-independent since the PCh binding site of mut CRP is abolished (33).

Chronic Treatment with F66A/T76Y/E81A Mutant CRP Significantly Reduces Atherosclerotic Lesion Formation in the Aortae of LDLR$^{-/-}$ mice

To assess the potential therapeutic effects of mut CRP on atherosclerotic burden in the early stages of atherosclerosis, LDLR$^{-/-}$ mice were fed on HFD for 1 week and randomly assigned to receive injections of vehicle or mut CRP (50 μg/injection*)*. The experiment was performed twice with n = 6 mice in each group at every given data collection time point. In the first set of experiment, administration of mut CRP had no effect on the degree of atherosclerotic lesion throughout the aorta at 1, 3, and 5 weeks. However, after 7 and 9 weeks of mut CRP treatment, the total atherosclerotic lesion area was significantly lower when compared to the lesion area in untreated mice (Fig 2.3 B). In comparison to untreated mice, the median aortic lesion area was reduced by 29% after 7 weeks ($p = 0.05$) and 33% after 9 weeks ($p = 0.002$) in mice injected with mut CRP. After 5 weeks, the atherosclerotic lesion area was 15% less in mut CRP treated mice when compared to untreated mice, however the reduction did not reach statistical significance ($p = 0.06$). In untreated group, the burden of atherosclerotic degree progressed in an incremental manner from week 1 through week 7, where it reached a plateau and remained constant at week 9. In contrast, progression of atherosclerosis in mice treated with mut CRP also progressed incremently until week 5, but it reached a plateau and remained constant at week 9.

In a replicate experiment, treatment with mut CRP did not affect the burden of atherosclerotic lesion area at early time points (1, 3, and 5 weeks) but, resulted in a statistically

significant reduction in aortic lesion area when compared to untreated mice (Fig 2.3 C). In comparison to the untreated mice, the lesion area in mice treated with mut CRP was reduced by 52% after 7 weeks ($p = 0.04$) and 55% after 9 weeks ($p = 0.03$). Similar to the first experiment, atherosclerosis steadily increased in the untreated mice from week 1 through week 9 but similar disease progression was not observed in mice treated with mut CRP where the disease progressed from week 1 through week 5 and stayed almost constant until week 9.

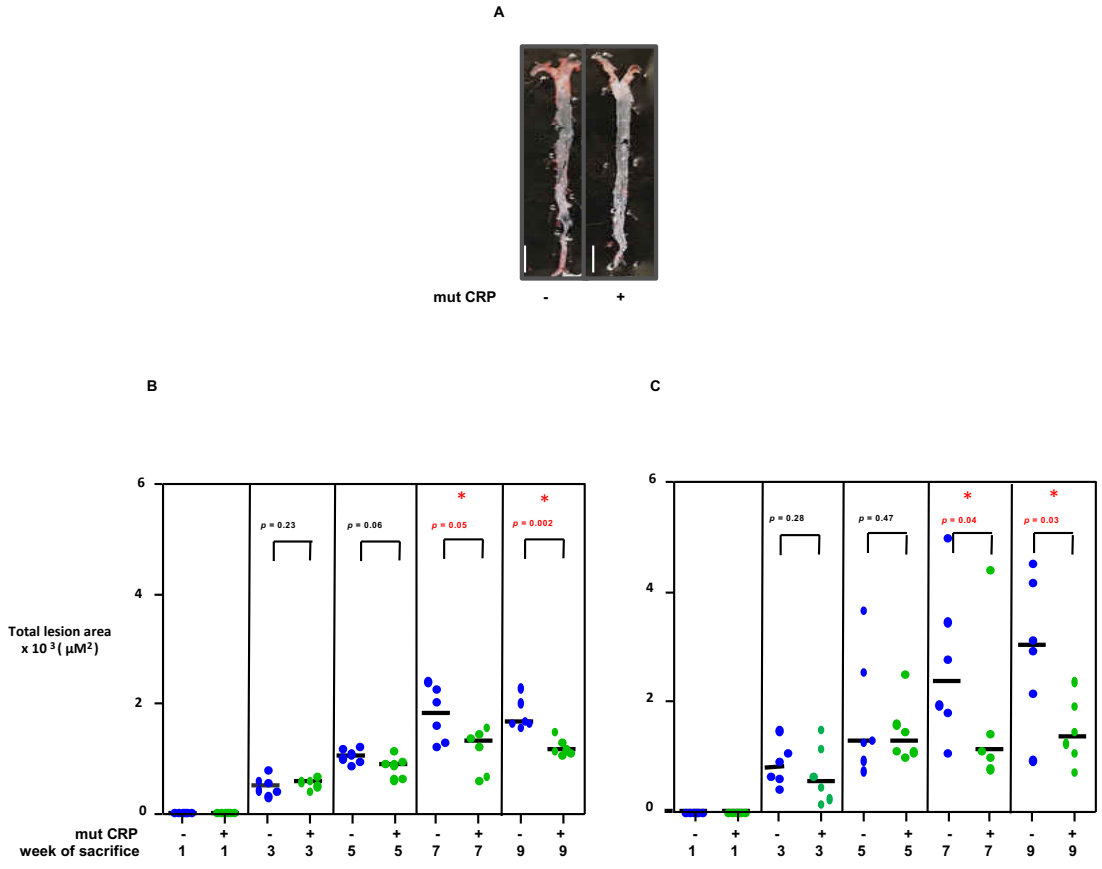

Figure 2.3: F66A/T76Y/E81A mutant CRP reduces atherosclerosis in the aorta of LDLR$^{-/-}$mice. Quantification of total atherosclerotic lesion area in *en face* aorta specimens from untreated and mut CRP treated LDLR$^{-/-}$ mice maintained on a high fat diet. *A,* A representative Sudan IV-stained aorta from male LDLR$^{-/-}$ mice maintained on a high fat diet demonstrating the spectrum of atherosclerosis is shown. The bright red colored areas reflect the atherosclerotic plaque or lesion (lipid rich deposits) in the aorta. Scale bar, 5 mm. *B*, Total atherosclerotic lesion coverage in *en face* aorta specimens from untreated and mut CRP treated LDLR$^{-/-}$ mice while *C,* Quantification of total atherosclerotic lesion coverage in *en face* aorta specimens from duplicate groups of untreated and mut CRP treated LDLR$^{-/-}$ mice. Data was collected at 5 different time points, i.e, 1, 3, 5, 7, and 9 weeks of mut CRP administration at alternate days (TBS was injected for untreated group). A scatterplot of total atherosclerotic lesion coverage is shown. Each symbol represents the total area of the entire aorta lumen that stained positive with Sudan IV. Values for untreated mice are indicated in blue and those for mut CRP treated are indicated in green. Horizontal lines indicate the median total lesion area for each group. Asterisks (red) denote statistically significant differences between groups (*$p \leq 0.05$).

These data, from two independently performed experiments, suggest that chronic treatment with mut CRP reduces the extent of atherosclerosis in the aortae of HFD fed LDLR$^{-/-}$ mice and slowed down the progression of the disease after 5 weeks of mut CRP administration.

Atherosclerosis in the Aortic Root of LDLR$^{-/-}$ mice is Unaffected by Chronic Treatment with F66A/T76Y/E81A Mutant CRP

We also investigated the effects of chronic administration of mut CRP on the development of atherosclerosis at the level of the aortic root in two independent experiments. The experiments were performed with n = 6 mice in each group at every given week time point. In the first experiment, the median lesion area in the aortic root of mice receiving mut CRP injections (every alternate day) was comparatively less than that of the corresponding control mice, at all timepoints as determined by evaluation of ORO-stained cross-sections. However, the decreases in the aortic root lesion areas of mice treated with mut CRP did not reach statistical significance for any time point. Interestingly, although mut CRP did not significantly decrease the size of aortic root atherosclerotic lesion area, it did delay the progression of the disease by approximately two weeks as the lesion area at 5 week and 9 weeks of mut CRP administration was similar to the lesion area at 3 and 7 weeks of untreated mice respectively (Fig 2.4 B). In the second experiment, administration of mut CRP did not have any affect on the atherosclerotic lesion area in the aortic root at any given time point (Fig 2.4 C). The data, from the first experiment, suggest that mutant CRP delayed the progression of atherosclerosis in the aortic root of LDLR$^{-/-}$ mice and the data from the second experiment suggest that mutant CRP had no effect on atherosclerosis in the aortic root of LDLR$^{-/-}$ mice. Hence, the combined data suggest that chronic administration of mut CRP had no effect on the development of atherosclerosis in the aortic root of LDLR$^{-/-}$ mice.

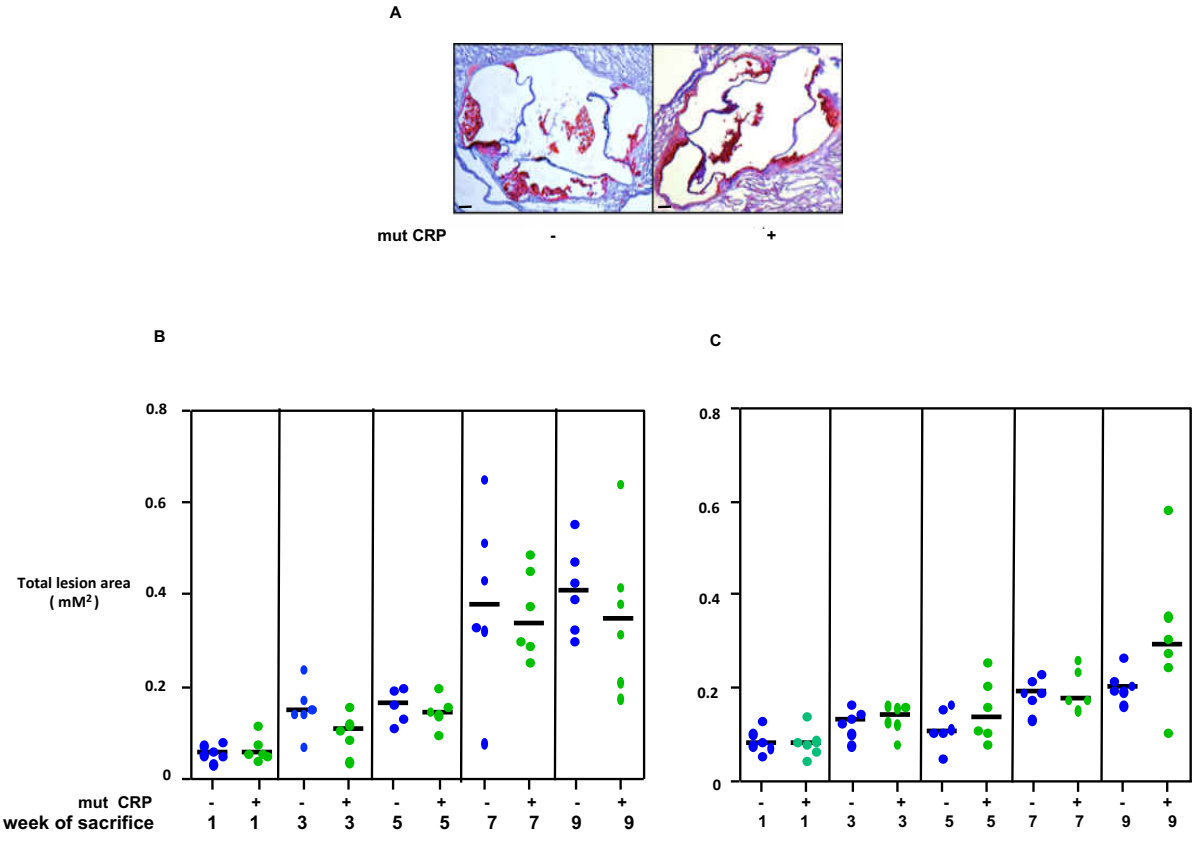

Figure 2.4: F66A/T76Y/E81A mutant CRP did not affect the development of atherosclerosis in the aortic root of LDLR$^{-/-}$mice. *A,* A representative ORO-stained aortic root section from male LDLR$^{-/-}$ mice maintained on a high fat diet demonstrating the spectrum of atherosclerosis is shown. The red colored areas reflect the atherosclerotic lesion (lipid rich deposits) in the aortic root. Scale bar, 100 µm. Quantification of total lesion area in the aortic root sections from untreated and mut CRP treated LDLR$^{-/-}$ mice maintained on a high fat diet from two independent experiments is shown (*B and C* respectively). Data was collected at 5 different time points (1, 3, 5, 7, and 9 weeks of mut CRP administration). A scatterplot of total atherosclerotic lesion coverage in the aortic

root is shown. Each symbol represents the aortic root lesion area determined for untreated (blue) and mut CRP treated (green) $LDLR^{-/-}$ mouse. Horizontal black lines indicate the median of total aortic root lesion area for each group of animals.

F66A/T76Y/E81A mutant CRP is Detected in Atherosclerotic Lesions of $LDLR^{-/-}$ mice

As shown above (Fig 2.4), chronic administration of mut CRP decreased the progression of atherosclerosis in the aortae of $LDLR^{-/-}$ mice. To elucidate, if the observed effect of reduced atherosclerosis in the lesions was due to chronic treatment with mut CRP, we performed, CRP immunostaining of aortae in both untreated and mut CRP treated mice (Fig 2.5). anti-CRP antibodies showed positive staining in atherosclerotic lesions of mice treated with mut CRP (Fig 2.5 A and 2.5 B). In comparison, no staining was observed with anti-CRP antibodies in the atherosclerotic lesion of aorta of untreated mice (Fig 2.5 A and 2.5 B). This result shows that chronic administration of mut CRP results in deposition of mut CRP within lesions, where it might be bound to modified lipoproteins.

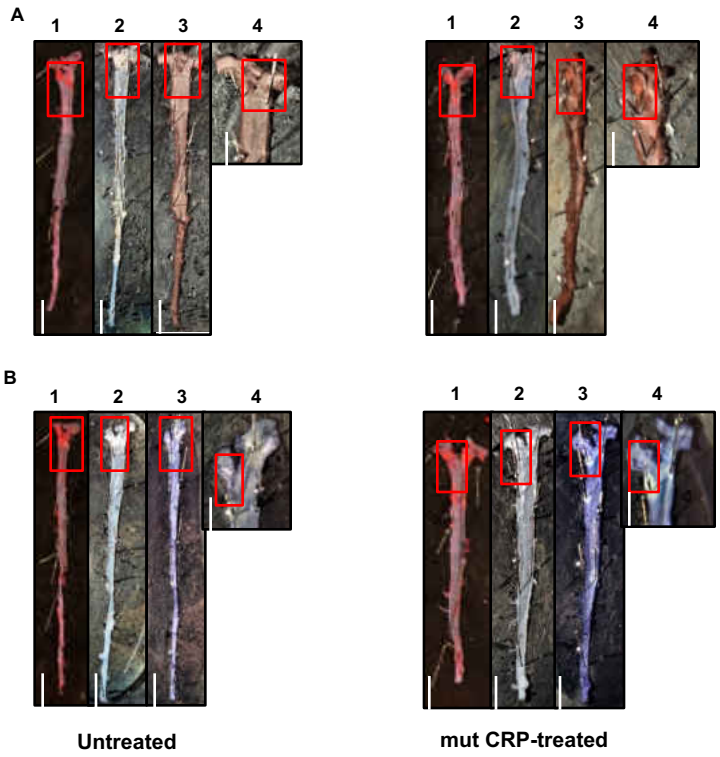

Figure 2.5: F66A/T76Y/E81A mutant CRP accumulation in atherosclerotic lesions of LDLR$^{-/-}$ mice. Representative aorta from untreated and mutant CRP treated LDLR$^{-/-}$ mice subjected to immunostaining for CRP are shown. Panel 1-4 depicts an *en face* aorta through different stages of staining procedures. (1) After Sudan IV staining to visualize atherosclerotic lesions. Red stained areas reflect positive atherosclerotic lesions (lipid rich deposits) in the aorta. (2) Aorta after destaining to remove Sudan IV. White colored areas reflect positive atherosclerotic lesion in the aorta. (3) Following staining for CRP. Brown stained areas are positive for CRP. (4) Enlarged view of aortic arch of the aorta showing CRP positive staining. A, CRP stained aorta using DAB as substrate that produces a brown colored reaction. B, CRP stained aorta using TMB as substrate that produces a blue colored reaction.. Scale bar, 5 mm.

F66A/T76Y/E81A mutant CRP did not Affect the Plasma Lipids Levels of LDLR$^{-/-}$ mice

In order to induce the development of atherosclerosis, LDLR$^{-/-}$ mice were fed HFD for 10 weeks. Chronic administration of mut CRP had no effect on the plasma LDL and HDL levels. At the dose and delivery route employed, no significant difference in plasma lipid levels (both LDL and HDL) were observed between untreated and mut CRP treated mice at any of the time points examined (Table 2.1). In addition, mut CRP administration did not affect LDLR$^{-/-}$ mice body weight as the body weights of untreated and mut CRP treated mice were in the same range (data not shown).

Week of sacrifice	HDL (mg/dL)		LDL (mg/dL)	
	Untreated	CRP-treated	Untreated	CRP-treated
1	61 ± 2	85 ± 19	864 ± 16	713 ± 31
3	91 ± 15	71 ± 19	838 ± 231	786 ± 246
5	78 ± 4	74 ± 12	754 ± 118	834 ± 185
7	131 ± 1	107 ± 15	932 ± 86	1086 ± 23
9	80 ± 3	105 ± 2	1054 ± 3	1103 ± 19

Table 2.1: Plasma HDL and LDL levels after treatment with and without F66A/T76Y/E81A mutant CRP. Samples were collected at 6 different time points, i.e, 1, 3, 5, 7, and 9 weeks of mut CRP administration, as indicated. Data is shown as Mean $\pm$ SE in pooled samples from two independent experiments (n = 6/group).

Mut CRP has been shown to bind to modified lipoproteins such as ox-LDL, however the observation that plasma lipid levels were unaffected by mut CRP administration suggests that mut CRP did not bind or affect lipoproteins in fluid phase circulation. These data shows that the reduction of atherosclerosis exhibited by mut CRP was likely not due to an effect on plasma lipoprotein metabolism.

Discussion

In this study we investigated the effect of a non-native pentameric CRP created by site-directed mutagenesis, F66A/T76Y/E81A mutant CRP, that does not bind to PCh since the PCh binding site of this mutant CRP is abolished due to mutations of critical amino acids forming the PCh-binding pocket, i.e., Glu^{81}, Phe^{66} and Thr^{76}, on the development of atherosclerosis employing LDL receptor knockout mouse model of atherosclerosis. Our major findings were as follows: 1) Mut CRP, unlike WT CRP, binds to ox-LDL (one of the modified forms of LDL) at physiological pH and it does not need the presence of an acidic environment to do so. Also, this binding is PCh-independent since its PCh binding site is abolished. 2) Chronic administration of mut CRP had an effect on the development and progression and of atherosclerosis throughout the aorta as evidenced by significantly reduced atherosclerotic lesion in *en face* aorta of $LDLR^{-/-}$ mice and halted progression of the disease post 5 weeks of mut CRP administration. 3) Administration of mut CRP did not affect the atherosclerotic lesion area in the aortic root of $LDLR^{-/-}$ mice. 4) Mut CRP administration did not affect the plasma lipid (HDL and LDL) levels of $LDLR^{-/-}$ mice.

Native pentameric CRP does not recognize and bind to immobilized, aggregated, and pathogenic proteins but it binds to cells and molecules with PCh groups exposed on its surface, in a Ca^{2+}-dependent manner (37-39). However, upon sensing a micro-inflammatory environment, CRP tends to gain the ability to change its pentameric structure from a native conformation to a non-native conformation (40). This structural conformation change, *in vitro*, can be attained by exposure to biological modifiers such as hydrogen peroxide, hypochlorous acid or even acidic pH but this structural change is reversible, i.e., as soon it senses physiological pH, it reverts back to its native pentameric conformation (18-19, 41-42). Non-native pentameric

CRP acquires the property to recognize and bind to immobilized, aggregated, and pathogenic proteins as its recognition function changes in comparison to native pentameric CRP (17, 40). For example, one of the functions of CRP in its non-native pentameric conformation is to bind to modified LDL irrespective of the presence of PCh and Ca^{2+}. Native CRP binds E-LDL, but not ox-LDL. It binds to ox-LDL only if the LDL is sufficiently oxidized to expose its PCh moiety and hence, it recognizes and binds to the exposed PCh moiety on ox-LDL. On contrary, non-native CRP binds to E-LDL with higher avidity compared to native CRP and it binds to ox-LDL irrespective of the oxidation extent of ox-LDL (18-19, 23,41,43-45).

The effects of supplementing native CRP has been investigated using three different murine models of atherosclerosis ($ApoE^{-/-}$, $LDLR^{-/-}$ and $ApoB^{100/100}$ $LDLR^{-/-}$) as well as a rabbit model of atherosclerosis. Supplementation of native CRP produced no effect on the development of atherosclerosis indicating it was neither pro-atherogenic nor anti-atherogenic (30-32, 45-53). However, native CRP was shown to slow the development of atherosclerosis in one study employing $ApoB^{100/100}$ $LDLR^{-/-}$ mouse model, wherein these mouse models are rich in LDL and have been shown to develop human-like hypercholesterolemia, suggesting that CRP might have an atheroprotective role (29). Although investigations to determine the effects of native CRP on the development of atherosclerosis in animal models provided conflicting results, a study for investigating the effect of monomeric CRP (mCRP) on atherosclerosis using $ApoE^{-/-}$ mice showed that mCRP was atheroprotective (52). Collectively, the data suggest that native pentameric CRP was either incapable or only partly capable for protecting against atherosclerosis in animal models. One of the potential reasons for the ineffectiveness of native CRP to affect atherosclerosis development and progression in these murine models is that the mouse models does not have the required inflammatory microenvironment, needed by CRP to change its

structure and therefore bind to modified LDL. In support of this, data obtained from *in vitro* studies revealed a non-native pentameric CRP, whose LDL-binding recognition functions differs from native pentameric CRP (54).

In the current study, we used a modified CRP, F66A/T76Y/E81A mutant CRP, designed by site-directed mutagenesis to mimic the properties of non-native pentameric CRP at physiological pH. This mut CRP was tested found to recognize and bind to ox-LDL, one of the modified forms of LDL, even in the absence of an acidic environment in a PCh-independent manner. Next, we studied the effect of chronic administration of mut CRP on the development and progression of atherosclerosis using HFD fed $LDLR^{-/-}$ mice in two independently performed experiments. We found that the size of atherosclerotic lesions in the aorta of mut CRP treated mice was reduced in comparison to the untreated mice. This effect was observed after 7 weeks of mut CRP administration at every alternate day. In addition, we observed that the progression of atherosclerosis was halted post 5 weeks of chronic mut CRP administration. The results obtained were consistent between the two independently performed experiments even though the disease was observed to be more aggressive in the second experiment when compared to the first experiment, but still mut CRP was able to take care of it. However, no such effect was observed when the extent of atherosclerosis was assessed in the aortic root area except, that, in the first experiment chronic mut administration of CRP slowed the progression of the disease but, it could not be replicated in the second experiment.

Such site-specific effects have been observed in various atherosclerotic studies using $LDLR^{-/-}$ mouse models wherein experimental manipulations exhibit development of the disease differently at different lesion-prone sites of the vasculature (55-59). Specifically, mut CRP was shown to be atheroprotective in the whole aorta but neither pro-atherosclerotic nor anti-

atherosclerotic in the aortic root. There were no region-specific effects observed in the different regions of aorta, i.e., aortic arch, thoracic and abdominal regions. Because the disease progression was studied in the earlier stages, the lesions formed mostly in the aortic arch area and were only sporadically observed in the thoracic aorta. Although the aortic root may provide significant information on lesion initiation and progression, its lesion responses are not invariably reflective of the lesions throughout the whole aorta. The observed beneficial effects of mut CRP on atherosclerosis outside of the aortic root may reflect unknown region-specific functions of CRP. Alternatively, it is possible that the ability of mut CRP to retard lesion formation is too subtle to overcome the aggressive atherogenesis induced in the aortic root by the HFD employed in our study, i.e., the rate of lesion formation in the whole aorta is slower in comparison to aortic root and therefore, mut CRP is able to exhibit an observable effect.

The co-localization of native CRP with macrophages and LDL in atherosclerotic lesions in the aortic root has been reported. Modified LDL (ox-LDL, and E-LDL) have been shown to induce the formation of foam cells via uptake by macrophages. (5, 60-66). Because in the current study, mut CRP showed an atheroprotective effect in the whole aorta, we determined the presence of administered mut CRP at atherosclerotic lesion in the whole aorta and we found that mut CRP was localized in the *en face* atherosclerotic lesion. This suggest that mut CRP co-localizes with LDL at the atherosclerotic lesion in the whole aorta. We hypothesize a mechanism for the atheroprotective effect exhibited by mut CRP, where mut CRP recognizes and interacts with modified LDL at the atherosclerotic lesions and prevents the formation of foam cells by blocking the uptake of LDL by macrophages. This hypothesized mechanism, although yet to be studied, is in accordance with a previously published study, where they reported that *in vitro* CRP-bound E-LDL prevents the transformation of macrophages to foam cell (67). The

atheroprotective effect of mut CRP in the whole aorta was observed in the absence of any observable changes in the plasma lipid (HDL and LDL) concentrations suggesting that mut CRP did not bind or had any effect on the lipoproteins in fluid phase.

As discussed above, the co-localization of CRP with LDL and its deposition in atherosclerotic lesions indicates the presence of a structurally altered or non-native CRP at the lesions. Interaction of LDL with CRP is mediated through PCh, apolipoprotein B and, cholesterol moieties (68-70). The moiety on modified LDL and the binding site on non-native pentameric CRP with which this interaction is mediated, is still unknown. One of the possible binding sites involved in this interaction might be the inter-subunit contact region in CRP since this region is inaccessible in native CRP but accessible in non-native CRP (18, 40). Another possible binding site involved in this interaction might be the cholesterol binding sequence (amino acid 35 to 47) since it has been found that to mediate the interactions of monomeric CRP with diverse ligands (71). In conclusion, non-native pentameric CRP such as *in vitro*-modified CRP (F66A/T76Y/E81A mutant CRP) binds to modified LDL without the requirement of an inflammatory microenvironment and shows a site-specific atheroprotective effect by decreasing the size of atherosclerotic lesion in the whole aorta post 8 weeks of high fat diet and halted the progression of atherosclerosis post 6 weeks of high fat diet. This study provides a proof of principle for the ability of a mut CRP to be further described as an atheroprotective molecule. Since, this is a single dose-one model regimen, further studies are required to define potential mechanisms that are responsible for the observed protective effect of CRP on atherosclerosis.

Highlights:

1. A triple mutant CRP (F66A/T76Y/E81A mutant CRP), locked in an alternate pentameric structural conformation, binds to oxidized LDL at physiological pH.
2. Chronic administration of F66A/T76Y/E81A mutant CRP, decreased atherosclerotic lesion development and progression in a site-specific manner, wherein it decreased atherosclerotic lesion in whole aorta but had no effect in the aortic root.
3. F66A/T76Y/E81A mutant CRP or CRP in its non-native pentameric conformation is an atheroprotective molecule and represents a potential novel therapy for the treatment of atherosclerosis.

Acknowledgement

The work was supported by NIH Grant: R01 AR068787 (Agrawal ; P.I.)

References

1. Libby P. Inflammation in atherosclerosis. *Nature*. 2002; 420*:* 868-874.
2. Galkina E, and Ley K. Immune and inflammatory mechanisms of atherosclerosis. *Annu Rev Immunol*. 2009; 27*:*165-197.
3. Lu H, and Daugherty A. Atherosclerosis: Cell Biology and lipoproteins. *Curr Opin Lipidol*. 2013; 24*:* 455-456.
4. Moore KJ, and Tabas I. Macrophages in the pathogenesis of atherosclerosis. *Cell*. 2011; 145: 341-355.
5. Orsó E, Grandl M, and Schmitz G. Oxidized LDL-induced endolysosomal phospholipidosis and enzymatically modified LDL-induced foam cell formation determine specific lipid species modulation in human macrophages. *Chem Phys Lipids*. 2011; 164: 479-487.
6. Leake DS. Does an acidic pH explain why low density lipoprotein is oxidised in atherosclerotic lesions? *Atherosclerosis*. 1997; 129: 149-157.
7. Björnheden T, Levin M, Evaldsson M, and Wiklund O. Evidence of hypoxic areas within the arterial wall *in vivo*. *Arterioscler Thromb Vasc Biol*. 1999; 19: 870-876.
8. Naghavi M, John R, Naguib S, Siadaty MS, Grasu R, Kurian KC, van Winkle WB, Soller B, Litovsky S, Madjid M, Willerson JT, and Casscells W. pH heterogeneity of human and rabbit atherosclerotic plaques: A new insight into detection of vulnerable plaque. *Atherosclerosis*. 2002; 164: 27-35.
9. Sneck M, Kovanen PT, and Öörni K. Decrease in pH strongly enhances binding of native, proteolyzed, lipolyzed, and oxidized low density lipoprotein particles to human aortic proteoglycans. *J Biol Chem*. 2005; 280: 37449-37454.

10. Haka AS, Grosheva I, Chiang E, Buxbaum AR, Baird BA, Pierini LM, and Maxfield FR. Macrophages create an acidic extracellular hydrolytic compartment to digest aggregated lipoproteins. *Mol Biol Cell*. 2009; 20: 4932-4940.
11. Ji SR, Wu Y, Zhu L, Potempa LA, Sheng F-L, Lu W, and Zhao J. Cell membranes and liposomes dissociate C-reactive protein (CRP) to form new, biologically active structural intermediate: $mCRP_m$. *FASEB J*. 2007; 21: 284-294.
12. Agrawal A, Gang TB, and Rusiñol AE. Recognition functions of pentameric C-reactive protein in cardiovascular disease. *Mediators Inflamm*. 2014; 2014: 319215.
13. Wu Y, Potempa LA, El Kebir D, and Filep JG. C-reactive protein and inflammation: Conformational changes affect function. *Biol Chem*. 2015; 396: 1181-1197.
14. Braig D, Nero TL, Koch H-G, Kaiser B, Wang X, Thiele JR, Morton CJ, Zeller J, Kiefer J, Potempa LA, Mellett NA, Du XJ, Meikle PJ, Huber-Lang M, Stark GB, Parker MW, Peter K, and Eisenhardt SU. Transitional changes in the CRP structure lead to the exposure of proinflammatory binding sites. *Nat Commun*. 2017; 8:14188.
15. McFadyen JD, Kiefer J, Braig D, Loseff-Silver J, Potempa LA, Eisenhardt SU, and Peter K. Dissociation of C-reactive protein localizes and amplies inflammation: Evidence for a change direct biological role of C-reactive protein and its conformational changes. *Front Immunol*. 2018; 9: 1351.
16. Salazar J, Martinez MS, Chávez-Castillo M, Núñez V, Añez R, Torres Y, Toledo A, Chacín M, Silva C, Pacheco E, Rojas J, and Bermúdez V. C-reactive protein: An in-depth look into structure, function, and regulation. *Intl Sch Res Notices*. 2014; 2014: 653045.
17. Lv J-M, and Wang M-Y. In vitro generation and bioactivity evaluation of C-reactive protein intermediate. *PloS One*. 2018; 13: e0198375.

18. Hammond DJ Jr, Singh SK, Thompson JA, Beeler BW, Rusiñol AE, Pangburn MK, Potempa LA, and Agrawal A. Identification of acidic pH-dependent ligands of pentameric C-reactive protein. *J Biol Chem*. 2010; 285: 36235-36244.
19. Singh SK, Thirmulai A, Pathak A, Ngwa DN, and Agrawal A. Functional transformation of C-reactive protein by hydrogen peroxide. *J Biol Chem*. 2017; 292: 3129-3136.
20. Bhakdi S, Torzewski M, Klouche M, and Hemmes M. Complement and atherogenesis: Binding of CRP to degraded, nonoxidized LDL enhances complement activation. *Arterioscler Thromb Vasc Biol*. 1999; 19: 2348-2354.
21. He W, Ren Y, Wang X, Chen Q, and Ding S. C-reactive protein and enzymatically modified LDL cooperatively promote dendritic cell-mediated T cell activation. *Cardiovasc Pathol*. 2017; *29*: 1-6.
22. De Beer FC, Soutar AK, Baltz ML, Trayner IM, Fienstein A, and Pepys MB. Low density lipoprotein and very low density lipoprotein are selectively bound by aggregated C-reactive protein. *J Exp Med*. 1982; 156: 230-242.
23. Ji S-R, Wu Y, Potempa LA, Qiu Q, and Zhao J. Interaction of C-reactive protein with low-density lipoproteins: Implications for an active role of modified C-reactive protein in atherosclerosis. *Int J Biochem Cell Biol*. 2006; 38: 648-661.
24. Torzewski J, Torzewski M, Bowyer DE, Fröhlich M, Koenig W, Waltenberger J, Filtzsimmons C, and Hombach V. C-reactive protein frequently colocalizes with the terminal complement complex in the intima of early atherosclerotic lesions of human coronary arteries. *Arterioscler Thromb Vasc Biol*. 1998; 18: 1386-1392.

25. Zhang YX, Cliff WJ, Schoefl GI, and Higgins G. Coronary C-reactive protein distribution: Its relation to development of atherosclerosis. *Atherosclerosis*. 1999; 145: 275-379.

26. Sun H, Koike T, Ichikawa T, Hatakeyama K, Shiomi M, Zhang B, Kitajima S, Morimoto M, Watanabe T, Asada Y, Chen YE, and Fan J. C-reactive protein in atherosclerotic lesions: Its origin and pathophysiological significance. *Am J Pathol*. 2005; 167: 1139-1148.

27. Norja S, Nuutila L, Karhunen PJ, and Goebeler S. C-reactive protein in vulnerable coronary plaques. *J Clin Pathol*. 2007; 6*0*: 545-8.

28. Yu Q, Li Y, Wang Y, Zhao S, Yang P, Chen Y, Fan J, and Liu E. C-reactive protein levels are associated with the progression of atherosclerotic lesions in rabbits. *Histol Histopathol.* 2012; 27: 529-535.

29. Kovacs A, Tornvall P, Nilsson R, Tegnér J, Hamsten A, and Björkegren J. Human C-reactive protein slows atherosclerotic development in a mouse model with human-like hypercholesterolemia. *Proc Natl Acad Sci USA*. 2007; 104: 13768-13773.

30. Koike T, Kitajima S, Yu Y, Nishijima K, Zhang J, Ozaki Y, Morimoto M, Watanabe T, Bhakdi S, Asada Y, Chen YE, and Fan J. Human C-reactive protein does not promote atherosclerosis in transgenic rabbits. *Circulation*. 2009; 120: 2088-2094.

31. Teupser D, Weber O, Rao TN, Sass K, Thiery J, and Fehling HJ. No reduction of atherosclerosis in C-reactive protein (CRP)-deficient mice. *J Biol Chem*. 2011; 286: 6272-6279.

32. Yu Q, Liu Z, Waqar AB, Ning B, Yang X, Shiomi M, Graham MJ, Crooke RM, Liu E, Dong S, and Fan J. Effects of antisense oligonucleotides against C-reactive protein on the

development of atherosclerosis in WHHL rabbits. *Mediators Inflamm*. 2014; *2014*: 979132.

33. Gang TB, Hammond DJ Jr, Singh SK, Ferguson DA Jr, Mishra VK, and Agrawal A. The phosphocholine-binding pocket on C-reactive protein is necessary for initial protection of mice against pneumococcal infection. *J Biol Chem*. 2012; 287(51): 43116-43125.
34. Netherland CD, Pickle TG, Bales A, and Thewke DP. Cannabinoid receptor type 2 (CB2) deficiency alters atherosclerotic lesion formation in hyperlipidemic Ldlr-null mice. *Atherosclerosis*. 2010; 213(1):102-8.
35. Schneider CA, Rasband WS, and Eliceiri KW. NIH Image to ImageJ: 25 years of image analysis. *Nat Methods*. 2012; 9(7):671-5.
36. Fu Z, Yan K, Rosenberg A, Jin Z, Crain B, Athas G, Heidi RS, Howard T, Everett AD, Herrington D, and Van Eyk JE. Improved protein extraction and protein identification from archival formalin-fixed paraffin-embedded human aortas. *Proteomic Clin Appl*. 2013; 7(3-4):217-24.
37. Volanakis JE, and Kaplan MH. Specificity of C-reactive protein for choline phosphate residues of pneumococcal C-polysaccharide. *Pros Soc Exp Biol Med*. 1971;136:612-614.
38. Volanakis JE, and Wirtz KWA. Interaction of C-reactive protein with artificial phosphatidylcholine bilayers. *Nature*. 1979; 281:155-157.
39. Black S, Wilson A, and Samols D. An intact phosphocholine binding site is necessary for transgenic rabbit C-reactive protein to protect mice against challenge with platelet-activating factor. *J Immunol*.2005; 175: 1192-1196.
40. Agrawal A, Gang TB, and Rusiñol AE. Recognition functions of pentameric C-reactive protein in cardiovascular disease. *Mediators Inflamm.* 2014; 2014: 319215.

41. Singh SK, Hammond DJ Jr, Beeler BW, and Agrawal A. The binding of C-reactive protein, in the presence of phosphoethanolamine, to low-density lipoproteins is due to the phosphoethanolamine-generated acidic pH. *Clin Chim Acta.* 2009; 409: 143-4.
42. Boncler M, Kehrel B, Szewczyk R, Stec-Martyna E, Bednarek R, Brodde M, and Watala C. Oxidation of C-reactive protein by hypochlorous acid leads to the formation of potent platelet activating factor. *Int J Biol Macromol*. 2018; 107: 2701-2714.
43. Chang M-K, Binder CJ, Torzewski M, and Witztum JL. C-reactive protein binds to both oxidized LDL and apoptotic cells through recognition of a common ligand: Phosphorylcholine of oxidized phospholipids. *Proc Natl Acad Sci USA*. 2002; 99: 13043-13048.
44. Biró A, Thielens NM, Cervenák L, Prohászka Z, Füst G, and Arlaud GJ. Modified low density lipoproteins differentially bind and activate the C1 complex of complement. *Mol Immunol.* 2007; 44: 1169-1177.
45. Bian F, Yang X, Zhou F, Wu P-H, Xing S, Xu G, Li W, Chi J, Ouyang C, Zhang Y, Xiong B, Li Y, Zheng T, Wu D, Chen X, and Jin S. C-reactive protein promotes atherosclerosis by increasing LDL transcytosis across endothelial cells. *Br J Pharmacol*. 2014; 171: 2671-2684.
46. Hirschfield GM, Gallimore JR, Kahan MC, Hutchinson WL, Sabin CA, Benson GM, Dhillon AP, Tennent GA, and Pepys MB. Transgenic human C-reactive protein is not proatherogenic in apolipoprotein E-deficient mice. *Proc Natl Acad Sci USA*. 2005; 102: 8309-8314.
47. Reifenberg K, Lehr H-A, Baskal D, Wiese E, Schaefer SC, Black S, Samols D, Torzewski M, Lackner KJ, Husmann M, Biettner M, and Bhakdi S. Role of C-reactive

protein in atherogenesis: Can the apolipoprotein E knockout mouse provide the answer? *Arterioscler Thromb Vasc Biol*. 2005; 25: 1641-1646.

48. Trion A, de Matt MPM, Jukema JW, van der Laarse A, Mass MC, Offerman EH, Havekes LM, Szalai AJ, Princen HM, and Emeiss JJ. No effect of C-reactive protein on early atherosclerosis development in apolipoprotein E*3-leiden/human C-reactive protein transgenic mice. *Arterioscler Thromb Vasc Biol.* 2005; 25: 1635-1640.
49. Tennent GA, Hutchinson WL, Kahan MC, Hirschfield GM, Gallimore JR, Lewin J, Sabin CA, Dhillon AP and Pepys MB. Transgenic human CRP is not pro-atherogenic, pro-atherothrombotic or pro-inflammatory in apoE$^{-/-}$ mice. *Atherosclerosis*. 2008; 196: 248-255.
50. Ortiz MA, Campana GL, Woods JR, Boguslawski G, Soja MJ, Walker CL, and Labarrere CA. Continuously-infused human C-reactive protein is neither proatherosclerotic nor proinflammatory in apolipoprotein E-deficient mice. *Exp Biol Med*. 2009; 234: 624-631.
51. Paul A, Ko KWS, Li L, Yechoor V, McCroy MA, Szalai AJ, and Chan L. C-reactive protein accelerates the progression of atherosclerosis in apolipoprotein E-deficient mice. *Circulatio***n**. 2004; 109: 647-655.
52. Schwedler SB, Amann K, Wernicke K, Krebs A, Nauck M, Wanner C, Potempa LA, and Galle J. Native C-reactive protein increases whereas modified C-reactive protein reduces atherosclerosis in apolipoprotein E-knockout mice. *Circulation*. 2005; 112: 1016-1023.
53. Torzewski M, Reifenberg K, Cheng F, Wiese E, Küpper I, Crain J, Lackner KJ, and Bhakdi S. No effect of C-reactive protein on early atherosclerosis development in LDLR$^{-/-}$/human C-reactive protein transgenic mice. *Thromb Haemost*. 2008; 99: 196-201.

54. Singh SK, Thirumalai A, Hammond DJ Jr, Pangburn MK, Mishra VK, Johnson DA, Rusiñol AE, and Agrawal A. Exposing a hidden functional site of C-reactive protein by site-directed mutagenesis. *J Biol Chem*. 2012; 287: 3550-3558.

55. VanderLaan PA, Reardon CA, and Getz GS. Site specificity of atherosclerosis: Site-selective responses to atherosclerotic modulators. *Arterioscler Thromb Vasc Biol*. 2004; 24: 12-22.

56. Goel R, Schrank BR, Arora S, Boylan B, Fleming B, Miura H, Newman PJ, Molthen RC, and Newman DK. Site-specific effects of PECAM-1 on atherosclerosis in LDL receptor-deficient mice**.** *Arterioscler Thromb Vasc Biol*. 2008; 28: 1996-2002.

57. King VL, Szilvassy SJ, and Daugherty A. Interleukin-4 deficiency decreases atherosclerotic lesion formation in a site-specific manner in female LDL-receptor$^{-/-}$ mice. *Arterioscler Thromb Vasc Biol*. 2002; 22: 456-461.

58. Schiller NK, Kubo N, Boisvert WA, and Curtiss LK. Effect of gamma-irradiation and bone marrow transplantation on atherosclerosis in LDL receptor-deficient mice. *Arterioscler Thromb Vasc Biol*. 2001; 21(10):1674-1680.

59. Babaev VR, Patel MB, Semenkovich CF, Fazio S, and Linton MF. Macrophage lipoprotein lipase promotes foam cell formation and atherosclerosis in low density lipoprotein receptor-deficient mice. *J Biol Chem.* 2000; 275(34): 26293-26299.

60. Obradovic MM, Trpkovic A, Bajic V, Soskic S, Jovanovic A, Stanimirovie J, Panic M, and Isenovic ER. Interrelatedness between C-reactive protein and oxidized low-density lipoprotein. *Clin Chem Lab Med*. 2015; 53: 29-34.

61. Moorkerja S, Francis J, Hunt D, Yong CY, and Nagpurkar A. Rat C-reactive protein causes a charge modification of LDL and stimulates its degradation by macrophages. *Arterioscler Thromb Vasc Biol*. 1994; 14: 282-287.

62. Krayem I, Bazzi S, and Karam M. The combination of CRP isoforms with oxLDL decreases TNF-α and IL-6 release by U937-derived macrophages. *Biomed Rep*. 2017; 7: 272-276.

63. Rufail ML, Ramage SC, van Antwerpen R. C-reactive protein inhibits in vitro oxidation of low-density lipoprotein. *FEBS Lett*. 2006; 580: 5155-5160.

64. Nayeri H, Naderi GA, Moghadam MS, Mohamadzadeh S, Boshtam M, Dinani NJ, and Dehkordi AA. Effect of CRP on some of the in vitro physicochemical properties of LDL. *ARYA Atheroscler*. 2010; 6: 85-89.

65. Eisenhardt SU, Starke J, Thiele JR, Murphy A, Stark GB, Bassler N, Sviridov D, Winkler K, and Peter K. Pentameric CRP attenuates inflammatory effects of mmLDL by inhibiting mmLDL-monocyte interactions. *Atherosclerosis*. 2012; 224: 384-393.

66. Chang M-K, Hartvigsen K, Ryu J, Kim Y, and Han KH. The pro-atherogenic effects of macrophages are reduced upon formation of a complex between C-reactive protein and lysophosphatidylcholine. *J Inflamm*. 2012; 9: 42.

67. Singh SK, Suresh MV, Praythe DC, Moorman JP, Rusiñol AE, and Agrawal A. C-Reactive Protein bound enzymatically modified low-density lipoprotein does not transform macrophages into foam cells. *J Immunol.* 2008; 180(6):4316-4322.

68. Nunomura W, and Hatakeyama M. Binding of low density lipoprotein (LDL) to C-reactive protein (CRP): A possible binding through apolipoprotein B in LDL at phosphorylcholine-binding site of CRP. *Hokkaido Igaku Zasshi*. 1990; 65: 474-480.

69. Saxena U, Nagpurpkar A, Dolphin PJ, and Mookerjea S. A study on the selective binding of apoprotein B- and E-containing human plasma lipoproteins to immobilized rat serum phosphorylcholine-binding protein. *J Biol Chem*. 1987; 262: 3011-3016.

70. Taskinen S, Kovanen PT, Jarva H, Meri S, Pentikäinen MO. Binding of C-reactive protein to modified low-density-lipoprotein particles: Identification of cholesterol as a novel ligand for C-reactive protein. *Biochem J*. 2002; 367: 403-412.

71. Li H-Y, Wang J, Meng F, Jia Z-K, Su Y, Bai Q-F, Lv LL, Ma FR, Potempa LA, Yan YB, Ji SR, and Wu Y. An intrinsically disordered motif mediates diverse actions of monomeric C-reactive protein. *J Biol Chem*. 2016; 291: 8795-8804.

CHAPTER 3

Identical functions of native *Limulus polyphemus* C-reactive protein and structurally altered human C-reactive protein

Running title: Ligand recognition functions of *Limulus* CRP

Asmita Pathak[1], Sanjay K. Singh, Avinash Thirumalai, Peter B. Armstrong[†], and Alok Agrawal[1*]

[1]Department of Biomedical Sciences, James H. Quillen College of Medicine, East Tennessee State University, Johnson City, TN 37614; and [†]Marine Biological Laboratory, Woods Hole, MA, 02543

Number of words: 7196

Number of figures: 3

[*] Correspondence should be addressed to: AA (agrawal@etsu.edu)

Keywords: C-reactive protein, Limulus Polyphemus, Phosphocholine, Amyloid

Abstract

C-reactive protein (CRP) has been conserved throughout evolution. Human native CRP exhibits calcium-dependent binding specificity for phosphocholine. Human CRP in its non-native structure expresses the capability to bind to deposited and conformationally-altered proteins, which can be achieved by several means including treatment of CRP with acidic pH. The ligand-binding property of human CRP in its non-native structure has implications for toxic and inflammatory conditions and favors the conservation of CRP throughout evolution. It is not known, however, whether CRP from invertebrates exhibits structure-based ligand-binding properties similar to that of human CRP. The aim of this study was to investigate the ligand-binding properties of CRP from American horseshoe crab *Limulus polyphemus*. We used different protein ligands immobilized on microtiter plates as a model for deposited and conformationally-altered proteins. We found that *Limulus* CRP binds to immobilized protein ligands at physiological pH, in contrast to human CRP which requires acidic pH to do so. The binding of *Limulus* CRP to these immobilized protein ligands occurred even in the absence of calcium, suggesting that the binding was not mediated through exposed phosphocholine molecules. We conclude that the structure-based ligand recognition function of CRP evolved with the development of the immune system to expose a ligand-binding specificity only when needed, that is, an inflammatory microenvironment would have to be sensed by CRP and that CRP would change its structure to execute its function. *Limulus CRP* also provides us with a tool to investigate the structure-function relationships of human CRP in animal models of inflammation.

Introduction

C-reactive protein (CRP), a member of the short pentraxin family, is a phylogenetically conserved protein (1). From arthropods to humans, CRP has been found to be present in every organism with similarity in three properties (2-6). First, structurally it is a cyclic oligomer of almost identical subunits with subunit molecular weight ranging from 20-30 kDa. Second, it recognizes and binds to phosphocholine (PCh) in a calcium-dependent manner and third, it exhibits immunological cross-reactivity with human CRP. In humans, CRP is an acute phase plasma protein but in some species it acts as a constitutive protein. CRP, from all species have an amino acid sequence ranging from 206-218 amino acids, although the sequence homology differs between species. Apart from human CRP, the function of CRP in other species is not known (7).

Amongst all species, human CRP is the most studied protein in terms of structure and function. CRP is a major acute phase hepatic protein in humans, the concentration of which increases more than 1000-fold in acute inflammatory conditions (8). Structurally, human CRP is a symmetrical pentamer consisting of five non-covalently attached subunits with an amino acid sequence of 206 amino acids. It is a 120 kDa protein with subunit molecular weight of approximately 23 kDa. Topologically, every subunit is folded into two anti-parallel beta sheets depicting a jellyroll (9-10). Each subunit has a recognition face that consists of a PCh- binding site with two coordinated calcium ions. PCh-binding site consists of Phe66, Thr76, and Glu81 along with residues 134-148 that forms the calcium ion binding site (11-14). The face opposite to the recognition face is the effector face that has been shown to bind to C1q and activate complement (15-17).

In contrast to human CRP, CRP from the arthropod horseshoe crab (*Limulus polyphemus*), is a constitutively expressed hepatopancreatic, glycosylated protein with a concentration of approximately 1-7 mg/ml. It is the most abundant pentraxin followed by SAP-like pentraxin in the hemolymph (18-19). Structurally, it is a dodecamer consisting of two rings of doubly stacked hexagons with an amino acid sequence of 218 amino acids. The molecular weight of *Limulus* CRP is known to be approximately 300 kDa with subunit molecular weight ranging between 25-30 kDa. It has been shown to be present in three different polymorphisms with variable glycosylation (24-27). It has 25-30% sequence homology with human CRP along with conserved protein structure of a jellyroll consisting of two anti-parallel beta sheets (20-26). High resolution X-ray crystallographic studies revealed the structural similarity of the PCh-binding site between *Limulus* and human CRP as Phe66, which is one of the amino acids involved in forming the PCh-binding site in human CRP, is conserved in *Limulus* CRP. Residues 139-153 show sequence homology with residues 134-148 (calcium-ion binding site in human CRP) in 9 out of 15 positions providing evidence for the conservation of the calcium ion binding site (7,27).

It has been shown that human CRP, in its native conformation does not have the ability to recognize and bind to immobilized, denatured and aggregated proteins. However, when exposed to an acidic environment, the native pentameric structure transforms into another pentameric configuration which further exposes a hidden ligand-binding site for non-PCh ligands. This structural change enables CRP to bind to such aggregated proteins, thus providing a unique structure dependent recognition feature to human CRP (28-30). However, it is not known if this feature of human CRP has been conserved during evolution. Therefore, the aim of this study was to investigate the structure-dependent ligand binding function of *Limulus* CRP. We found that

CRP from an evolutionarily distant species, *Limulus polyphemus,* can recognize and bind to immobilized, denatured and aggregated proteins in its native structural conformation. Therefore, the ligand recognition feature is inherent in *Limulus* CRP, in contrast to human CRP.

Materials and Methods

Purification of CRP from hemolymph of *Limulus polyphemus*

Limulus polyphemus hemolymph (blood; 50 ml) was centrifuged at 15000g for 15 minutes in order to pellet the cells yielding a clear blue plasma. *Limulus* plasma was then subjected to Sepharose 4B absorption for the removal of carbohydrate binding proteins. Approximately 10 ml Sepharose 4B beads (Sigma Aldrich; cat# 4B200) were packed in a column and equilibrated with 10 ml of TBS (10 mM Tris + 150 mM NaCl; pH 7.2) + 2 mM $CaCl_2$. *Limulus* plasma was then passed through packed Sepharose 4B beads and the plasma was collected. The column was washed with TBS + 2 mM $CaCl_2$ until the blue color disappeared from the beads (approximately 10 ml of TBS + 2 mM Ca^{2+}). The plasma was further subjected to polyethylene glycol (PEG) treatment for the removal of hemocyanin by adding 3% of PEG 8000 to the plasma. The treatment with PEG 8000 was carried out on a shaker for 16 hours at 4^0C. Following PEG treatment, plasma was centrifuged at 30000g for 30 minutes and the dark blue pellet was discarded leaving a clear, transparent plasma. CRP was isolated from the plasma of *Limulus polyphemus* in a series of three chromatography that included affinity chromatography, anion exchange chromatography and HPLC (Gel filtration protein purification system).

PCh affinity chromatography was performed for purifying PCh-binding *Limulus* CRP (CRP-I), using commercially available PCh-conjugated Sepharose beads (Pierce), as described previously (31). Briefly, 1ml PCh-Sepharose beads were packed into a column and equilibrated with 10 ml of BBS (0.1M borate-buffered saline; pH 8.3) +3 mM $CaCl_2$ [BBS-Ca]. The clear, transparent *Limulus* plasma obtained after Sepharose absorption, high speed centrifugation and PEG treatment was diluted 1:3 with BBS-Ca and passed through the column at a slow flow rate. The flow-through from the column was collected and saved to purify further *Limulus* protein still

present in the hemolymph. The column was washed with BBS-Ca and CRP was eluted from the column by passing BBS + 5 mM EDTA (BBS-EDTA). 0.5 ml fractions were collected and A_{280} for each fraction was measured. Fractions were collected until the $A_{280} < 0.02$. After all bound CRP was eluted, fractions containing CRP were pooled and dialyzed against TBS + 2 mM $CaCl_2$. PEt-binding *Limulus* CRP (CRP-II) was purified using phosphoethanolamine (PEt) affinity chromatography, as described previously (31). Briefly, 1ml PEt conjugated Sepharose beads were packed into a column and equilibrated with 10 ml of BBS-Ca. PEt binding protein was purified from PEt-Sepharose column in the manner similar to the one described above for purification using PCh-Sepharose column. After purification, CRP-containing fractions were dialyzed against TBS + 2 mM $CaCl_2$ and both PCh-binding *Limulus* CRP (CRP-PCh) and PEt-binding *Limulus* CRP (CRP-PEt) were processed for gel filtration chromatography.

Gel filtration chromatography was performed using Superose 12 (10/300 GL Pharmacia) column connected to the BioRad's Biologic Duo Flow Protein Purification System, as described previously (31). Briefly, the column was equilibrated with 20 ml of filter-sterilized and degassed TBS + 5 mM EDTA at a flow rate of 0.3 ml/min. Concentrated CRP (400 µl) was injected into the Superose12 column using a loop and CRP was eluted with TBS + 5 mM EDTA. Fractions (0.25 ml) were collected and A_{280} measured to determine the elution volume of CRP from the column. CRP-containing fractions were pooled and dialyzed against TBS+2mM $CaCl_2$.

Molecular weight determination of Limulus CRP by Gel filtration calibration

In order to elucidate molecular weight of *Limulus* CRP (CRP-I and CRP-II), we performed gel filtration chromatography, as described above, of three known molecular weight proteins [Apoferritin (440 kDa), human CRP (120 kDa) and BSA (66 kDa)]. *Limulus* CRP (both PCh and PEt binding protein) were then subjected to gel filtration purification. Apoferritin,

human CRP and BSA were eluted from the column using TBS + 2 mM $CaCl_2$ while *Limulus* CRP was purified using TBS + 5 mM EDTA. A_{280} of the fractions was measured and the elution volume of the protein was determined by the area of the single peak obtained in the purification profile. Log molecular weight of the proteins were plotted against elution volume (ml) and based on the molecular weight of the standard proteins, the molecular weight of *Limulus* CRP species was determined.

SDS PAGE (sodium dodecyl sulfate polyacrylamide gel electrophoresis)

In order to determine purity of *Limulus* CRP (both CRP-I and CRP-II), a denaturing, 4-20% gradient gel electrophoresis was performed. A 4-20% resolving gel (30% acrylamide + 1.5M Tris HCl pH 8.8+ 10% SDS + Glycerol + TEMED + 10% APS+ H_20) was prepared using a gradient mixer and following its polymerization, 4% stacking gel (30% acrylamide + 0.5M Tris HCl pH 6.8+ 10% SDS + TEMED + 10% APS+ H_20) was added and allowed to polymerize. Protein (10 μg) diluted with 4X sample loading buffer (1M Tris HCl pH 6.8 + 40% glycerol + SDS +0.5% Bromophenol blue +β-mercaptoethanol) was loaded and 1X running buffer (3g Tris base + 14.4g Glycine + 1g SDS+ H_20) was added to the tank. Gel was subjected to electrophoresis at 80 volts until protein enters the resolving gel and then, at 150 volts for 5 hours. Following electrophoresis, the gel was stained in Coomassie staining solution (45% methanol + 0.25% Coomassie brilliant blue G250 + 7.5% glacial acetic acid + H_20) overnight at room temperature and destained (45% methanol + 7.5% glacial acetic acid) until the background was clear and the and the bands were visible.

Anti-Limulus CRP

Rabbit polyclonal antibodies to preferred Limulus CRP-I were generated commercially (Thermofischer). In order to evaluate the binding avidity of anti- *Limulus* CRP for CRP-I and its cross reactivity with CRP-II, ELISA was performed. Briefly, microtiter wells (96 well plate) were coated with CRP-I and CRP-II (10 μg/ml-0; two fold serial dilution) and incubated at 37^0 C for 2 hours. The wells were then blocked with TBS containing 0.5% gelatin (Sigma-Aldrich) for 45 minutes at room temperature. After washing with TBS-Ca (TBS containing 2 mM $CaCl_2$, 0.1% gelatin, and 0.02% Tween 20), rabbit anti- *Limulus* CRP Ab, diluted in TBS-Ca (1:500 dilution), was added to the well and incubated for 1 hour to detect bound CRP. HRP-conjugated donkey anti-rabbit IgG, diluted in TBS-Ca (1:1000 dilution), was used as the secondary antibody. Color was developed using ABTS as the substrate and the *A* value was read at 405 nm using a microplate spectrophotometer.

Amino acid sequencing

Amino acid sequencing of gel filtration purified *Limulus* CRP (CRP-I and CRP-II) was performed by the Molecular Structure Facility, University of California, Davis.

Protein Ligand Binding Assay

The protein ligand binding assay was used to determine the binding of *Limulus* CRP (CRP-I and CRP-II) to a variety of immobilized proteins. Factor H (Complement Technology; cat# A137), IgG (Sigma-Aldrich; cat # I2511), BSA (Sigma-Aldrich; cat# 05470), amyloid β peptide 1–42 (Aβ) (Bachem; cat# 4014447), Ac-LDL (acetylated LDL), ox-LDL (oxidized LDL), and gelatin (Sigma-Aldrich; cat# G6650) were used as protein ligands. Ac-LDL and ox-LDL were prepared as described previously (28). Microtiter wells were coated with 10 μg/ml

protein ligands diluted in TBS (100 µl/well) and incubated overnight at 4 °C. The unreacted sites in the wells were blocked with TBS containing 0.5% gelatin. *Limulus* CRP I (20 µg/ml-0; two fold serial dilution) and *Limulus* CRP II (40 µg/ml-0; two fold serial dilution) were diluted in TBS-Ca (presence of calcium) or TBS-EDTA (TBS containing 5 mM EDTA, 0.1% gelatin, and 0.02% Tween 20; absence of calcium), added to the wells, and incubated overnight at 4 °C. The wells were then washed with the appropriate buffers, TBS-Ca (presence of calcium) or TBS-EDTA (absence of calcium) prior to the addition of anti- *Limulus* CRP Ab, diluted in TBS-Ca (1:500 dilution) was used to detect bound CRP. After 1 hour, incubation at 37 °C, the wells were rinsed again and HRP-conjugated donkey anti-rabbit IgG (GE Healthcare) diluted in TBS-Ca was added for 1 h at 37 °C. Color was developed using ABTS as the HRP substrate, and the absorbance was read at 405 nm using a microplate reading spectrophotometer.

Deglycosylation of Limulus CRP

Deglycosylation of CRP-I and CRP-II was performed using chemical and enzymatic methodolgy. Chemical deglycosylation was performed using trifluoromethanesulfonic acid (TFMS) (Sigma; cat# 34,781-7) and methodology was followed according to manufacturer's instructions for Glycoprofile IV chemical deglycosylation kit (Sigma; cat # PP0510). Briefly, 150 µl of chilled TFMS was added to 1 mg of pre-cooled lyophilized *Limulus* CRP samples and incubated for 25 minutes on ice with occasional shaking. Bromophenol blue solution (0.2%; 4 µl) was added to the reaction followed by dropwise addition of 60% pyridine solution (Sigma; cat# P 5496) in a methanol-dry ice bath until the color of the reaction changes from red to light purple or blue. The deglycosylated samples (CRP-I and CRP-II) were dialyzed against 1x TBS overnight with four changes of buffer.

Enzymatic deglycosylation was performed under denaturing and non-denaturing conditions using a protein deglycosylation mix II kit (New England Biolabs, cat# P6044) according to manufacturer's instructions. Following deglycosylation, the protein samples were dialyzed against TBS for 16 hours at 4^0C with two changes of buffer. Deglycosylated proteins were then subjected to SDS PAGE. The binding activity of deglycosylated *Limulus* CRP species (CRP-I and CRP-II) to immobilized protein ligands at physiological pH was evaluated by an ELISA-based assay using Aβ was used as the representative protein ligand.

Data Plotting

All experiments were performed three times, and comparable results were obtained each time. The results of a representative experiment are shown in the figures where the raw data (A_{405}) were used to plot the curves.

Results

Two CRP species with varying affinities for PCh and PEt were isolated from the hemolymph of *Limulus polyphemus*. The gel filtration elution profiles of both CRP- I (PCh-binding protein) and CRP- II (PEt-binding protein) were similar as both proteins eluted as a single peak at the same elution volume and the molecular weight was estimated to be approximately 300 kDa (Fig 3.1 A and B). Denaturing SDS PAGE analysis of CRP- I and CRP-II revealed two bands of molecular mass 29.5 kDa and 26.9 kDa respectively (Fig 3.1 C). Although, both CRP-I and CRP-II contained two bands but, the intensity of the bands differed between the two species, with the 26.9 kDa band having similar intensity for both CRP-I and CRP-II while the intensity of the 29.5 kDa band was more prominent for CRP-I as compared to CRP-II. Another difference between CRP-I and CRP-II was observed during affinity purification where CRP-I, eluted either by EDTA or PCh, produced identical bands on denaturing SDS-PAGE gels while CRP-II eluted by EDTA, contained an additional band (32.3 kDa) that was not observed by PEt elution.

The molecular weight of the protein as determined by gel filtration profile and the molecular mass of the subunits for both CRP-I and CRP-II, suggests that it is composed of 12 subunits, six copies of each subunit stacked together as an oligomer. This result is consistent with a previously published study that states the determined molecular weight and subunit composition of *Limulus* CRP (25). Because *Limulus* CRP is a glycoprotein, the differential purification and the intensity of the subunits between CRP-I and CRP-II may be attributed to the differential glycosylation patterns on the two CRP species. When the binding affinity for antibody (rabbit polyclonal anti-CRP-I) was analyzed for CRP-I and CRP-II, we found that rabbit polyclonal anti-CRP-I binds to CRP-II with similar affinity as it does to CRP-I (Fig 3.1

D). Further, purified CRP-I and CRP-II were subjected to amino acid sequencing. The amino acid sequence of first ten amino acids of CRP-I was LEEGEITSKV and CRP-II was LEEGEITSKI. The amino acid sequence of CRP-I and CRP-II was similar for the first nine residues. However, it differed at the tenth residue. Evidence of polymorphism for *Limulus* CRP has been reported, where the amino acid sequence of the different isoforms of *Limulus* CRP were identical except at certain amino acid positions (23).

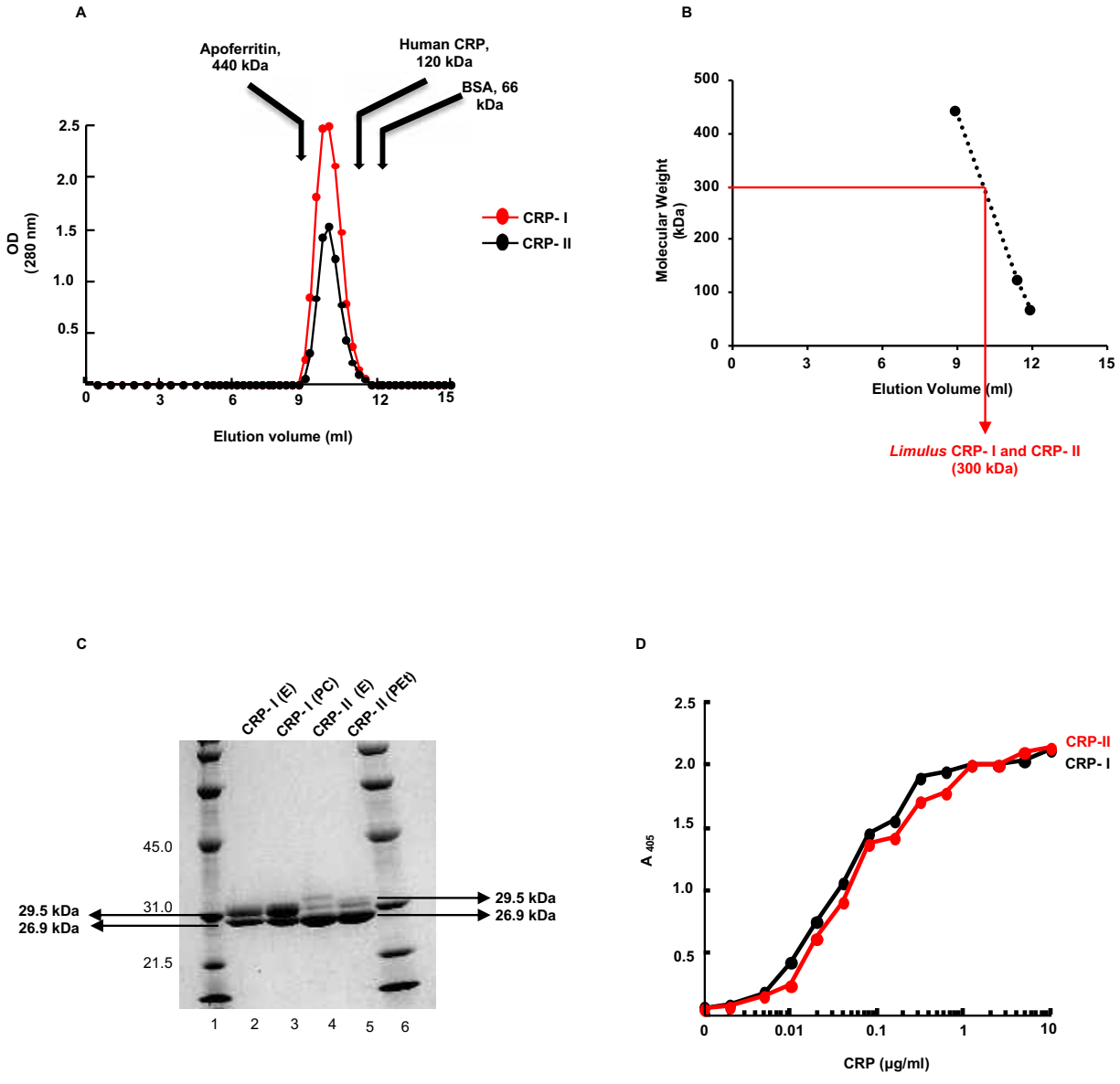

Figure 3.1: Purification and characterization of CRP-I and CRP-II. (A) Gel filtration elution profiles of of CRP-I (*red*) and CRP-II (*black*) purified from the hemolymph of *Limulus polyphemus* are shown. Molecular weight of CRP-I and CRP-II was determined by using gel filtration elution profiles of Apoferritin (440 kDa), human CRP (120 kDa), and BSA (66 kDa). Chromatography was performed in TBS, pH 7.2, containing 5 mM EDTA. A representative of three chromatograms from the Superose 12 gel filtration column is shown. (B) Molecular weight of *Limulus* CRP-I and CRP-II was determined to be 300 kDa. A linear regression plot of (A) is shown, where the molecular weight of standards are plotted against their gel filtration elution volume. *Limulus* CRP-I and CRP-II (red), based on their gel filtration elution volume, are extrapolated and their molecular weight determined. (C) Coomassie blue-stained SDS-PAGE comparing the pattern of proteins present in *Limulus* CRP purified by either phosphocholine (PCh) or phosphoethanolamine (PEt). CRP-I and CRP-II (10 μg) were electrophoresed on a 4–20% gradient SDS-PAGE gel under denaturing conditions Lanes 1 and 6, molecular weight standards. Lanes 2 and 3, CRP-I eluted by EDTA and PCh respectively. Lanes 4 and 5, CRP-II eluted by EDTA and PEt respectively. (D) Rabbit polyclonal antibody to CRP-I displays cross- reactivity with CRP-II. Enzyme-linked immunosorbent assay (ELISA) plates were coated with increasing amounts CRP-I and CRP-II, as indicated. The binding of anti-CRP-I antibody was detected using HRP-conjugated donkey anti-rabbit IgG, a colorimetric substrate, and quantified by measuring the absorbance at 405 nm using a microplate reading spectrophotometer.

The binding of CRP-I and CRP-II to a variety of immobilized protein ligands, such as Aβ, ox-LDL, Ac-LDL, Factor-H, aggregated IgG (agg IgG), BSA, and gelatin was investigated at physiological pH. All ligands were used at a concentration of 10 μg/ml to coat the wells. As shown (Fig 3.2 A), CRP-I bound to these immobilized protein ligands in a concentration-dependent manner, in the following order Aβ > Ac-LDL > ox-LDL > agg-IgG > Factor-H. We did not detect binding of CRP-I to either BSA or gelatin. We next sought to determine if calcium binding site is critical for CRP-I to recognize and bind to these immobilized ligands by performing the experiment in the presence of EDTA (absence of calcium). As shown (Fig 3.2 B), the binding curves of CRP-I binding to immobilized ligands are similar to the ones observed above, in the presence of calcium (Fig 3.2 A).

When the binding of CRP-II to immobilized protein ligands was analyzed at physiological pH, similar results were obtained as for CRP -I, where CRP-II bound to these immobilized protein ligands in a concentration-dependent manner, in the following order Aβ > ox-LDL > Ac-LDL $\geq$ agg-IgG > Factor-H while no binding was observed to either BSA or gelatin (Fig 3.2 C). Also, the binding of CRP-II to immobilized protein ligands was also calcium independent as it recognized and bound to these immobilized ligands in the absence of calcium (Fig 3.2 D). The manner in which CRP-II bound to these immobilized ligands, in the absence of calcium was similar as observed in the presence of calcium with the exception of Ac-LDL and ox-LDL (Ac-LDL > ox-LDL). Because both Ac-LDL and ox-LDL are modified versions of lipoproteins, the differential binding in the absence of calcium does not correlate with the change in binding specificities of CRP-II.

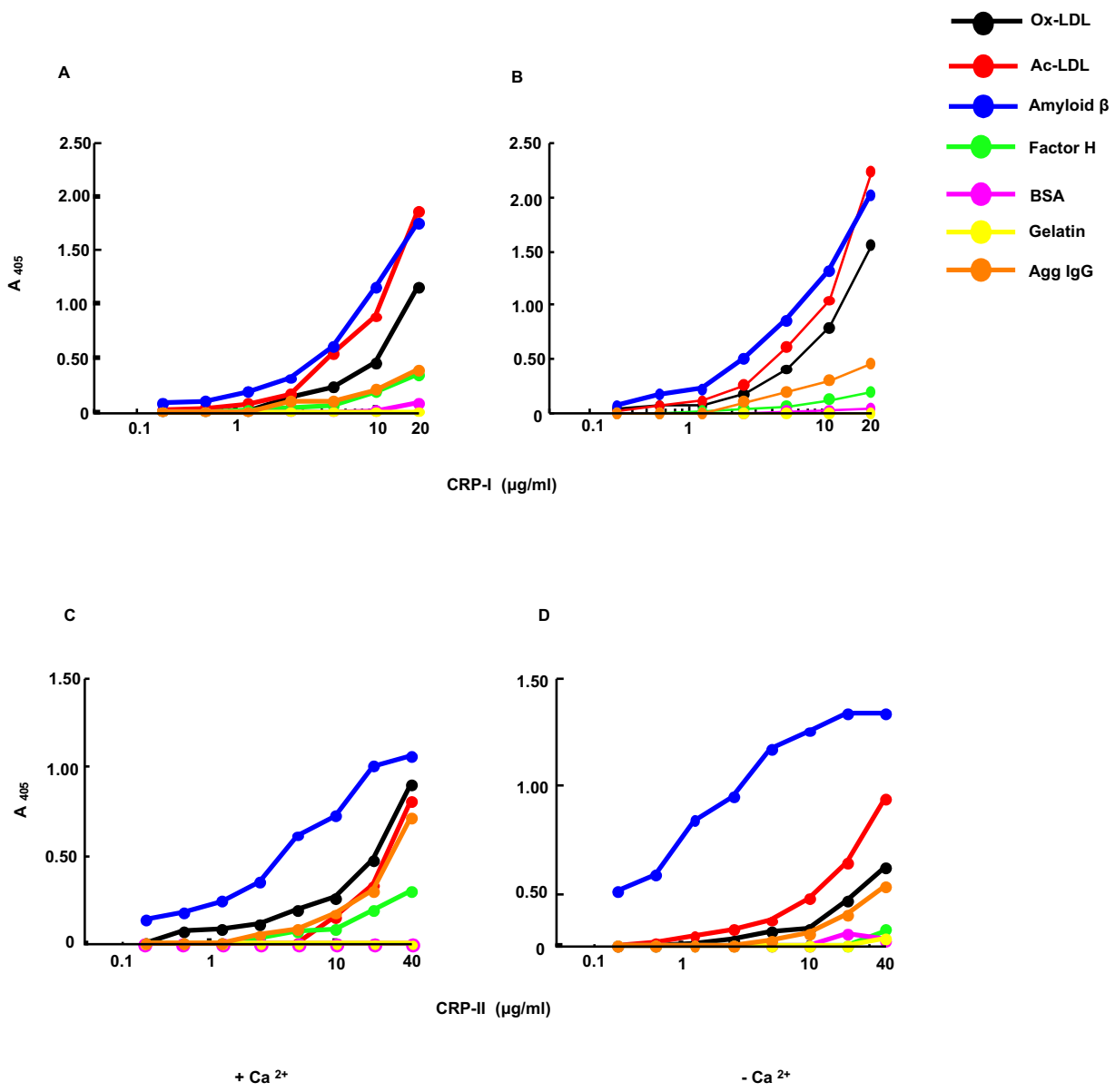

Figure 3.2: *Limulus* CRP-I and CRP-II recognizes and binds to immobilized protein ligands at physiological pH. (A and C) For analyzing binding of CRP-I (A) and CRP-II (C) to immobilized ligands, microtiter wells were coated with 10 µg/ml of amyloid β peptide 1–42 (Aβ), ox-LDL, ac-LDL, factor H, aggregated IgG (agg IgG), BSA, and gelatin. Increasing concentration of CRP-I (0-20 µg/ml) and CRP-II (0-40 µg/ml) diluted

in TBS-Ca were then added to the wells and incubated for 2 hours at 37 °C. Bound CRP was detected by using rabbit anti-CRP-I antibody and HRP-conjugated donkey anti-rabbit IgG. Color was developed, and the *A* value was read at 405 nm. A representative of three experiments is shown. (B and D) Representative result for the binding of CRP-I (B) and CRP-II (C) to the above mentioned immobilized ligands, in the absence of calcium (TBS-EDTA), are shown.

These data indicate that both CRP-I and CRP-II have the ability to recognize immobilized and conformationally altered, denatured, and aggregated proteins at physiological pH. Also, these proteins might be recognizing and binding to amyloid-like like structures that are exposed by the protein ligands upon immobilization (30) because as the extent of the exposure of these amyloid-like structures after immobilization decreases (Aβ < ox-LDL $\leq$ Ac-LDL < agg IgG < Factor-H < BSA < gelatin), the ability of CRP-I and CRP-II to recognize them and bind to them also decreases. Also, this binding is calcium independent and calcium binding site doesn't play a role in recognition of conformationally altered, denatured, and aggregated proteins by CRP-I and CRP-II.

Both species of *Limulus* CRP, CRP-I and CRP-II, are glycosylated proteins, unlike human CRP (25, 26). In order to investigate the role of carbohydrate moieties present on CRP-I and CRP-II, we subjected both proteins to chemical and enzymatic deglycosylation. Denaturing SDS PAGE analysis of CRP-I following enzymatic deglycosylation (deglycosylation performed under denaturing and non-denaturing conditions), revealed no alteration in the mobility of either of the two bands. However, when CRP-I was subjected to chemical deglycosylation, only one band of molecular mass 23.2 kDa was observed (Fig 3.3 A). In comparison, enzymatic

deglycosylation of CRP-II, altered (reduced) the intensity of the 29.5 kDa band. Chemical deglycosylation of CRP-II affected the mobility of the observed three bands resulting in two bands of molecular mass 26 kDa and 23.2 kDa, respectively (Fig 3.3 C). Although, three bands were observed in denaturing SDS-PAGE analysis of native CRP-II, anti-CRP-I antibody recognized only two bands of molecular mass 29.5 kDa and 26.9 kDa, respectively (data not shown). Thus, the deglycosylated band of 26 kDa observed post chemical deglycosylation of CRP-II could either be a deglycoylsylated product of the non-specific 32.3 kDa band or could be a result of partial deglycosylation. While we could fully deglycosylate CRP-I and CRP-II, it could not be evaluated in functional assays since deglycosylation by chemical and enzymatic (under denaturing conditions) methodology rendered the protein in a non-native state (confirmed by ELISA; data not shown).

Although, enzymatic deglycosylation (performed under non-denaturing conditions), did not produce a shift in the mobility of CRP-I and CRP-II bands in a denaturing SDS-PAGE, we wanted to determine any differences in the functional binding between native and deglycosyated state of *Limulus* CRP species. Because there lies a possibility that the protein was partially deglycosyated but there was no noticeable change in the SDS-PAGE band pattern. This might be explained in lieu of the extent of glycosylation on these proteins, as they are not fully known. Therefore, we compared the functional binding activity of native and deglycosylated CRP-I and CRP-II to an immobilized protein ligand, Aβ. As shown (Fig 3.3 B), native CRP-I bound to Aβ in a CRP concentration dependent manner. However, enzymatically deglycosylated CRP-I bound to Aβ with approximately 100-fold less avidity when compared to native CRP-I. Similar results were observed for CRP-II (Fig 3.3 D).

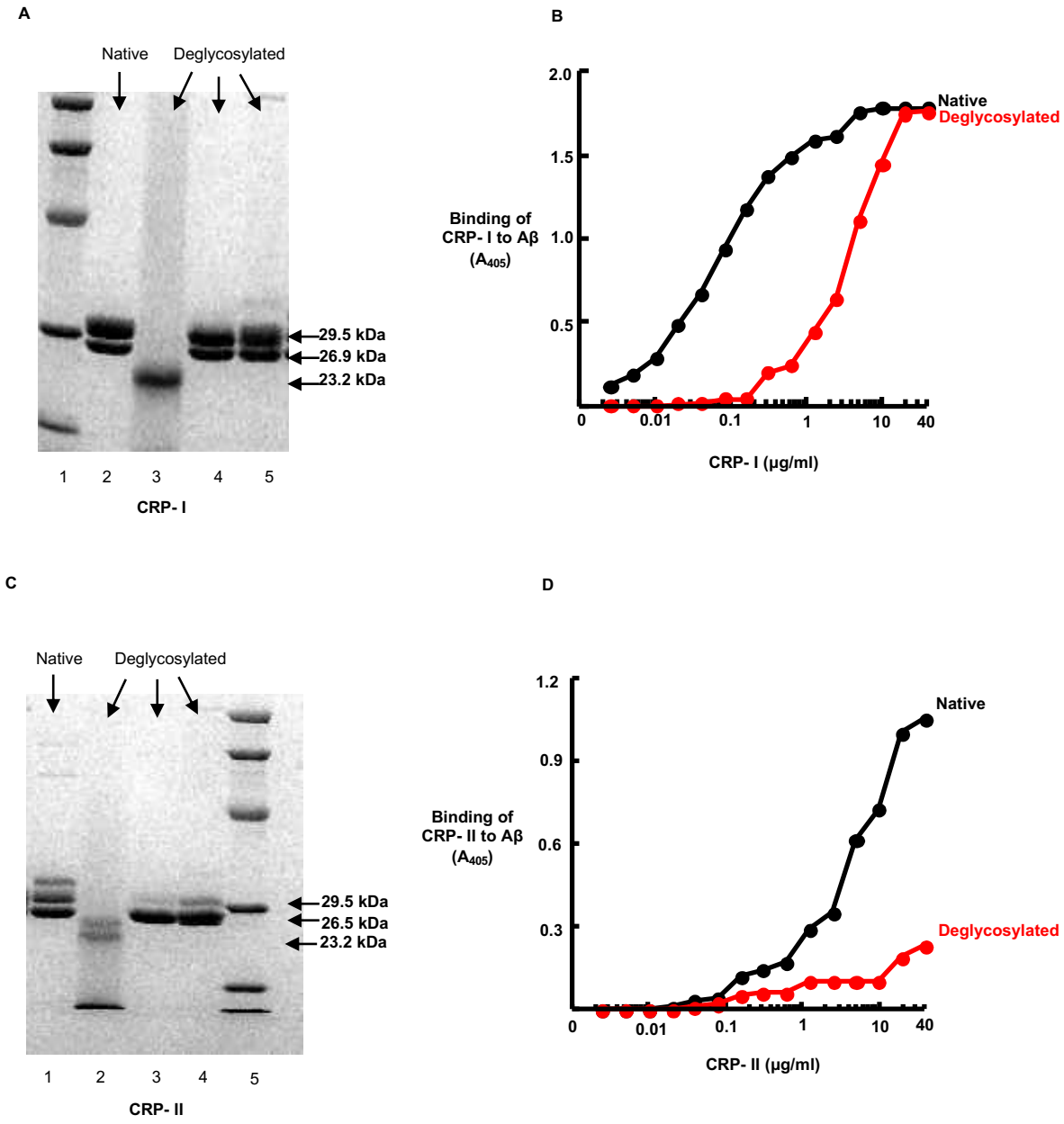

Figure 3.3: Deglycosylation of CRP-I and CRP-II reduces binding to immobilized amyloid β peptide 1–42: (A) CRP-I was deglycosylated using chemical, enzymatic (under denaturing), and enzymatic (under non- denaturing) means. Native CRP-I (10 µg) and deglycosylated CRP-I (10 µg) were subjected to SDS-PAGE under reducing conditions in a 4–20% gradient gel. A representative Coomassie Blue-stained gel is

shown; lane 1: molecular weight marker, lane 2: Native CRP-I, lane 3: Chemically deglycosylated CRP-I, lane 4: Enzymatically (under denaturing conditions) deglycosylated CRP-I, and lane 5: Enzymatically (under non-denaturing conditions) deglycosylated CRP-I. (B) Microtiter wells were coated with amyloid β peptide 1–42 (10 μg/ml). The unreacted sites in the wells were blocked with gelatin. Native CRP-I *(black)* and enzymatically (under non-denaturing conditions) deglycosylated CRP-I *(red)* (both; 0-40 μg/ml) diluted in TBS-Ca were added to the wells and incubated for 2 hours at 37 °C. Bound CRP was detected by using rabbit anti-CRP-I antibody and HRP-conjugated donkey anti-rabbit IgG. Color was developed, and the *A* value was read at 405 nm. A representative of three experiments is shown. (C) CRP-II was deglycosylated using chemical, enzymatic (under denaturing), and enzymatic (under non- denaturing) means. Native CRP-II (10 μg) and deglycosylated CRP-II (10 μg) were subjected to SDS-PAGE under reducing conditions in a 4–20% gradient gel. A representative Coomassie Blue-stained gel is shown; lane 1: Native CRP-II, lane 2: Chemically deglycosylated CRP-II, lane 3: enzymatically (under denaturing conditions) deglycosylated CRP-II, lane 4: enzymatically (under non-denaturing conditions) deglycosylated CRP-II, and lane 5: molecular weight marker. (D) Microtiter wells were coated with amyloid β peptide 1–42 (10 μg/ml). The unreacted sites in the wells were blocked with gelatin. Native CRP-II *(black)* and enzymatically (under non-denaturing conditions) deglycosylated CRP-II *(red)* (both; 0-40 μg/ml) diluted in TBS-Ca were added to the wells and incubated for 2 hours at 37 °C. Bound CRP was detected by using rabbit anti-CRP-I antibody and HRP-conjugated donkey anti-rabbit IgG. Color was developed, and the *A* value was read at 405 nm. A representative of three experiments is shown.

These data indicated that the presence of carbohydrate moieties on CRP-I and CRP-II plays a role in its ability to recognize and bind to conformationally altered, denatured, and aggregated proteins since, removal of these moieties leads to loss of these protein's ability to recognize immobilized proteins.

Discussion

A SAP-like pentraxin has been shown to be present in the hemolymph of *Limulus polyphemus* along with CRP (34). As opposed to *Limulus* CRP which has an affinity for PCh and PEt, *Limulus* SAP-like pentraxin has an affinity for PEt and carbohydrate moieties but not PCh. Therefore, we pre-absorbed the SAP-like pentraxins from hemolymph by using Sepharose-affinity chromatography prior to purifying CRP. We then purified CRP by two means, PCh dependent affinity chromatography and PEt dependent affinity chromatography and investigated the ligand recognition function of *Limulus* CRP. Our major findings were as follows: 1) *Limulus* CRP is a 300 kDa protein that exists as a dodecamer with two rings of six subunits each, as published previously (25); 2) The differential glycosylation patterns on *Limulus* CRP might be playing a role in its differential affinity for PCh and PEt; 3) *Limulus* CRP can recognize and bind to immobilized, denatured, and aggregated proteins in a calcium independent manner, at physiological pH; and 4) The ligand recognition function of *Limulus* CRP is dependent on its carbohydrate moieties since partial enzymatic deglycosylation greatly affected its ligand binding properties.

American horseshoe crab, *Limulus polyphemus*, is an evolutionarily distant species the origin of which dates back to 300-500 million years. Amongst the entire taxa of arthropods, this is the only species in which CRP along with other pentraxins has been identified as the vertebrate pentraxins counterpart (18). Along with hemocyanin and α_2- macroglobulin, pentraxins are the third most abundant proteins present in the hemolymph of these arthropods (34-35). The two major pentraxins are CRP (constituting about 80% of pentraxin population) and SAP-like pentraxins (constituting about 8-19% of pentraxin population). The N-terminal amino acid sequence differs significantly between CRP and SAP-like pentraxin along with the affinity for

ligands. CRP has an affinity for PCh and PEt but not carbohydrate moieties while SAP-like pentraxins has an affinity for PEt and carbohydrate moieties but not PCh (18-19). A third pentraxin, limulin (approximately 1% of pentraxin population), was also identified in the hemolymph of these animals. Initially, limulin and *Limulus* CRP were considered to be the same because of identical N terminal amino acid sequence. However, it was later on shown that though closely related, the two proteins are unique with differences in their ligand affinity. CRP has an affinity for PCh and PEt but not sialic acid while limulin has an affinity for PCh, PEt, and sialic acid (20-21, 37-40). In our study, we purified two different isoforms of *Limulus* CRP with differences in their ligand affinity for PCh and PEt. Since, our protein of interest was CRP, passage of hemolymph over Sepharose column eliminated SAP-like pentraxin. Also, neither of the two isoforms of *Limulus* CRP, CRP-I and CRP-II are likely to be limulin because when both CRP isoforms were passed over fetuin-sepharose column (sialic acid affinity chromatography), none of them bound to the column (data not shown).

CRP is present in the hemolymph of *Limulus polyphemus* in a wide concentration range of 0.2-6 mg/ml (25). We purified CRP-I at a concentration of 0.2 mg/ml and CRP-II at a concentration of 0.006 mg/ml. We observed that the affinity of *Limulus* CRP for PCh-sepharose is about 5 mg/ml beads in contrast to human CRP whose affinity is over 10 mg/ml beads which is consistent with a previously reported study (37). In contrast, the affinity of *Limulus* CRP for PEt-sepharose is about 2 mg/ml beads, which is consistent with the behavior of human CRP as human CRP has much higher affinity for PCh-sepharose as compared to PEt-sepharose (25). The lower affinity of Limulus CRP for PCh-sepharose in comparison to human CRP could be attributed to its higher molecular weight that can limit its access to the PCh moieties when complexed with Sepharose. *Limulus* CRP, purified by PCh affinity chromatography (CRP-I) and

PEt affinity chromatography (CRP-II), is a high molecular weight protein with estimated molecular weight of 300 kDa organized as double stacked, identical hexameric assembly (dodecamer) (22-23). Each subunit molecular mass was estimated as 26-32 kDa. As opposed to human CRP that exists in mammalian circulation as a non-glycosylated protein, *Limulus* CRP has been known to exist in three different polymorphisms with differences attributed to the glycosylation pattern as these three polymorphisms share similar amino acid sequencing with only 10 % microheterogeniety amongst them (23-27). The N terminal amino acid sequencing of CRP-I and CRP-II were similar (Leu-Glu-Glu-Gly-Glu-Gly-Ile-Thr-Ser-Lys-Val), suggesting that the differential glycosylation of the two CRP's contributes to their variable affinity for PCh and PEt. *Limulus* CRP subunits are glycosylated by a single oligosaccharide chain of composition $Man_2GlcNAc_2$ (differential glycosylations of $Man_3GlcNAc_2$, $Man_4GlcNAc_2$, or $Man_5GlcNAc_2$) (26). The difference in the mannose chains in the CRP subunits gives differential intensity to the bands in SDS PAGE for CRP-I and CRP-II (two bands of molecular mass 26.9 kDa and 29.5)

Human CRP has been shown to be present in two structural configurations: a native pentameric CRP at physiological pH that does not recognize immobilized, denatured and aggregated proteins and a non-native pentameric CRP at acidic pH that can recognize and bind to immobilized, denatured and aggregated proteins (29). In order to determine if this structure-based ligand binding property of human CRP is inherent in *Limulus* CRP, we performed ligand binding assays. We found that unlike human CRP, *Limulus* CRP in its native structural configuration at physiological pH can recognize and bind to immobilized, denatured and aggregated proteins. Both CRP-I and CRP-II does not need any structural modification to gain the ligand binding property of non-native pentameric human CRP. However, upon exposure to

an acidic environment, both CRP-I and CRP-II recognized and bound to immobilized, denatured and aggregated proteins more efficiently than it did at physiological pH (data not shown). The functional ligand binding ability of CRP-I and CRP-II at both physiological and acidic pH might provide protection against enhanced protein toxicity in these arthropods, as they are constantly being exposed to harsh environments. Non-native human CRP has an exposed ligand binding site that can recognize and bind non-PCh containing ligands (immobilized, denatured and aggregated proteins) in a calcium-independent manner. This property of non-native human CRP is consistent with native *Limulus* CRP, as it also recognizes and binds to immobilized ligands in the presence and absence of calcium. This ligand binding property of *Limulus* CRP in the absence of calcium further suggests that it does not bind to the PCh moieties , if exposed, on these ligands as presence of calcium is critical for PCh-binding. The pattern of CRP-I and CRP-II binding to immobilized ligands suggests that it recognizes and bind to amyloidogenic-like structures expressed by the proteins upon immobilization as it binds more efficiently to Aβ compared to factor-H and doesn't bind at all to BSA and gelatin.

Over the course of evolution, the glycosylation patterns on CRP have changed, where *Limulus* CRP-I and CRP-II are glycosylated while human CRP is non-glycosylated. Human CRP does possess sites of glycosylation but they are hidden in its native conformation and therefore may provide no functional advantage to native CRP (41-43). In order to determine if the glycosylated moieties have any role in the structure-ligand function of *Limulus* CRP, we de-glycosylated CRP-I and CRP-II and observed that the ability of the deglycosylated CRP-I and CRP-II, to recognize and bind to immobilized, denatured and aggregated proteins was greatly decreased (approximately 100 fold) when compared to their glycosylated counterparts.

Therefore, native glycosylated *Limulus* CRP displays similar ligand binding function as non-native human pentameric CRP.

An innate immune system has a pivotal role in host-defense mechanism where its major function is identification of pathogens and its clearance or inactivation. The innate immune system is unique in these arthropods as they have complement-like activity but without the acquired immunoglobulin-dependent immunity that is present in vertebrates. Hence, the immune system evolved from these ancient species, where α_2- macroglobulin and pentraxins exhibit the function of immune defense proteins using cytolysis for pathogen elimination, to humans where this function is taken over by acute phase reactants and complement activation (18). As the immune system evolved, the nature of CRP gene expression also evolved from a constitutively expressed protein in *Limulus polyphemus* to an acute phase protein in humans.

We conclude that though the ligand-binding properties of *Limulus* CRP are not identical to that of native human CRP, they overlap the ligand-binding properties of non-native pentameric human CRP that can be generated at inflammatory microenvironments. Also, changing the glycosylation state of *Limulus* CRP, changes its ligand-binding and overlapping with native human CRP. This suggests that CRP evolved as a component of and along with the development of the entire immune system.

Acknowledgement

The work was supported by NIH Grant: R01 AR068787 (Agrawal ; P.I.)

Abbreviations:

CRP	C-reactive protein
PCh	Phosphocholine
PEt	Phosphoethanolamine
CRP-I	PCh-binding Limulus CRP
CRP-II	PEt-binding Limulus CRP
Aβ	Amyloid β peptide 1-42
Ox-LDL	Oxidized low-density lipoprotein
Ac-LDL	Acetylated low-density lipoprotein
TFMS	Trifluoromethanesulfonicacid
TBS-Ca	TBS, pH 7.2, containing 0.1% gelatin, 0.02% Tween 20 and 2 mM $CaCl_2$
TBS-EDTA	TBS, pH 7.2, containing 0.1% gelatin, 0.02% Tween 20 and 5 mM EDTA

References

1. Agrawal, A., Singh, P.P., Bottazzi, B., Garlanda, C., Mantovani, A. (2009) Pattern recognition by pentraxins. *Adv Exp Med Biol*. **653**, 98-116.
2. Pepys, M.B., Dash, A.C., Fletcher, T.C., Richardson, N., Munn, E.A., Feinstein, A. (1978) Analogues in other mammals and in fish of human plasma proteins, C-reactive protein and amyloid P component. *Nature*. **273**, 168–170.
3. Baltz, M.L., De Beer, F.C., Feinstein, A., Munn, E.A., Milstein, C.P., Fletcher, T.C., March, J.F., Taylor, J., Bruton, C., Clamp, J.R., Davies, A.J., Pepys, M.B. (1982) Phylogenetic aspects of C-reactive protein and related proteins. *Ann NY Acad Sci USA*. **389**, 49–75.
4. Maudsley, S., Pepys, M.B. (1987) Immunochemical cross-reactions between pentraxins of different species. *Immunology*. **62**, 17–22.
5. Ying, S-C., Marchalonis, J.J., Gewurz, A.T., Siegel, J.N., Jiang, H., Gewurz, B.E., Gewurz, H. (1992) Reactivity of anti-human C-reactive protein (CRP) and serum amyloid P component (SAP) monoclonal antibodies with limulin and pentraxins of other species. *Immunology*. **76**, 324–330.
6. Nunomura, W. (1992) C-reactive protein (CRP) in animals: its chemical properties and biological functions. *Zool Sci*. **9**, 499–513.
7. Pathak, A., Agrawal, A. (2019) Evolution of C-reactive protein. *Front Immunol*. **10**, 93.
8. Kushner, I. (1982) The phenomenon of the acute phase response. *Ann NY Acad Sci USA*. **389**, 39–48.

9. Shrive, A.K., Cheetham, G.M.T., Holden, D., Myles, D.A.A., Turnell, W.G., Volanakis, J.E., Pepys, M.B., Bloomer, A.C., Greenhough, T.J. (1996) Three-dimensional structure of human C-reactive protein. *Nature Struct Biol*. **3**, 346–354.
10. Woo, P., Korenberg, J.R., Whitehead, A.S. (1985) Characterization of genomic and complementary DNA sequence of human C-reactive protein, and comparison with the complementary DNA sequence of serum amyloid P component. *J Biol Chem*. **260**, 13384–13388.
11. Agrawal, A., Lee, S., Carson, M., Narayana, S.V.L., Greenhough, T.J., Volanakis, J.E. (1997) Site-directed mutagenesis of the phosphocholine-binding site of human C-reactive protein: role of Thr^{76} and Trp^{67}. *J Immunol.* **158**, 345–350.
12. Thompson, D., Pepys, M.B., Wood, S.P. (1999) The physiological structure of human C-reactive protein and its complex with phosphocholine. *Structure.* **7**, 169–177.
13. Agrawal, A., Simpson, M.J., Black, S., Carey, M.P., Samols, D. (2002) A C-reactive protein mutant that does not bind to phosphocholine and pneumococcal C-polysaccharide. *J Immunol*. **169**, 3217–3222.
14. Mikolajek, H., Kolstoe, S.E., Pye, V.E., Mangione, P., Pepys, M.B., Wood, S.P. (2011) Structural basis of ligand specificity in the human pentraxins, C-reactive protein and serum amyloid P component. *J Mol Recognit*. **24**, 371–377.
15. Kaplan, M.H., Volanakis, J.E. (1974) Interaction of C-reactive protein complexes with the complement system. I. Consumption of human complement associated with the reaction of C-reactive protein with pneumococcal C-polysaccharide and with the choline phosphatides, lecithin and sphingomyelin. *J Immunol.* **112**, 2135–2147.

16. Agrawal, A., Volanakis, J.E. (1994) Probing the C1q-binding site on human C-reactive protein by site-directed mutagenesis. *J Immunol.* **152**, 5404–5410

17. Agrawal, A., Shrive, A.K., Greenhough, T.J., Volanakis, J.E. (2001) Topology and structure of the C1q-binding site on C-reactive protein. *J Immunol.* **166**, 3998–4004.

18. Armstrong, P.B. (2015) Comparative biology of the pentraxin protein family: evolutionarily conserved component of innate immune system. *Int Rev Cell Mol Biol*. **316**, 1–47.

19. Tharia, H.A., Shrive, A.K., Mills, J.D., Arme, C., Williams, G.T., Greenhough, T.J. (2002) Complete cDNA sequence of SAP-like pentraxin from Limulus polyphemus: implications for pentraxin evolution. *J Mol Biol.* **316(3)**, 583-597.

20. Robey, F.A., Liu, T.Y. (1981) Limulin: A C-reactive protein from *Limulus polyphemus*. *J Biol Chem* **256**, 969-975.

21. Misquith, S., Surolia, A., Subita, S., Armstrong, P. (1994) Preliminary investigation of the molecular basis for the functional differences between the two pentraxins Limulin and C-reactive protein from the plasma of the American horseshoe crab, *Limulus polyphemus*. *Biol Bull.* **187**, 229-230.

22. Myles, D.A.A., Bailey, S., Rule, S.A,, Jones, G.R., Greenhough, T.J. (1990) Preliminary crystallographic study of C-reactive protein from *Limulus polyphemus*. *J Mol Biol.* **213**, 223-225.

23. Nguyen, N.Y., Suzuki, A., Boykins, R.A., Liu, T.Y. (1986) The amino acid sequence of *Limulus* C-reactive protein: Evidence of polymorphism. *J Biol Chem.* **261**, 10456-10465.

24. Nguyen, N.Y., Suzuki, A., Cheng, S.M., Zon, G., Liu, T.Y. (1986) Isolation and characterization of *Limulus* C-reactive protein genes. *J Biol Chem.* **261**, 10450-10455.

25. Tennent, G.A., Bulter, P.J.G., Hutton, T., Woolfitt, A.R., Harvey, D.J., Rademacher, T.W., Pepys, M.B. (1993) Molecular characterization of *Limulus polyphemus* C-reactive protein. I. Subunit composition. *Eur J Biochem.* **214**, 91-97.

26. Amatayakul-Chantler, S., Dwek, R.A., Tennent, G.A., Pepys, M.B., Rademacher, T.W. (1993) Molecular characterization of *Limulus polyphemus* C-reactive protein. II. Asparagine-linked oligosaccharides. *Eur J Biochem.* **214**, 99-100.

27. Liu, T.Y., Syin, C., Nguyen, N.Y., Suzuki, A., Boykins, A., Lei, K-J., Goldman, N. (1987) Comparison of protein structure and genomic structure of human, rabbit, and Limulus C-reactive proteins: Possible implications for function and evolution. *J Prot Chem.* 6, **263**-271.

28. Singh, S.K., Thirumalai, A., Hammond, D.J. Jr, Pangburn, M.K., Mishra, V.K., Johnson, D.A., Rusińol, A.E., Agrawal, A. (2012) Exposing a hidden functional site of C-reactive protein by site-directed mutagenesis. *J Biol Chem.* **287**(5), 3550-3508.

29. Hammond, D.J. Jr., Singh, S.K., Thompson, J.A., Beeler, B.W., Rusinol, A.E., Pangburn, M.K., Potempa, L.A., Agrawal, A. (2010) Identification of acidic pH-dependent ligands of pentameric C-reactive protein. *J Biol Chem.* **285**, 36235–36244.

30. Singh, S.K., Thirumalai, A., Pathak, A., Ngwa, D.N., Agrawal, A. 2017. Functional transformation of C-reactive Protein by hydrogen peroxide. *J Biol Chem.* **292(8)**, 3129-3136.

31. Thirumalai, A., Singh, S.K., Hammond, D.J. Jr, Gang, T.B., Ngwa, D.N., Pathak, A., Agrawal, A. (2017) Purification of recombinant C-reactive protein mutants. *J Immunol Methods.* **443**, 26-32.

32. Gang, T.B., Hammond, D.J., Singh, S.K., Ferguson Jr, D.A., Mishra ,V.K., Agrawal, A. (2012) The Phosphocholine-binding Pocket on C-reactive Protein Is Necessary for Initial Protection of Mice against Pneumococcal Infection. *J. Biol. Chem*. **287**, 43116-43125

33. Shrive, A.K., Metcalfe, A.M., Cartwright, J.R., Greenhough, T.J. (1999) C-reactive protein and SAP-like pentraxin are both present in *Limulus polyphemus* haemolymph: Crystal structure of *Limulus* SAP. *J Mol Biol.* **290**, 997-1008.

34. Armstrong, P.B., Armstrong, M.T., Quigley, J.P. (1993) Involvement of α_2-macroglobulin and C-reactive protein in a complement-like hemolytic system in the arthropod, *Limulus polyphemus*. *Mol Immunol.* **30**, 929-934.

35. Quigley, J.P., Armstrong, P.B. (1985) A Homologue of a2-Macroglobwlin Purified from the Hemolymph of the Horseshoe Crab Limulus Polyphemus. *J. Biol. Chem*. **260**, 17215-17219.

36. McSweegan, E.F., Pistole, T.G. (1982) Interaction of the lectin limulin with capsular polysaccharides from *Neisseria meningitidis* and *Escherichia coli*. *Biochem Biophys Res Commun.* **106**, 1390-1397.

37. Robey, F.A., Liu, T.Y. (1983) Synthesis and use of new spin labeled derivatives of phosphorylcholine in a comparative study of human, dogfish, and *Limulus* C-reactive proteins. *J Biol Chem.* **258**, 3895-3900.

38. Liu, T., Lin, Y., Cislo, T., Minetti, C.A.S.A., Baba, J.M.K., Liu, T.Y. (1991) Limunectin: A phosphocholine-binding protein from *Limulus* amebocytes with adhesion-promoting properties. *J Biol Chem*. **266**, 14813-14821.

39. Saito, T., Hatada, M., Iwanaga, S., Kawabata, S.I. (1997) A newly identified horseshoe crab lectin with binding specificity to O-antigen of bacterial lipopolysaccharides. *J Biol Chem*. **272**, 30703-30708.

40. Liu, T.Y., Minetti, C.A., Fortes-Dias C.L., Liu, T., Lin, L., Lin, Y. (1994) C-reactive proteins, limunectin, lipopolysaccharide-binding protein, and coagulin. Molecules with lectin and agglutinin activities from Limulus polyphemus. *Ann NY Acad Sci.* **712**, 146-154.

41. Ansar, W., Mukhopadhyay, S., Habib, S.K., Basu, S., Saha, B., Sen, A.K., Mandal, C.N., Mandal, C. (2009) Disease-associated glycosylated molecular variants of human C-reactive protein activate complement-mediated hemolysis of erythrocytes in tuberculosis and Indian visceral leishmaniasis. *Glycoconj J*. **26**, 1151–1169.

42. Das, T., Sen, A., Kempf, T., Pramanik, S.R., Mandal, C., Mandal, C. (2003) Induction of glycosylation in human C-reactive protein under different pathological conditions. *Biochem J*. **373**, 345–355.

43. Das, T., Mandal, C., Mandal, C. (2004) Variations in binding characteristics of glycosylated human C-reactive proteins in different pathological conditions. *Glycoconj J*. **20**, 537–543.

CHAPTER 4

Transcriptional activation and regulation of C-reactive protein gene by two distinct STAT3 sites

Running title: IL-6 induces C-reactive protein expression through multiple STAT3 sites on the promoter

Asmita Pathak[1], and Alok Agrawal[1*]

[1]Department of Biomedical Sciences, James H. Quillen College of Medicine, East Tennessee State University, Johnson City, TN, USA

Number of words: 6516

Number of figures: 6

[*] Correspondence should be addressed to: AA (agrawal@etsu.edu)

Keywords: C-reactive protein, STAT3, transcriptional regulation, gene expression, cytokine induction

Abstract

Gene expression regulation of C-reactive protein (CRP) occurs at transcriptional level by various cytokine inducible and constitutively active transcription factors. IL-6 is the major cytokine that is known to induce CRP expression by activation of transcription factors STAT3 and C/EBPβ. The proximal 157 bp region of the CRP promoter has been shown to be sufficient to induce CRP transcription in response to IL-6 and binding sites for both these transcription factors are present within the -157 bp region of CRP promoter. It has been previously reported that the proximal 300 bp region of the CRP promoter elicits a higher IL-6 response compared to the 157 bp region. An additional C/EBPβ site has been shown to be present at position -222, but additional binding sites for STAT3 have not been located between -157 to -300 bp region. In the current study, we discovered multiple putative IL-6 inducible STAT3 binding sites, located at position -72, -134, and -165 respectively, in addition to the previously reported transcriptionally active STAT3 site at -108. We found that, although STAT3 binds to its cognate site at positions -134 and -165, the STAT3 binding site at -134 is transcriptionally active, unlike -165. The STAT3 site at position -134 does not activate CRP transcription but rather regulates the gene expression of CRP. We hypothesize that IL-6 inducible STAT3 binding sites at position -134 and -108 act co-operatively with each other to activate CRP transcription wherein STAT3 (-134) regulates a crosstalk mechanism between STAT3 (-108) and other transcription factors.

Introduction

C-reactive protein (CRP) is an acute phase protein of the innate immune response of humans, serum concentration of which increases significantly followed by either a chronic or an acute inflammatory insult (1-6). It is a multifunctional, host defense protein that is produced by hepatocytes (7,8). The regulation of CRP synthesis occurs at transcriptional level wherein cytokines such as interleukin 6 (IL-6) and interleukin 1β (IL-1β) induce CRP expression via activation of various transcription factors (9,10). IL-6, alone or in synergy with IL-1β, actuates CRP transcription by activating C/EBP (CCAAT/enhancer-binding protein) family of transcription factors and STAT (signal transducers and activators of transcription) family members. IL-1β alone does not activate CRP transcription but it does so in synergy with IL-6 via activation of nuclear factor kappaB (NF-κB) (8, 11-17). Cytokine (IL-6 + IL-1β)-induced CRP transcription has been observed in human hepatoma cell line Hep3B while IL-6 activated transcription factors have been shown to induce CRP expression in other hepatic cell lines as well (11, 14-16, 18).

The proximal 157 bp region of the CRP promoter (-157/+1) has been shown to be sufficient for inducing CRP transcription in response to IL-6 as IL-6 activated transcription factors such as C/EBPβ and STAT3 have binding sites on the CRP promoter, centered at position -52 and -108, respectively (9,13). Also, IL-1β activated transcription factor, NF-κB binds to its site located at position -69 on CRP promoter (Fig 1A). NF-κB regulates CRP transcription via formation of homodimers or heterodimers of five NF-κB proteins namely p50, p52, p65, c-Rel, and c-Rel B (8). In addition to the cytokine activated transcription factors, other constitutively active transcription factors such as C/EBPζ, RBP-Jκ, Oct-1, HNF-1, and HNF-3 have been

shown to regulate CRP gene expression (7,12,19).

STAT3, one of the STAT family members, transitions from a non-active cytoplasmic non-phosphorylated monomeric state to an active nuclear tyrosine-phosphorylated dimeric state. This transition is initiated by IL-6 binding to its receptor complex that initiates a pathway of Janus kinase kinases phosphorylation with subsequent phosphorylation, dimerization, and nuclear translocation of STAT3 (20,21). STAT3 has been shown to bind to acute phase response elements on the promoter regions containing $TT(N)_4AA$ or $TT(N)_5AA$ motifs specifically (22-24). One such IL-6 induced STAT3 response element, centered at position -108 on the proximal human CRP promoter containing the sequence TTCCCGAA, has been shown to induce CRP transcription (13).

It has been previously reported that the proximal 300 bp region of the CRP promoter (-300/+3) elicits a higher IL-6 response when compared to the 157 bp region. In addition to the IL-6 induced transcriptionally active C/EBPβ site positioned at -52, another C/EBPβ site has been shown to be present at position -222. However, additional binding sites for STAT3 are not known between -157 bp to -300 bp region. In the current study, the aim was to locate putative IL-6 responsive STAT3 binding sites in the -300 bp region of CRP promoter and if located, determine whether these sites are transcriptionally active. We revisited the -300/+3 region of CRP promoter and found three additional, putative STAT3 binding sites centered at position -72, -134, - 165 along with the previously reported STAT3 site at position -108. Our data indicates that, in addition to the STAT3 site at position -108, STAT3 binds to IL-6 responsive STAT3 binding sites located at position -134 and -165, but only the STAT3 site at -134 is transcriptionally active. Also, STAT3 site at -134 does not activate CRP transcription but rather regulates CRP expression via facilitating crosstalk between other transcription factors.

Experimental Procedures

Identification of putative STAT3-binding sites in -300 bp region of the CRP promoter

Putative STAT3- binding sites were identified by visual inspection of the proximal 300 bp region of the CRP promoter. $TT(N)_4AA$ or $TT(N)_5AA$ containing motifs were considered potemtial STAT3-binding regions.

Preparation of Nuclear Extract and EMSA (Electrophoretic mobility gel shift assay)

Hep3B cells were used as the source of nuclear extracts. Cells were cultured in a 100 mm dish using RPMI media (containing 10% FBS and 1% Penicillin-Streptomycin stock) and at 60% confluency, were subjected to serum starvation overnight. Post overnight serum starvation, cytokine treatment was performed using IL-6 and IL-6 + IL-1β, for 15 minutes. IL-6 and IL-1β (R & D systems; cat# 206-IL and 201-LB, respectively) were used at concentrations of 10 ng/ml and 1 ng/ml, respectively. Nuclear extracts were prepared using NE-PER nuclear and cytoplasmic kit (Pierce; cat# 78835), as described previously (25). Putative STAT3-containing oligonucleotide (oligo) sequences that are used in EMSA are shown in Figure 1B. Oligos were obtained from Integrated DNA Technologies. Probes were prepared by annealing complementary oligos, followed by labelling with [γ ^{32}P] ATP (MP Biomedicals; SKU 013502005) using end labelling with T4 Polynucleotide kinase (Promega; M4101). Probe-nuclear extract reaction mixture was incubated in gel shift incubation buffer (40 mM KCl, 20 mM Hepes pH 7.9, 1 mM $MgCl_2$, 0.05 mM EGTA, 0.5 mM dithiothrietol, 4% Ficoll, and 1 μg of poly dI-dC) for 20 minutes at room temperature. For supershift experiments, antibody to STAT3 (F20X, Santa Cruz Biotechnologies) was added to the nuclear extract, prior to addition of the

probe. DNA- protein complexes were resolved in 5% polyacrylamide native gels containing 2.5% glycerol and analyzed in a phosphorimager using ImageQuant software (GE Healthcare).

CRP Promoter-Luciferase (Luc) Reporter Constructs

The engineering of Luc-157 (−157/+1 of CRP gene and Luc-300 (-300/+3 of CRP promoter) wild-type (WT) constructs, have been described previously (8,25,28). The WT constructs were used as templates for mutagenesis. Constructs containing mutated STAT3 sites were generated using the QuickChange site-directed mutagenesis kit (Stratagene) on both Luc-157 WT and Luc-300 WT. The STAT3-site (-108) was mutated by substituting $^{-111}$TCCCGA^{-106} with $^{-111}$GATATC^{-106} using mutagenic primers 5'-GCTTCCCCTCTGATATCAGCTCTGACACCTG and 5'-CAGGTGTCAGAGCTGATATCAGAGGGGAAGC. The STAT3-site (-134) was mutated by substituting $^{-138}$TTCTGAAA^{-131} with $^{-138}$TCCGGCCA^{-131} using mutagenic primers: 5'-TCACATTGATTTCTCTGTCCGGCCATAATTTTGCTTCCCC and 5'-GGGGAAGCAAAATTATGGCCGGACAGAGAAATCAATGTGA. The STAT3-site (-165) was mutated by substituting $^{-169}$TTGTAATAA^{-161} with $^{-169}$TTCGCAGTA^{-161} using mutagenic primers 5'-GGTAATTCAGTAGTCATAGGAGTTCGCAGTACATAACTCACATTGATTTCTCTG and 5'-CAGAGAAATCAATGTGAGTTATGTACTGCGAACTCCTATGACTACTGAATTACC. A double STAT3 mutant with both -108 and -134 site mutated was generated by using Luc- 157 mut STAT3 (-108) and Luc- 300 mut STAT3 (-108) as the template and STAT3-site (-134) mutagenic primers, as described above. Double STAT3 mutant with both -108 and -165 site mutated was generated by using Luc- 300 mut STAT3 (-108) as the template and STAT3-site (-

165) mutagenic primers, as described above. Plasmids were purified using maxiprep plasmid isolation kit (Eppendorf) and mutations were verified by sequencing at the Molecular Biology Core Facility at ETSU,

Luciferase (Luc) Transactivation Assay

Hep3B cells were cultured overnight for transfection and cytokine treatment using serum-free medium as described previously (26). The confluency of cells at the time of transfection was approximately 60%. Cells were plated into 6-well plates for transient transfections, and transfection was carried out using FuGENE 6 reagent (Promega). Briefly, per well, 10 µl FuGENE 6 was added to 125 µl RPMI-1640 and incubated for 5 minutes. Further, 1µg of Luciferase reporter-CRP promoter construct was added to the RPMI- FuGENE 6 cocktail, incubated for 20 minutes at RT and added to the well. Cytokine treatment was performed 16 hours post-transfection. IL-6 and IL-1β (R & D systems) were used at concentrations of 10 ng/ml and 1 ng/ml, respectively, and incubation continued for 24 hours. Post-transfection (40 hours) and post-cytokine treatment (24 hours), luciferase assays were performed (Luciferase assay system with reporter lysis buffer; Promega) as described previously (27). Luciferase activity was measured in a luminometer (Molecular Devices), which was programmed for the integration time of 10 s with no post-injection delay time. Results were projected as mean ± SD of three experiments and statistical analysis was performed using unpaired student t-test.

Results

Multiple IL-6 inducible putative STAT3-binding sites are located within the first 300 bp (-300/+3) region of CRP promoter

We examined the proximal 300 bp region of the CRP promoter and located three previously undescribed, putative STAT3-binding sites containing $TT(N)_4AA$ or $TT(N)_5AA$ motifs. Two sites were located downstream of -157/+1 region of the CRP promoter, at -72 (-76/-69: TTGGAAAA) and -134 (-138/-131: TTCTGAAA), while one was located upstream at -165 (-169/-161: TTGTAATAA) in the -300/+3 region (Fig 4.1 A).

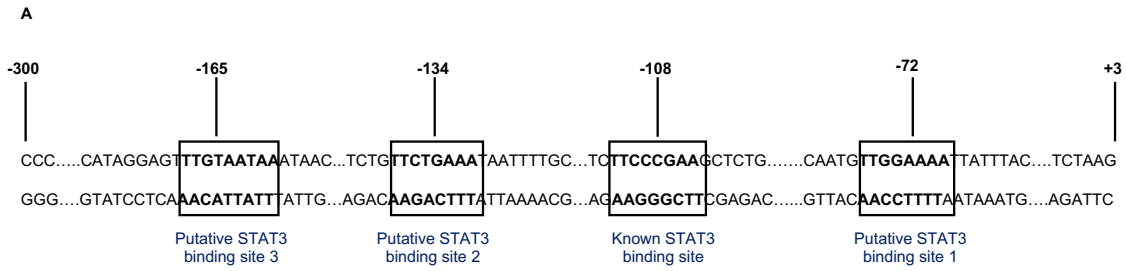

B

Probes for EMSA:

Oligo 1 [STAT3 (-72)] **-92** 5' GCCCCAACAAGCAATG**TTGGAAAA**TTATTTACATAGTGCG 3' **-53**
GCGCACTATGTAAATAATTTTCCAACATTGCTTGTTGGGG

Oligo 2 [STAT3 (-134)] **-154** 5' GCGCGTGATTTCTCTG**TTCTGAAA**TAATTTTTGCTGCGTG 3' **-115**
GCACGCAGCAAAAATTATTTCAGAACAGAGAAATCACGCG

Oligo 3 [STAT3 (-165)] **-182** 5' GGCGCATAGGAGT**TTGTAATAA**ATAACTCACCGC 3' **-149**
GGCGGTGAGTTATTTATTACAAACTCCTATGCGC

Oligos used to construct mutated STAT Luc promoter:

WT **TTCCCGAA**
mSTAT (-108) 5' GCTTCCCCTC**TGATATCA**GCTCTGACACCTG 3'
CAGGTGTCAGAGCTGATATCAGAGGGGAAGC

WT **TTCTGAAA**
mSTAT (-134) 5' TCACATTGATTTCTCTG**TCCGGCCA**TAATTTTGCTTCCCC 3'
GGGGAAGCAAAATTATGGCCGGACAGAGAAATCAATGTGA

WT **TTGTAATAA**
mSTAT (-165) 5' GGTAATTCAGTAGTCATAGGAG**TTCGCAGTA**CATAACTCACATTGATTTCTCTG 3'
CAGAGAAATCAATGTGAGTTATGTACTGCGAACTCCTATGACTACTGAATTACC

Figure 4.1: The −300 / +3 region of the CRP gene promoter and the sequences of the oligos used in this study. (A) The putative binding sites for STAT3 on the CRP promoter are shown along with the previously known STAT3 binding site at -108. (B) Sequence of the oligos used as probes in EMSA and to construct mutated STAT promoter for luciferase assays. Putative STAT3 binding sites are shown, highlighted in blue. Mutated nucleotides are indicated in red.

IL-6 activated STAT3 binds to its cognate site at position -134 and -165 on CRP promoter

Binding of STAT3 to the newly identified putative STAT3-binding sites on the CRP promoter was analyzed by EMSA. Nuclear extracts from Hep3B cells treated with IL-6 alone and (IL-6 + IL-1β; 15 minutes) were used as source of activated STAT3. Wild- type (WT) oligos, containing putative STAT3 sites (-72, -134, and -165), are shown in Fig 4.1 B. When WT oligo (-72) was used as probe, several complexes were observed (Fig 4.2 A), however, none were clearly abolished or super-shifted by inclusion of anti-STAT3 antibodies. Two STAT3-containing complexes were observed with WT oligo (-134) as probe (Fig 4.2 B). The intensity of the two bands was greater using nuclear extracts from (IL-6 + IL-1β)-treated Hep3B cells compared to nuclear extracts from cells treated with IL-6 alone. Using nuclear extracts from IL-6 treated cells, only one band (complex II) was clearly visible (Fig 4.2 B, lane2), which was supershifted by anti-STAT3 antibody (Fig 4.2 B, lane 4). Nuclear extracts from (IL-6 + IL-1β)-treated cells, produced two bands (Complex I and complex II) (Fig 4.2 B, lane3) both of which were abolished in the presence of anti- STAT3 antibody (Fig 4.2 B, lane 5). EMSA revealed one STAT3-containing complex formed with WT oligo (-165) with nuclear extracts from both IL-6

(Fig 4.2 C, lane 2) and (IL-6 + IL-1β) (Fig 4.2 C, lane 3) treated cells. Although the intensity of the EMSA bands observed with WT oligo (-165) was not as intense as those observed with WT oligo (-134) and WT oligo (-72), they were abolished in the presence of anti- STAT3 antibody (Fig 4.2 C, lane 4 and 5 respectively). The abolition of complexes by anti-STAT3 antibodies observed with WT oligo (-134) and WT oligo (-165) confirms that these complexes contain STAT3. Therefore, out of the identified, putative STAT3 binding sites, STAT3 was shown to bind to -134 and -165.

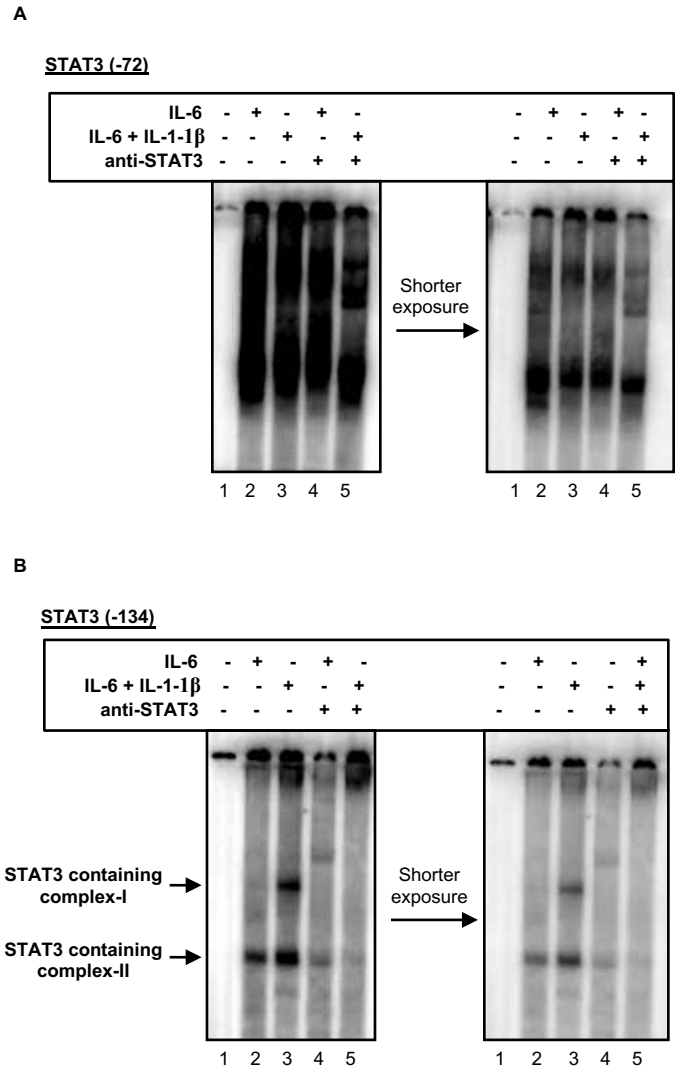

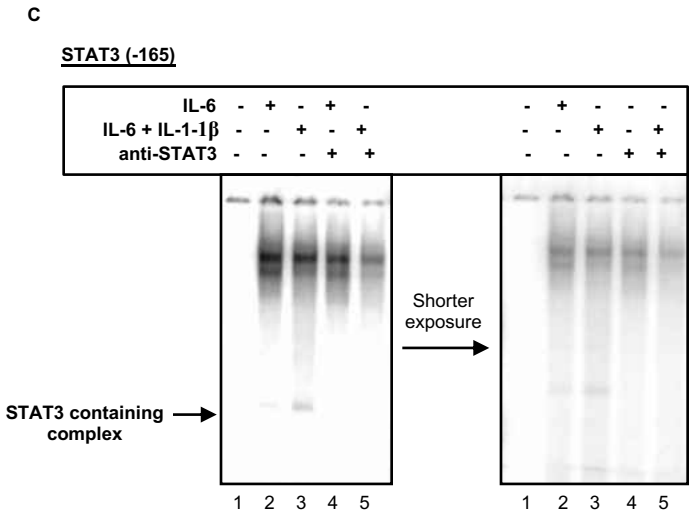

Figure 4.2: STAT3 binds to its cognate position at -134 and -165. A representative EMSA demonstrating the binding of STAT3 to its putative binding sites on the CRP promoter is shown. Radiolabeled WT oligos [(A) Oligo 1: -72 (-92/-55), (B) Oligo 2: -134 (-154/-115), and (C) oligo 3: -165 (-182/-149)] were used as probe and nuclear extract derived from cytokine (IL-6 and IL-6 + IL-β; 15 minutes)-treated Hep3B cells were used as the source of STAT3. Anti-STAT3 was added to nuclear extracts before the addition of the probe. DNA probe–protein complexes were visualized using a phosphorimager. Complexes containing STAT3 are indicated by arrows and free probe mobility is not shown.

The proximal 157bp region of the CRP promoter is sufficient for transactivation but -300/+3 region elicits a greater response

The proximal 157 bp region of CRP promoter has been shown to be sufficient for synergistic induction of CRP gene expression. We compared the transactivation of CRP gene expression between the proximal 157 bp (Luc 157-WT) and 300 bp (Luc 300-WT) region of CRP promoter by Luciferase transactivation assays (Fig 4.3 A). The synergy between IL-6 and IL-1β was observed with both Luc-157 WT and Luc-300 WT, with the CRP expression being ~90 % greater (*; $p = 0.004$) in cells treated with (IL-6 + IL-1β) as compared to cells treated with IL-6 alone. IL-1β-treated cells displayed similar transactivation as basal (data not shown). In all cells treated with IL-6 alone and in cells treated with (IL-6 + IL-1β), Luc-300-WT displayed a greater transactivation that Luc-157 WT [~53% and ~33% (*) respectively]. These results indicate that the region between -157 and -300 contribute to an elevated CRP gene expression.

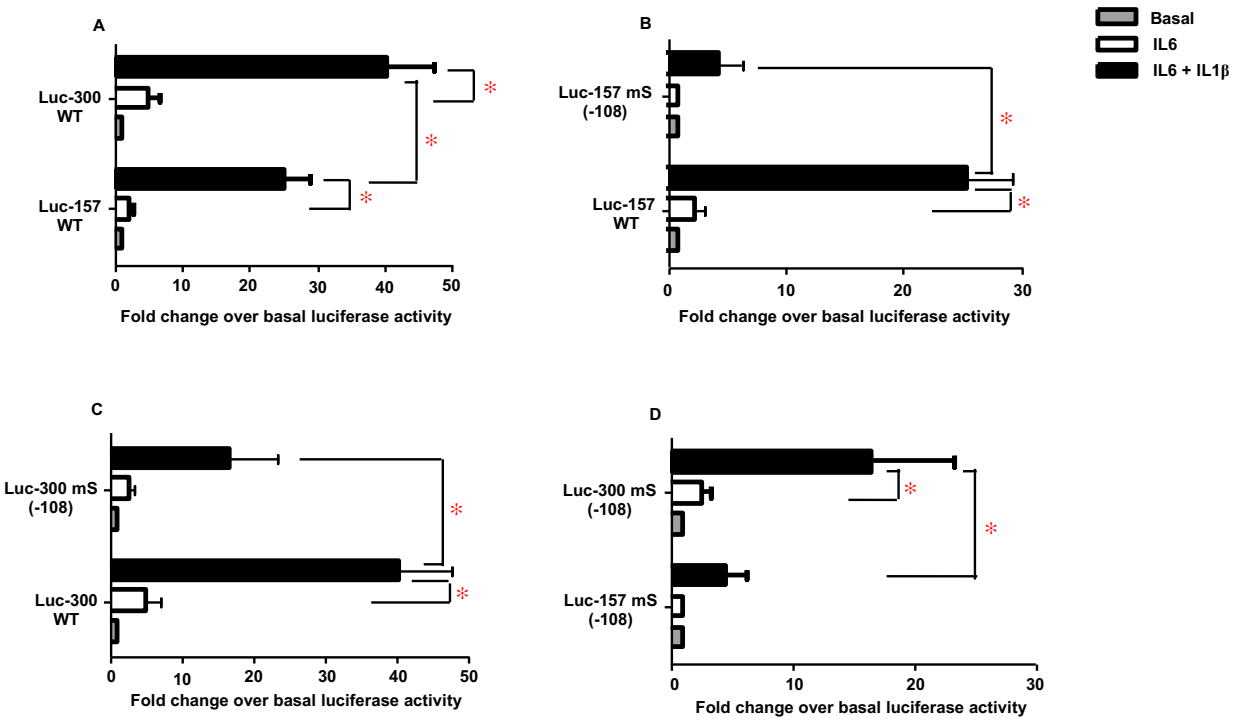

Figure 4.3: The -300/+3 region of CRP promoter elicits a greater cytokine-induced response when compared to the proximal 157 region and the STAT3 site at -108 is critical for CRP transcription. (A) Luciferase transactivation assay of Hep3B transfected with Luc-157 WT and Luc-300 WT CRP promoter constructs is shown. ((B-D) Luciferase transactivation assay showing the effect of mutated STAT3 site at -108 on cytokine (IL-6 and IL-6 + IL-1β)-induced CRP expression, is shown. Hep3B cells were transfected with Luc-157 WT and Luc-157 mS (-108) (B), Luc-300 WT and Luc-300 mS (-108) (C), and Luc-157 mS (-108) and Luc-300 mS (-108) (D) CRP promoter constructs, 24 h post cytokine treatment and 40 h post transfection, CRP transcription was measured as Luc activity. Fold change over basal luciferase activity is plotted on the *x*-axis. Results are expressed as mean ± SD for three experiments. *p* value of ≤ 0.05 are considered statistically significant (*).

Role of STAT3-site positioned at -134 in IL-6 and (IL-6 + IL1-β)- induced CRP expression

The binding of STAT3 to its transcriptionally active site at -108 has been well documented (13) and as shown in Fig 4.3 B and 4.3 C, mutation of STAT3 (-108) leads to reduced IL-6 and (IL-6 + IL-1β) induced gene expression in both proximal 157 and 300 bp region of CRP promoter. However, mutation of STAT3 (-108) in the proximal 300 bp region did not completely abolish the activation of CRP expression by IL-6, unlike the proximal 157 bp region (Fig 4.3 D).

To investigate the role of potential STAT3 binding site at -134, in regulating cytokine [IL-6 and (IL-6 + IL1-β)] induced CRP expression, we performed Luciferase transactivation assays using Luc 157-WT, Luc 300-WT, Luc 157-mS (-134), and Luc 300-mS (-134) promoter constructs. In addition, CRP promoter constructs with mutation in both (-108 and -134) STAT3 sites [Luc-157 mS (-108) + (-134) and Luc-300 mS (-108) + (-134)], were used to analyze the combined function of of STAT3 on CRP promoter activity in response to IL-1β, IL-6, and (IL-6 + IL-1β) induced CRP expression respectively. Treatment with IL-1β alone did not induce CRP expression above basal levels (data not shown). Mutation of STAT3 (-134) in the 157 bp region of CRP promoter, Luc-157 mS (-134) has no effect on (IL-6 + IL-1β)- induced CRP expression while the IL-6 induced CRP expression was ~47 % higher (*; $p = 0.04$) compared to Luc-157 WT (Fig 4.4 A). However, mutation of STAT3 (-134) in the 300 bp region, Luc-300 mS (-134) resulted in greater IL-6 and (IL-6 + IL1-β) -induced CRP expression (~88% and ~40% (*), respectively) (Fig 4.4 B). Consistent with results for mutation of STAT3 (-108), mutating STAT3 (-134) in the proximal 300 bp region of CRP promoter produced a higher CRP expression as compared to the same mutation in the proximal 157 bp promoter region (Fig 4.4 C).

Mutation of both STAT3 sites (-108 and -134), Luc-300 mS (-108) + (-134) completely eliminated IL-6 and (IL-6 + IL1-β)-induced CRP expression when compared to Luc 300-WT (Fig 4.4 E). However, mutation of both STAT3 sites in the 157 bp region, Luc-157 mS (-108) + (-134) induced ~49% lower (*) (IL-6 + IL-1β)- induced CRP expression compared WT and no effect was observed in IL-6-induced CRP expression (Fig 4.4 E). Mutation of STAT3 sites at -108 and -134 in the proximal 300 bp region of the promoter lead to loss of the cytokine-induced CRP expression, however, the cytokine-induced CRP expression was observed in the 157 bp promoter region with both STAT3 sites mutated (Fig 4.4F).

As reported previously (13) and shown here, the STAT3 (-108) site is involved in activating CRP transcription as its mutation reduced (IL-6+IL-1β)-induced CRP expression in both proximal 157 bp and 300 bp region. Our results suggest that the STAT3 (-134) site alone does not contribute to enhance CRP expression but rather regulates the interaction/crosstalk between other transcription factors as mutation of this site enhanced CRP expression in the proximal 300 bp region but not in 157 bp promoter region. Consistent with this, is the observation that complete elimination of STAT3 binding sites (mutated -134 and -108) reduced CRP expression to basal levels. This raises the possibility of the involvement of an active site present between -300 bp and -157 bp region that is involved in the crosstalk. Also, because the effect is observed in both IL-6 and (IL-6+IL-1β)-induced CRP expression, IL-6 activated transcription factors appear to be involved in the crosstalk. Compared to the proximal 157 bp region of CRP promoter, the proximal 300 bp of CRP promoter elicits a greater cytokine induced CRP expression. Mutation of -108 site or -134 site alone did not significantly affect this observation. When both STAT3 sites were mutated in the proximal 300 bp region, the cytokine-induced expression of CRP gene was reduced to basal levels, however a similar effect was not

observed on the cytokine-induced CRP expression in the proximal 157 bp region. This further supports the possibility of a crosstalk mechanism between transcription factors present in the proximal 300 bp promoter region and STAT3 sites (-108 and -134) along-with other transcription factors present in -157 bp region of CRP promoter.

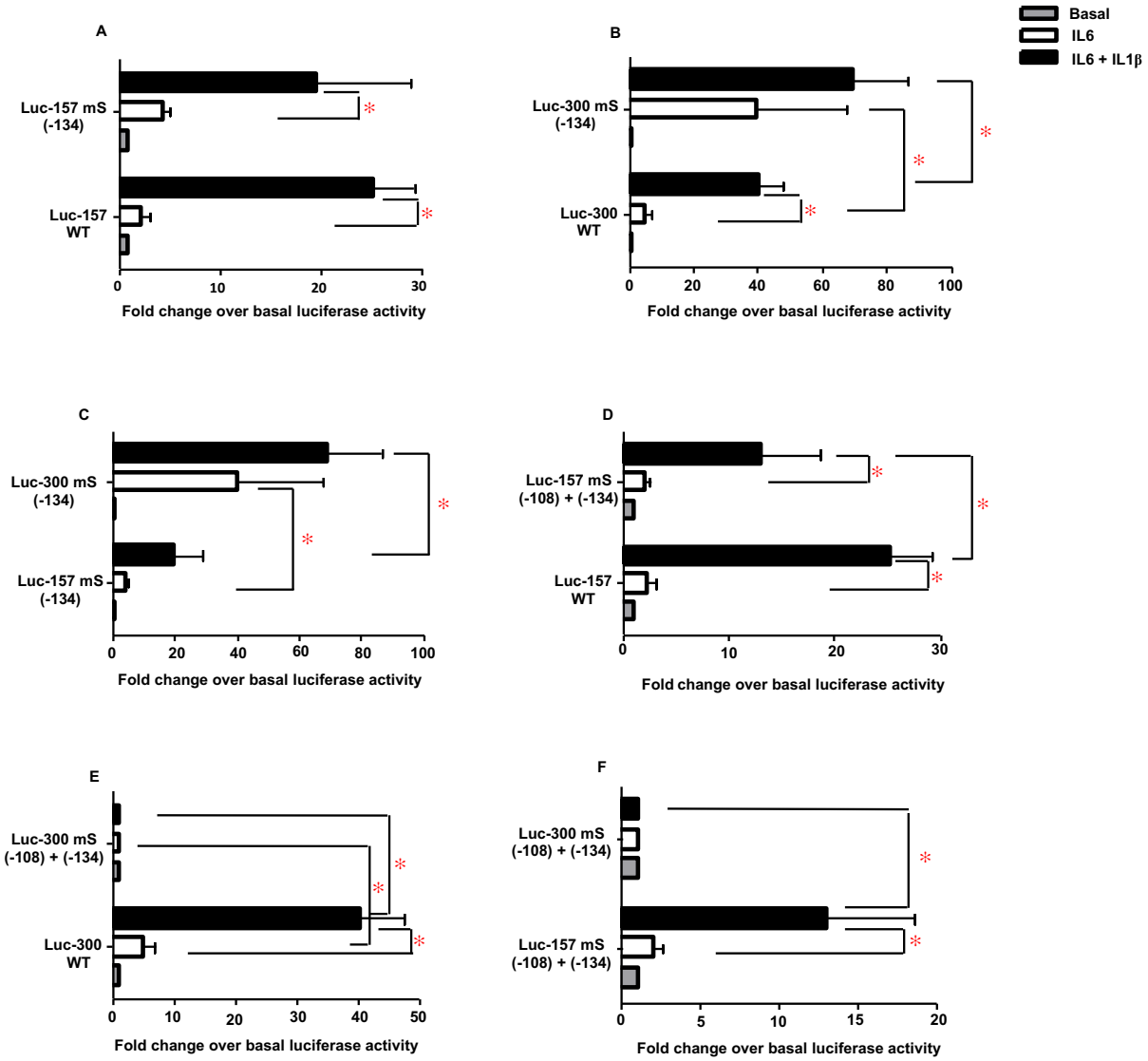

Figure 4.4: STAT3 binds to its cognate site at position -134 on the CRP promoter and regulates cytokine (IL-6 and IL-6 + IL-1β)-induced CRP expression. (A-C) Luciferase transactivation assay shows the effect of mutated STAT3 site at -134 on cytokine (IL-6 and IL-6 + IL-1β)-induced CRP expression. Hep3B cells were transfected with Luc-157 WT and Luc-157 mS (-134) (A), Luc-300 WT and Luc-300 mS (-134) (B), and Luc-157 mS (-134) and Luc-300 mS (-134) CRP promoter constructs. (D-F) A luciferase transactivation assay, where the effect of mutated STAT3 sites at -108 and -134 on cytokine (IL-6 and IL-6 + IL-1β)-induced CRP expression, is shown. Hep3B cells were transfected with Luc-157 WT and Luc-157 mS (-108) + (-134) (D), Luc-300 WT and Luc-300 mS (-108) + (-134) (E), and Luc-157 mS (-108) + (-134) and Luc-300 mS (-108) + (-134) (F) CRP promoter constructs at 24 h post cytokine treatment and 40 h post transfection, CRP transcription was measured as Luc activity. Fold change over basal luciferase activity is plotted on the *x*-axis. Results are expressed as mean ± SD for three experiments. *p* value of ≤ 0.05 are considered statistically significant (*).

STAT3 binds to its cognate site at -165 but does not participate in the transcriptional activation of CRP gene expression

In order to investigate the role of STAT3 (-165) in cytokine [IL-6 and (IL-6 + IL1-β)] induced CRP expression, we performed Luciferase transactivation assays using Luc 300-WT, and Luc 300-mS (-165) promoter constructs, as well a, CRP promoter constructs with both -108 and -165 STAT3 sites mutated, Luc-300 mS (-108) + (-165). IL-1β-induced CRP expression was similar to basal expression (data not shown). Mutation of STAT3 at -165 in the 300 bp promoter

region, Luc-300 mS (-165) did not affect the cytokine induced CRP expression (Fig 4.5 A). However, mutation of STAT3 at both -108 and -165, significantly reduced (IL-6 + IL-1β)-induced CRP expression by ~75% (*) (Fig 4.5 B), but when compared with mutation of STAT3 at -108 and -134, the cytokine induced CRP expression is significantly greater (Fig 4.5 C).

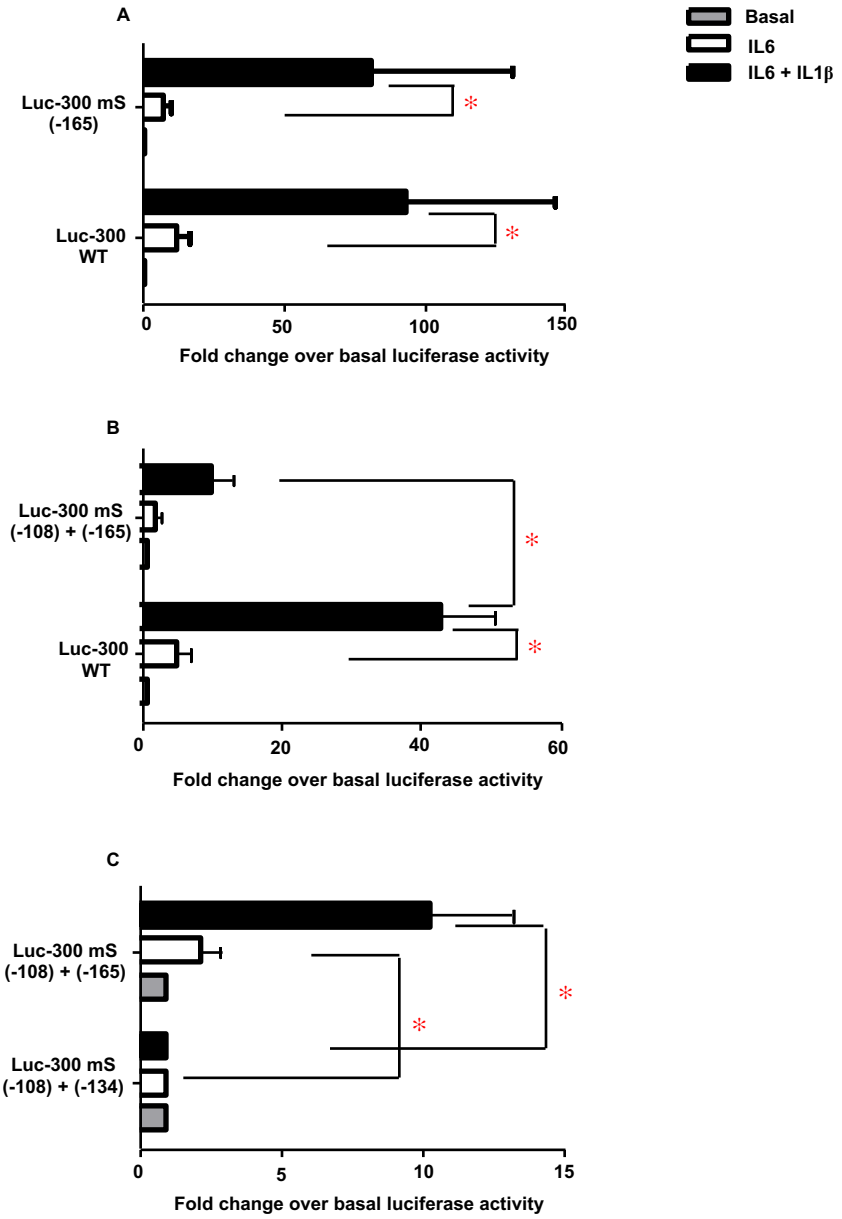

Figure 4.5: STAT3 site at -165 neither activates nor regulates cytokine (IL-6 and IL-6 + IL-1β)-induced CRP expression. Luciferase transactivation assays of Hep3B cells transfected with Luc-300 WT and Luc-300 mS (-165) (A), Luc-300 WT and Luc-300 mS (-108) + (-165) (B), and Luc-300 mS (-108) + (-134) and Luc-300 mS (-108) + (-165) CRP promoter constructs at 24 h post cytokine treatment and 40 h post transfection, CRP transcription was measured as Luc activity. Fold change over basal luciferase activity is plotted on the *x*-axis. Results are expressed as Mean ± SD for three experiments. *p* value of ≤ 0.05 are considered statistically significant (*).

These results indicate that the putative STAT3 site at -165 does not play a significant role in either activating or regulating CRP gene expression as the cytokine induced CRP expression after mutating STAT3 site at -165 was not different than WT. Furthermore, since mutation of STAT3 at -108 alone reduces cytokine induced CRP expression, the effect of abolition of both STAT3 site at -108 and -165 did not contribute enough to the CRP gene expression.

Discussion

The aim of the study was to locate additional transcriptionally active, IL-6-inducible STAT3 binding sites in the -300/+3 region of the CRP promoter. Our major findings were 1) Multiple putative IL-6 inducible STAT3 binding sites, centered at position -72, -134, and -165, -134, are located in the proximal -300 bp region of CRP promoter,. 2) IL-6 activated STAT3 binds to its cognate site at position -134 and -165, in addition to binding to another previously identified site at position -108. 3) STAT3 binds to its cognate site positioned at -165 but it does not activate or regulate CRP gene transcription. 4) Cytokine [IL-6 and (IL-6 + IL-1β)]- induced CRP expression increased dramatically when STAT3 site positioned at -134 was mutated, however, CRP expression curtailed back at basal levels when STAT3 was unable to bind to either of its two sites (-134 and -108) on the CRP promoter. This effect of STAT3 was observed only in the proximal 300 bp region and not in the 157 bp region. Taken together, these data suggest that in addition to transcriptionally active STAT3 site at position -108, STAT3 binds to another site centered at -134 but unlike STAT3 (-108), STAT3 (-134) does not activate transcription but rather regulates the crosstalk of STAT3 (-108) with C/EBPβ (-222) and C/EBPβ-β-NFκB complex (-52/-47) in the -300/+3 region of CRP promoter.

In humans, the acute phase nature of CRP has been observed in various acute and chronic inflammatory states (1-6). Because CRP is a hepatocyte derived protein, the regulation of its synthesis at the transcriptional level has been studied and observed in various hepatocyte derived cell lines such as Hep3B. The activation of CRP gene expression occurs in response to IL-6 and IL-1β wherein IL-6 induces CRP expression via activation and binding of transcription factor C/EBPβ to its sites centered at position -52 and -222 and STAT3 to its site centered at position -

108 respectively, on the CRP promoter (12,13,17, 26, 29). IL-1β alone, in contrast, does not induce CRP expression but rather synergistically enhances IL-6 induced expression via activation and binding of NF-κB to its site centered at position -69 and a nonconsensus κB site centered at position -47 on the CRP promoter (8,9,25). Initially, the proximal 157 bp region of CRP promoter was found to be sufficient to induce CRP expression (9,13) but later it was reported that the proximal 300 bp region induces more CRP expression compared to the 157 bp region alone. One of the possible explanations for the differential induction of CRP expression between the -157/+1 and -300/+3 regions of the promoter can be attributed to the presence of an additional C/EBPβ site at position -222. No additional NF-κB sites have been found between -157 bp and -300 bp region of CRP promoter. Also, in the proximal 300 bp region of the CRP promoter, the presence of additional STAT3 responsive sites have not been sought yet.

In the current study, we found multiple putative IL-6 inducible STAT3 binding sites, located at position -72, -134, and -165 respectively, in addition to the previously reported transcriptionally active STAT3 site at position -108. Out of these newly identified putative binding sites, STAT3 was found to bind to its cognate site at position -134 and -165. Although, STAT3 binds specifically to $TT(N)_4AA$ or $TT(N)_5AA$ motifs, the spacing between the TT and AA core half-sites affects the ability of STAT3 to bind to its responsive elements on the CRP promoter. Other STAT complexes have the ability to bind to $TT(N)_5AA$ motifs while STAT3 binds specifically to $TT(N)_4AA$ motifs (30). This explains the inability of putative STAT3 site positioned at -165 to activate transcription since it contained $TT(N)_5AA$ motif. The other putative STAT3 site at -72 remains to be evaluated and studied further since this area of CRP promoter contains overlapping binding sites for various constitutively active transcription factors such as HNF-1, HNF-3 and a repressive transcription factor Oct-1 along with a NF-κB binding

site (8,12,19,32).

Fig 4.6 depicts our hypothetical model based on the findings in the current study illustrating the role of STAT3 site at position -134 in regulating CRP gene expression. The proposed mechanism of regulation of CRP gene transcription in lieu of STAT3 (-134) is as follows: 1. As shown in Fig 4.5 A, when IL-6 activated STAT3 binds to its cognate site at position -134 and -108, CRP transcription is activated by STAT3 (-108) and other transcription factors; 2. Mutation or abolition of STAT3 (-134) leads to enhanced IL-6 and (IL-6 + IL-1β)-induced CRP expression in contrast to STAT3 (-108) wherein its abolition leads to decreased CRP expression. The effect of mutation or abolition of STAT3 (-108) on CRP expression is observed only in (IL-6 + IL-1β)- induced transcriptional activation and not in IL-6 induced transcriptional activation alone; 3. Also, abolition of both STAT3 binding sites, i.e., STAT3 (-108) and STAT3 (-134) completely diminishes CRP expression down to basal levels. Therefore, STAT3 (-134) acts as a regulatory site for STAT3 (-108) wherein it regulates the crosstalk of STAT3 (-108) with other transcription factors. Since, similar effect of STAT3 (-134) is not observed in proximal 157 bp region, we hypothesize that C/EBPβ site at position -222 is involved in the crosstalk with STAT3 (-108). Along with it, the discrepancy in the IL-6 and (IL-6 +IL-1β)-induced activation of CRP transcription by STAT3 (-108) further raises the possibility of the involvement of NFκB in the crosstalk mechanism since NFκB is the only transcription factor induced by IL-1β; and 4. Taken together, as shown in Fig 4.6 B, the absence of STAT3 (-134) enables STAT3 (-108) to cross talk and form a complex with C/EBPβ (-222) and this STAT3- C/EBPβ complex further cross-talks with C/EBPβ-NFκB complex (-52/-47).

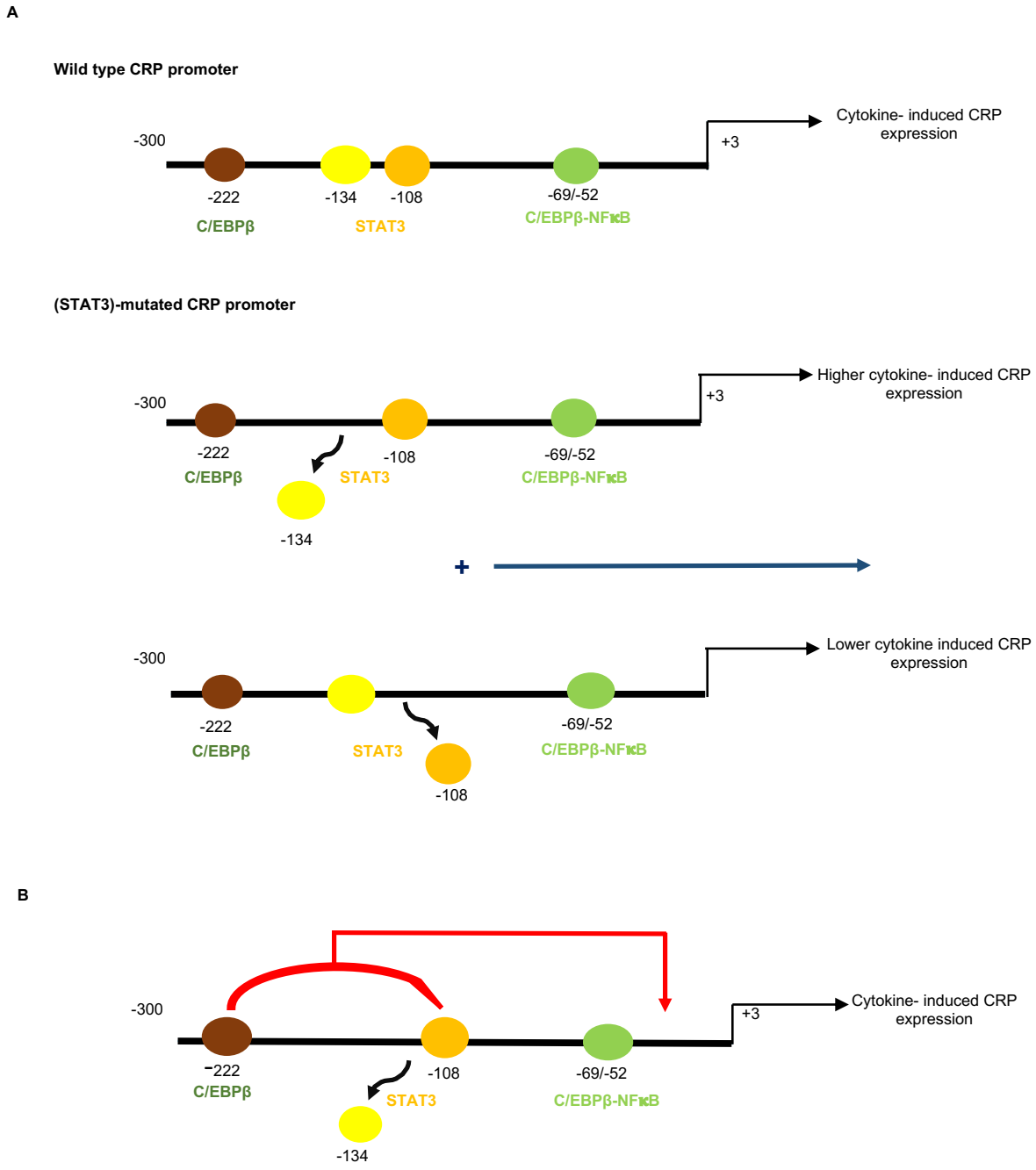

Figure 4.6: A hypothetical model representing the role of STAT3 site at position -134 in regulating CRP expression. (A) Cytokines [IL-6 and (IL-6 + IL-1β)] induce CRP expression of WT promoter (-300/+3) via activation of various transcription factors such as C/EBPβ (-222; brown), STAT3 (-134 & -108; yellow), and C/EBPβ-NFκB complex (-

69/-52; green). Mutation of STAT3 (-134) increases cytokine induced CRP expression while mutation of STAT3 (-108) decreases (IL-6 + IL-1β)-induced CRP expression. (B) Deletion of STAT3 (-134) allows STAT3 (-108) to crosstalk with C/EBPβ (-222) and this C/EBPβ-STAT3 complex further cross-talks with C/EBPβ- NFκB complex (-69/-52). These cross-talks, highlighted in red, mediates cytokine induced CRP expression.

The mechanism of synergy or crosstalk between C/EBPβ, STAT3, and NF-κB has been observed in transactivation of CRP gene expression (33). In addition to CRP gene promoter, synergy between these transcription factors has also been observed to induce expression in promoters of various other model proteins such as synergistic interaction between NF-κB and C/EBPβ (26,27,29,35-37), NF-κB and STAT proteins (37-40), and C/EBPβ and STAT proteins (41-44). Our observation that STAT3- C/EBPβ complex (-222/-108) crosstalk with C/EBPβ-NFκB complex (-52/-47) is based on the previously reported studies that shows that NF-κB p65 inhibits STAT3 dependent activation of gene. Therefore, STAT3 cannot crosstalk with NF-κB site at position -69 since it contains p50-p65 heterodimers. In contrast, NF-κB p50 acts in synergy with STAT3 to activate gene transcription (20) and NF-κB p50 has been reported to form a complex with C/EBPβ on the CRP promoter via the nonconsensus κB site (-47) overlapping the proximal C/EBP binding site (-52) (26). Another critical regulatory region on the CRP promoter that participates in transactivation of CRP gene is the -54 to -74 region, where NF-κB, HNF-1, HNF-3, and Oct-1form complexes. STAT3 has been reported to form a transcriptional complex with c-Fos and HNF-1α that aid in the synergistic induction of CRP gene expression (45). This raises the possibility that STAT3 might be involved in regulating CRP gene expression via the -54 to -74 region. However, this is just a speculation and needs to

be studied in detail further.

In summary, we report another STAT3 binding site at position -134 in addition to the transcriptionally active STAT3 site at position -108 and in contrast to STAT3 (-108) that activates transcription of the CRP gene, STAT3 (-134) regulates CRP transcription by regulating the STAT3 (-108). This study also provides a proof of principle for a possible mechanism of crosstalk between STAT3 (-108), C/EBPβ (-222) and C/EBPβ-NF-κB p50 (-52/-47). Further studies using overexpressed STAT3 would provide more insight into the mechanism of activation and transcriptional regulation of CRP gene by STAT3. Also, future studies at chromatin levels need to be addressed as transiently transfected promoter constructs are not appropriate models for endogenous genes due to the packaging of these genes in chromatin structures (46).

Acknowledgement

The work was supported by NIH Grant: R01 AR068787 (Agrawal ; P.I.)

Abbreviations

CRP	C-reactive protein
C/EBP	CCAAT/enhancer-binding protein
IL-6	Interleukin-6
IL-1β	Interleukin-1β
Luc	Luciferase
NF-κB	Nuclear factor kappaB
Oligo	Oligonucleotide
WT	Wild-type
STAT	Signal inducers and activators of transcritption

References

1. Kushner, I., D. Rzewnicki, D. Samols. 2006. What does minor elevation of C-reactive protein signify?.Am. J. Med. **119**: 166.e17-166.e28.
2. Agrawal, A. 2005. CRP after 2004. Mol. Immunol. **42**: 927-930.
3. Suresh, M. V., S. K. Singh, D. A. Ferguson, Jr, A. Agrawal. 2006. Role of the property of C-reactive protein to activate the classical pathway of complement in protecting mice from pneumococcal infection. J. Immunol. **176**: 4369-4374.
4. Agrawal, A., Singh, P.P., Bottazzi, B., Garlanda, C., Mantovani, A. 2009. Pattern recognition by pentraxins. *Adv Exp Med Biol*. **653**: 98-116.
5. Jialal, I., Devaraj, S., Venugopal S.K. 2004. C-reactive protein: risk marker or mediator in atherothrombosis?. *Hypertension*. **44**: 6-11.
6. Ridker, P.M., Hennekens, C.H., Buring, J.E., Rifai, N. 2000. C-reactive protein and other markers of inflammation in the prediction of cardiovascular disease in women. *N Engl J Med*. **342**: 836-843.
7. Singh, P.P., Voleti, B., Agrawal, A. 2007. A novel RBP-Jκ- dependent switch from C/EBPβ to C/EBPζ at the C/EBP binding site on the C-reactive protein promoter. *J Immunol*. **178(11)**: 7302-7309.
8. Voleti, B., Agrawal, A. 2005. Regulation of Basal and Induced Expression of C-Reactive Protein through an Overlapping Element for OCT-1 and NF-κB on the Proximal Promoter. *J. Immunol.* **175 (5)**: 3386-3390.
9. Zhang, D., Jiang, S.L., Rzewnicki, D., Samols, D., Kushner, I. 1995. The effect of interleukin-1 on C-reactive protein expression in Hep3B cells is exerted at the transcriptional level. *Biochem J*. **310**: 143–148.

10. Goldberger, G., Bing, D.H., Sipe, J.D., Rits, M., Colten, H.R. 1987. Transcriptional regulation of genes encoding the acute-phase proteins CRP, SAA, and C3. *J Immunol.* **138**: 3967–3971.

11. Ochrietor, J.D., Harrison, K.A., Zahedi, K., Mortensen, R.F. 2000. Role of STAT3 and C/EBP in cytokine-dependent expression of the mouse serum amyloid P-component (SAP) and C-reactive protein (CRP) genes. *Cytokine*. **12**: 888–899.

12. Li, S.P., Goldman, N.D. 1996. Regulation of human C-reactive protein gene expression by two synergistic IL-6 responsive elements. *Biochemistry*. **35**: 9060–9068.

13. Zhang, D., Sun, M., Samols, D., Kushner, I. 1996. STAT3 participates in transcriptional activation of the C-reactive protein gene by interleukin-6. *J Biol Chem*. **271**: 9503–9509.

14. Wang, Y., Ripperger, J., Fey, G.H., Samols, D., Kordula, T., Wetzler, M., van Etten, R.A., Baumann, H. 1999. Modulation of hepatic acute phase gene expression by epidermal growth factor and Src protein tyrosine kinases in murine and human hepatic cells. *Hepatology*. **30**: 682–697.

15. May, P., Schniertshauer, U., Gerhartz, C., Horn, F., Heinrich, P.C. 2003.Signal transducer and activator of transcription STAT3 plays a major role in gp130-mediated acute phase protein gene activation. *Acta Biochim Pol*. **50**: 595–601.

16. Ganapathi, M.K., Rzewnicki, D., Samols, D., Jiang, S.L., Kushner, I. 1991. Effect of combinations of cytokines and hormones on synthesis of serum amyloid A and C-reactive protein in Hep 3B cells. *J Immunol*. **147**: 1261–1265.

17. Ganter, U., Arcone, R., Toniatti, C., Morrone, G., Ciliberto, G. 1989. Dual control of C-reactive protein gene expression by interleukin-1 and interleukin-6. *EMBO J.* **8**: 3773–3779.

18. Castell, J. V., M. J. Gomez-Lechon, M. David, R. Fabra, R. Trullenque, P. C. Heinrich. 1990. Acute-phase response of human hepatocytes: regulation of acute-phase protein synthesis by interleukin-6. Hepatology. **12**: 1179-1186.

19. Toniatti, C., Demartis, A., Monaci, P., Nicosia, A., Ciliberto, G. 1990. Synergistic trans-activation of the human C-reactive protein promoter by transcription factor HNF-1 binding at two distinct sites. *EMBO J.* **9**: 4467–4475.

20. Yoshida, Y., Kumar, A., Koyama, Y., Peng, H., Arman, A., Boch, J.A., Auron, P.E. 2004. Interleukin 1 activates STAT3/Nuclear Factor-κB cros-talk via a unique TRAF6- and p65-dependent mechanism. *J Biol Chem*. **279 (3**): 1768-1776.

21. Zhong Z., Wen Z., Darnell J. E. Jr. 1994. Stat3: a STAT family member activated by tyrosine phosphorylation in response to epidermal growth factor and interleukin-6. *Science.* **264***:* 95–98.

22. Wegenka, U.M., Buschmann, J., Lütticken, C., Heinrich, P.C, Horn, F. 1983. Acute-phase response factor, a nuclear factor binding to acute-phase response elements, is rapidly activated by interleukin-6 at the posttranslational level. *Mol Cell Biol*. **13**: 276-278.

23. Oliviero, S., Cortese, R. 1989. The human haptoglobin gene promoter: interleukin-6-responsive elements interact with a DNA-binding protein induced by interleukin-6. *EMBO J*. **8(4)**: 1145-1151.

24. Bao, J.J., Sifers, R.N., Kidd, V.J., Ledley, F.E., Woo, S.L.C. 1987. Molecular evolution of serpins: homologous structure of the human alpha 1-antichymotrypsin and alpha 1-antitrypsin genes. *Biochemistry*. **26**: 7755-7799.

25. Cha-Molstad, H., Agrawal, A., Zhang, D., Samols, D., Kushner, I. 2000. The rel family member p50 mediates cytokine-induced C-reactive protein expression by a novel

mechanism. *J. Immunol*. **165**: 4592-4597.

26. Agrawal, A., H. Cha-Molstad, D. Samols, and I. Kushner. 2001. Transactivation of C-reactive protein by IL-6 requires synergistic interactions of CCAAT/enhancer binding protein β (C/EBPβ) and Rel p50. *J. Immunol*. **166**: 2378-2384.
27. Agrawal, A., D. Samols, and I. Kushner. 2003. Transcription factor c-Rel enhances C-reactive protein expression by facilitating the binding of C/EBPβ to the promoter. *Mol. Immunol*. **40**: 373-380.
28. Kleemann, R., P. P. Gervois, L. Verschuren, B. Staels, H. M. G. Princen, and T. Kooistra. 2003. Fibrates down-regulate IL-1-stimulated C-reactive protein gene expression in hepatocytes by reducing nuclear p50-NF-κB-C/EBPβ complex formation. *Blood.* **101**: 545-551.
29. Majello, B., Arcone, R., Toniatti, C., Ciliberto, G. 1990. Constitutive and IL-6-induced nuclear factors that interact with the human C-reactive protein promoter. *EMBO J.* **9:** 457– 65.
30. Seidel, H.M., Milocco, L.H., Lamb, P., Darnell Jr, J.E., Stein, R.B., Rosen, J. 1995. Spacing of palindromic half sites as a determinant of selective STAT (signal transducers and activators of transcription) DNA binding and transcriptional activity. *Proc Natl Acad Sci USA*. 92: 3041-3045.
31. Murphy, C., Beckers, J., Rüther, U. 1995. Regulation of the human C-reactive protein in transgenic mice. *J Biol Chem*. **270(2):** 704-708.
32. Voleti, B., Hammond Jr, D., Thirumalai, A., Agrawal, A. 2012. Oct-1 acts as a transcriptional repressor on the C-reactive protein promoter. *Mol Immunol.* **52:** 242-248
33. Agrawal, A., Cha-Molstad, H, Samols, D., Kushner, I. 2003. Overexpressed nuclear

factor-κB can participate in endogenous C-reactive protein induction, and enhances the effects of C/EBPβ and signal transducer and activator of transcription-3. *Immunology*. **108 (4):** 539-547.

34. LeClair, K.P., Blanar, M.A., Sharp, P.A. 1992. The p50 subunit of NF-κB associates with the NF-IL6 transcription factor. *Proc Natl Acad Sci USA*. **89:** 8145– 9
35. Stein, B., Cogswell, P.C., Baldwin, A.S. 1993. Functional and physical associations between NF-κB and C/EBP family members: a Rel domain–bZIP interaction. *Mol Cell Biol*. **13:** 3964– 74
36. Xia, C., Cheshire, J.K., Patel, H., Woo, P.1997. Cross-talk between transcription factors NF-κB and C/EBP in the transcriptional regulation of genes. *Int J Biochem Cell Biol* 1997. **29:** 1525– 39.
37. Watchorn, T.M., Waddell, I.D., Dowidar, N., Ross, J.A. 2001. Proteolysis-inducing factor regulates hepatic gene expression via the transcription factors NF-κB and STAT3. *FASEB J*. **15**: 562– 564.
38. Ohmori, Y., Schreiber, R.D., Hamilton, T.A. 1997. Synergy between interferon-γ and tumor necrosis factor-α in transcriptional activation is mediated by cooperation between signal transducer and activator of transcription 1 and nuclear factor κB. *J Biol Chem.* **272:** 14899– 907.
39. Musikacharoen, T., Matsuguchi, T., Kikuchi, T., Yoshikai, Y. 2001. NF-κB and STAT5 play important roles in the regulation of mouse toll-like receptor 2 gene expression. *J Immunol*. **166:** 4516– 24.

40. Shen, C., Stavnezer, J. 1998. Interaction of STAT6 and NF–κB: direct association and synergistic activation of interleukin-4-induced transcription. *Mol Cell Biol*. **18:** 3395– 404.

41. Pietrangelo, A., Dierssen, U., Valli, L., Garuti, C., Rump, A., Corradini, E., Ernst, M., Klein, C., Trautwein, C. 2007. STAT3 is required for IL-6-gp130-dependent activation of Hepcidin in vivo. *Gastroenterology*. **132 (1):** 294-300.

42. Mikita, T., Kurama, M., Schindler, U. 1998. Synergistic activation of the germline ε promoter mediated by Stat6 and C/EBPβ. J Immunol. **161(4):** 1822-1828.

43. Kordula, T., Travis, J. 1996. The role of Stat and C/EBP transcription factors in the synergistic activation of rat serine protease inhibitor-3 gene by IL-6 and dexamethasone. *Biochem J*. **313(3):** 1019-1027.

44. Niehof, M., Streete, K., Rakemann, T., Bischoff, S.C., Mann, M.P., Friedemann, H., Trautwein, C. 2001. Interleukin-6 induced tethering of STAT3 to the LAP/C/EBPβ promoter suggests a new mechanism of transcriptional regulation by STAT3. *J Biol Chem*. **276:** 9016-9027.

45. Nishikawa, T., Hagihara, K., Serada, S., Tomoyasu, I., Atsumi, M., Song, J., Tanaka, T., Kawase, I., Naka, T., Yoshizaki, K. 2008. Transcriptional complex formation of c-Fos, STAT3, and Hepatocyte NF-1α is essential for cytokine-driven C-reactive protein gene expression. J Immunol. **180(5)**: 3492-3501.

46. Smith, C.L., Hager, G.L. 1997. Transcriptional regulation of mammalian genes in vivo. A tale of two templates. *J Biol Chem.* **272(44):** 27493-27496.

CHAPTER 5

SUMMARY

The major findings of our studies were:

1. A non-native pentameric CRP, F66A/T76Y/E81A mutant CRP, created by site-directed mutagenesis, binds to atherogenic LDL at physiological pH, i.e, it does not need the presence of an acidic environment to do so unlike native pentameric CRP.
2. F66A/T76Y/E81A mutant CRP demonstrated protection against atherosclerosis by decreasing the extent of atherosclerotic lesions along the aorta and slowing the progression of the disease. This atheroprotective effect of mutant CRP was observed in a site-specific manner as it showed an effect on lesion area in the whole aorta of HFD-fed $LDLR^{-/-}$ mice but had no effect on the size of atherosclerotic lesions in the aortic root.
3. Administration of F66A/T76Y/E81A mutant CRP did not affect the lipoprotein, i.e., HDL and LDL profile of HFD-fed $LDLR^{-/-}$ mice. Therefore, non-native pentameric human CRP that is a structurally altered form of native pentameric human CRP, is an atheroprotective molecule.
4. CRP from an evolutionary distant species *Limulus Polyphemus, Limulus* CRP, is different than native pentameric human CRP. *Limulus* CRP is a 300 kDa protein that exists as a dodecamer with two rings of six subunits each with differential glycosylation patterns, as opposed to human CRP which is a 120 kDa pentameric, non-glycosylated protein.
5. *Limulus* CRP exists in different isoforms that possess differential affinities for PCh and PEt containing ligands. *Limulus* CRP, purified either by PCh or by PEt, can recognize and bind to immobilized, denatured, and aggregated proteins in a calcium independent manner, at physiological pH.

6. The ligand recognition function of *Limulus* CRP is different than native pentameric human CRP but overlaps that of the non-native pentameric human CRP.
7. Therefore, ancient CRP such as *Limulus* CRP, inherently had the ability to bind to pathogenic proteins in a physiological environment. However, over the course of evolution, the structure of CRP changed and in order for CRP to recognize and bind to such pathogenic and toxic proteins an acidic or inflammatory environment was needed.
8. The proximal 300 bp region of human CRP promoter elicits a higher IL-6 mediated response when compared to the proximal 157 bp region. The proximal 300 bp region was found to contain three putative STAT3 binding sites, centered at position -165, -134, and -72, in addition to the known transcriptionally active site at position -108.
9. Amongst the identified, putative STAT3 binding sites, IL-6 activated STAT3 was found to bind to its cognate site at positions -134 and -165, in addition to binding to another previously identified site at position -108.
10. Cytokine [IL-6 and (IL-6 + IL-1β)]- induced CRP expression was shown to increase dramatically when STAT3 was unable to bind to its site positioned at -134, however, CRP expression curtailed back at basal levels when STAT3 was unable to bind to either of its two sites (-134 and -108) on the CRP promoter. This effect was observed only in the proximal 300 bp region and not in the 157 bp region. Taken together, these data suggest that in addition to transcriptionally active STAT3 site at position -108, STAT3 binds to another site centered at -134 but unlike STAT3 (-108), STAT3 (-134) does not activate transcription but rather regulates the cross-talk of STAT3 (-108) with possibly, C/EBPβ (-222) and C/EBP-β-NFκB complex (-52/-47) in the -300/+3 region of CRP promoter.

CRP has been linked to atherosclerosis, a chronic inflammatory disease, in terms of higher circulating levels, deposition at atherosclerotic lesion, and co-localization with LDL and macrophages within lesions. To elucidate the role of CRP as either a pro-atherogenic protein or an anti-atherosclerotic protein, various studies were performed using different animal models of atherosclerosis wherein native CRP was administered either passively or transgenically. In all studies, CRP was found to be neither pro-atherogenic nor anti-atherosclerotic with the exception of one study (84), where CRP was shown to slow the progression of the disease.

Human CRP has been shown to exists in two pentameric structural conformations, native and non-native and the ligand recognition functions of these two structural conformations differ. A micro-inflammatory environment is required by CRP to change its structure from a native pentameric state to a non-native pentameric state, that can be achieved *in vitro* by exposure to biological modifiers such as hydrogen peroxide, hypochlorous acid or even acidic pH, but this structural change is reversible at physiological pH. Non-native pentameric CRP acquires the property to recognize and bind to immobilized, aggregated, and pathogenic proteins as opposed to native pentameric CRP. Previous lab studies have shown that native CRP binds to E-LDL at physiological pH and this CRP-E-LDL complex prevents foam cell formation (88). However, it does not bind to ox-LDL unless the LDL is sufficiently oxidized to expose its PCh moieties. Non-native CRP binds to E-LDL with higher avidity compared to native CRP and binds to ox-LDL irrespective of the extent of oxidation.

Atherosclerotic lesions are often characterized as inflammatory sites wherein acidic pH predominates along with changes in the redox environment due to free radical generation. Further extending our current understanding of the role of CRP in atherosclerosis is the fact that the disease development differs between animal models and humans. This raises the possibility

that the atherosclerotic lesions in animal models might lack a suitable acidic micro-environment necessary for native CRP to undergo the required structural change and therefore, could not bind to atherogenic LDL. In this study, we used a modified CRP, F66A/T76Y/E81A (mutant CRP), created by site-directed mutagenesis, that binds to atherogenic LDL without the requirement of an acidic pH and we found that this mutant CRP delays and inhibits the progression of atherosclerosis in a site specific manner using $LDLR^{-/-}$ mouse models.

This study provides a proof of principle for the atheroprotective ability of CRP, wherein non-native CRP can be used as a novel therapeutic tool for treatment against atherosclerosis. One of the drawbacks of this study is that it is a single dose-one regimen model. There is a possibility that the amount of CRP administered was inadequate and CRP was not able to display an affect in its full capability, as we observed a site-specific atheroprotective effect. Future studies employing a non-native CRP transgenic mouse model on $LDLR^{-/-}$ background may provide further validation of the atheroprotective ability of this molecule along-with a comparative study using another atherosclerosis mouse model such as HFD-fed $ApoE^{-/-}$ mice. Another drawback is that no mechanism of action regarding how CRP affected the development and progression of atherosclerosis could be defined. The proposed mechanism of action is that non-native CRP recognizes and binds to modified LDL and prevents foam cell formation by blocking their uptake by macrophages. Further studies to support the proposed mechanism of action and to define other potential mechanisms that are responsible for the observed protective effect of CRP in atherosclerosis, are required. Atherosclerosis, being a major cause of cardiovascular mortality in developed countries, and inflammation playing a major role in it, constantly compels the need to find alternative treatments as available treatments such as statins or other cholesterol lowering drugs presents with side-effects and the natural treatment provide with contradictory results.

Using a slightly altered component of the immune system itself, as a therapeutic molecule might prove to be beneficiary.

CRP is an evolutionarily conserved protein that has been found in every organism where its presence has been sought. Over the course of evolution, the structure of CRP changed. Based on our finding in the study above, that a non-native pentameric human CRP acts as an atheroprotective molecule, it is imperative to understand the evolution of the structural change of CRP. Therefore, a parallel comparison of structure-function relationship of CRP between an evolutionary distant specie and humans would be useful. The conservation of CRP amongst various species across the animal phyla, led us to conclude that CRP is an important molecule of the immune system as it evolved along with the development of the entire immune system in terms of its structure and function. The sites that are relevant for the function of CRP, such as PCh-binding site, C1q-binding site, and an intrinsically disordered region, are also conserved amongst different species.

Using *Limulus polyphemus* as a model invertebrate organism that is also an evolutionary distant species, we studied the evolution of function CRP in terms of its structure. Unlike human CRP, *Limulus* CRP is a glycosylated protein that has varying affinities for PCh and PEt ligands. Surprisingly, human CRP do possess sites of glycosylation but they are hidden in its native conformation and therefore provide no functional advantage to native CRP. *Limulus* CRP is known to exist in three isoforms due to variable glycosylation (54). The isoform of *Limulus* CRP that has higher affinity for PCh was called as CRP-I (PCh-binding *Limulus* CRP) and the one that has higher affinity for PEt was called CRP-II (PEt-binding *Limulus* CRP). In order to see if these carbohydrate moieties have any role in the structure-ligand function of *Limulus* CRP, we de-glycosylated both CRP-I and CRP-II and found that the ability of these proteins to recognize

and bind to immobilized, denatured and aggregated proteins significantly decreased (approximately 100 fold) when compared to its glycosylated counterparts. However, upon exposure to acidic environment, they regained their ligand-recognition function. Therefore, de-glycosylated *Limulus* CRP behaves similar to native human CRP and native glycosylated *Limulus* CRP behaves similar to non-native human pentameric CRP. We conclude that though the ligand-binding properties of *Limulus* CRP are not identical to that of native human CRP, they overlap the ligand-binding properties of non-native pentameric human CRP that can be generated in inflammatory microenvironments. Also, changing the glycosylation state of *Limulus* CRP, alters its ligand-binding property to overlap with that of native human CRP.

The drawback of our study is that we could not de-glycosylate the protein completely and hence, could not understand the importance of the presence of carbohydrate moieties on the protein, since glycosylation is the major aspect where *Limulus* CRP differs from human CRP. Additionally, the enhanced ability of *Limulus* CRP to recognize and bind pathogenic proteins, in the presence of an acidic environment could not be understood. Further studies are required to understand the ligand-recognition functions between human CRP and *Limulus* CRP, in lieu of the glycosylation pattern along-with the presence of an acidic environment. In our study above, we showed the atheroprotective ability of a non-native pentameric human CRP whose ligand recognition functions parallels with native *Limulus* CRP. These effector functions of CRP that lies downstream of the recognition functions are dependent on the structural changes in the protein. Studies on structure-function relationships of CRP from most species is unknown and more studies are required from all species including invertebrate and vertebrate in order to have a complete understanding of the evolution of this protein.

Over the course of evolution, in addition to the structure, it appears that the gene expression of CRP changed from a constitutive protein to an acute phase protein. The concentration of CRP increases drastically, from several hundred to thousand fold, following an inflammatory stimulus. The regulation of CRP gene expression occurs at transcriptional level via various cytokine induced and constitutively active transcription factors. Since, CRP is a hepatocyte derived protein, various hepatic cell lines have been used to study its gene expression. Hep3B is the most commonly used cell line and the major cytokines that drive CRP transcription in these cell lines are IL-6 and IL-1β. IL-6 alone, or in synergy with IL-1β induces CRP expression. The proximal 157 bp region of the CRP promoter has been shown to be sufficient to induce CRP transcription in response to IL-6. We recently found that the proximal 300 bp region of the CRP promoter elicits a greater IL-6 response compared to the 157 bp region.

A previous study identified STAT3, an IL-6 inducible transcription factor, in activating CRP gene transcription via binding to its site at position -108 on the promoter (83). In this study, we identified multiple IL-6 inducible STAT3 binding sites on the proximal 300 bp region of CRP promoter. We found that, in addition to transcriptionally active STAT3 site at -108, STAT3 binds to its cognate site at position -134. We propose that instead of activating CRP expression, this site regulates CRP transcription via possibly regulating the cross talk between STAT3 at -108 and other IL-6 and IL-1β inducible transcription factors. This study provides a proof of principle for a possible mechanism of crosstalk between STAT3 (-108), C/EBPβ (-222) and C/EBPβ-NF-κB p50 (-52/-47).

The drawbacks of the study are that these findings are Hep3B cell line specific and studied on a defined, short DNA sequence of CRP promoter. It is possible that the present study for understanding the induction of CRP transcription in response to cytokines might not be

reproducible when using transgenic mice as the defined conditions and cytokine treatments used might not correlate with the physiological system of the transgenic mice (85). In addition, transcription of CRP or any gene occurs via interaction of variable transcription factors that regulates the transcription of the gene either positively or negatively. *In vitro* transcriptional studies using shorter DNA sequences might produce results that could not be reproduced when longer sequences are used, as some regulatory elements might be located several base pairs away (86). Future studies using longer DNA sequences of CRP promoters and overexpressed STAT3 would provide more insight into the mechanism of activation and transcriptional regulation of CRP gene by STAT3. Additionally, these findings need to be reproduced by using other hepatocyte derived cell lines such as HepG2, Huh7, and primary human hepatocytes. Also, future studies at the chromatin levels needs to be addressed as transiently transfected promoter constructs are not appropriate models for endogenous genes due to the packaging of these genes in chromatin structures (87).

REFERENCES

1. Abernethy, T. J., and Avery, O. T. (1941). The occurrence during acute infections of a protein not normally present in the blood: I. Distribution of the reactive protein in patients‟ sera and the effect of calcium on the flocculation reaction with C polysaccharide of Pneumococcus. J. Exp. Med. 73, 173–82.
2. Agrawal, A., Singh, P. P., Bottazzi, B., Garlanda, C., and Mantovani, A. (2009) Pattern recognition by pentraxins. Adv Exp Med Biol 653, 98–116.
3. Volanakis, J.E. and M.H. Kaplan. Specificity of C-reactive protein for choline phosphate residues of pneumococcal C-polysaccharide. Proc Soc Exp Biol Med, 1971. 136(2): p. 612-4.
4. Agrawal, A., et al., Topology and structure of the C1q-binding site on C-reactive protein. J Immunol, 2001. 166(6): p. 3998-4004.
5. Agrawal, A., CRP after 2004. Mol Immunol, 2005. 42(8): p. 927-30.
6. Shrive, A. K., Cheetham, G. M., Holden, D., Myles, D. A., Turnell, W. G., Volanakis, J. E., Pepys, M. B., Bloomer, A. C., and Greenhough, T. J. (1996) Three-dimensional structure of human C-reactive protein. Nat. Struct. Biol. 3, 346–354.
7. Thompson, D., Pepys, M. B., and Wood, S. P. (1999) The physiological structure of human C- reactive protein and its complex with phosphocholine. Struct. London Engl. 1993 7, 169–177.
8. Roux, K. H., Kilpatrick, J. M., Volanakis, J. E., and Kearney, J. F. (1983) Localization of the phosphocholine-binding sites on C-reactive protein by immunoelectron microscopy. J. Immunol. 131, 2411–5.

9. Black, S., Agrawal, A., and Samols, D. (2003) The phosphocholine and the polycation-binding sites on rabbit C-reactive protein are structurally and functionally distinct. Mol. Immunol. 39, 1045–54.
10. Szalai, A. J., Agrawal, A., Greenhough, T. J., and Volanakis, J. E. (1999) C-reactive protein: structural biology and host defense function. Clin. Chem. Lab. Med. 37, 265–70.
11. Agrawal, A., and Volanakis, J. E. (1994) Probing the C1q-binding site on human C-reactive protein by site-directed mutagenesis. J. Immunol. 152, 5404–10.
12. Bang, R., Marnell, L., Mold, C., Stein, M.-P., Clos, K. T. Du, Chivington-Buck, C., and Clos, T. W. Du (2005) Analysis of binding sites in human C-reactive protein for Fc{gamma}RI, Fc{gamma}RIIA, and C1q by site-directed mutagenesis. J. Biol. Chem. 280, 25095–102.
13. Gaboriaud, C., Juanhuix, J., Gruez, A., Lacroix, M., Darnault, C., Pignol, D., Verger, D., Fontecilla-Camps, J. C., and Arlaud, G. J. (2003) The crystal structure of the globular head of complement protein C1q provides a basis for its versatile recognition properties. J. Biol. Chem. 278, 46974–82.
14. Volanakis, J.E., Human C-reactive protein: expression, structure, and function. Mol Immunol, 2001. 38(2-3): p. 189-97.
15. Kaplan, M.H. and J.E. Volanakis, Interaction of C-reactive protein complexes with the complement system. I. Consumption of human complement associated with the reaction of C-reactive protein with pneumococcal C-polysaccharide and with the choline phosphatides, lecithin and sphingomyelin. J Immunol, 1974. 112(6): p. 2135-47.
16. Siegel, J., R. Rent, and H. Gewurz, Interactions of C-reactive protein with the complement system. I. Protamine-induced consumption of complement in acute phase

sera. J Exp Med, 1974. 140(3): p. 631-47.

17. Singh, S.K., Thirumalai, A., Pathak, A., Ngwa, D.N., Agrawal, A. Functional transformation of C-reactive protein by hydrogen peroxide. J Biol Chem. 292(8): 3129-3136.
18. Agrawal, A., Suresh, M.V, Singh, S.K., Ferguson, D.A. Jr. The protective function of human C-reactive protein in mouse models of *Streptococcus pneumoniae* infection. Endor Metab Immune Disord Drug Targets, 2008. 8:231-237.
19. Suresh, M.V., Singh, S.K., Ferguson, D.A. Jr, Agrawal, A. Human C-reactive protein protects mice from *Streptococcus pneumoniae* infection without binding to pneumococcal C-polysaccharide. J Immunol, 2007. 178:1158-1163.
20. Gang, T.B., Hammond D.J. Jr, Singh, S.K., Ferguson, D.A. Jr, Mishra, V.K., Agrawal, A. The phosphocholine binding pocket on C-reactive protein is necessary for initial protection of mice against pneumococcal infection. J Biol Chem, 2012. 287:43116-43125.
21. Gang, T.B., Hanley, G.A., Agrawal, A. C-reactive protein protects mice against pneumococcal infection via both phosphocholine-dependent and phosphocholine-independent mechanisms. Infect Immun, 2015. 83:1845-1852.
22. Ngwa, D.N., Agrawal, A. Structure-function relationships of C-reactive protein in bacterial infection. Front Immunol, 2019. 10:166.
23. Szalai, A.J., et al., Human C-reactive protein is protective against fatal Salmonella enterica serovar typhimurium infection in transgenic mice. Infect Immun, 2000. 68(10): p. 5652-6.

24. Libby, P. and P.M. Ridker, Inflammation and atherosclerosis: role of C-reactive protein in risk assessment. Am J Med, 2004. 116 Suppl 6A: p. 9S-16S.
25. Bhakdi, S., et al., Possible protective role for C-reactive protein in atherogenesis: complement activation by modified lipoproteins halts before detrimental terminal sequence. Circulation, 2004. 109(15): p. 1870-6.
26. Kovacs, A., et al., Human C-reactive protein slows atherosclerosis development in a mouse model with human-like hypercholesterolemia. Proc Natl Acad Sci U S A, 2007. 104(34): p. 13768-73.
27. Rodriguez, W., et al., Prevention and reversal of nephritis in MRL/lpr mice with a single injection of C-reactive protein. Arthritis Rheum, 2006. 54(1): p. 325-35.
28. Yang, J., et al., Human C-reactive protein binds activating Fcgamma receptors and protects myeloma tumor cells from apoptosis. Cancer Cell, 2007. 12(3): p. 252-65.
29. Kushner, I., The phenomenon of the acute phase response. Ann N Y Acad Sci, 1982. 389: p. 39-48.
30. Kushner, I. and G. Feldmann, Control of the acute phase response. Demonstration of C-reactive protein synthesis and secretion by hepatocytes during acute inflammation in the rabbit. J Exp Med, 1978. 148(2): p. 466-77.
31. Pepys, M. B., and Hirschfield, G. M. (2003) C-reactive protein: a critical update. J. Clin. Invest. 111, 1805–12
32. Gabay, C., and Kushner, I. (1999) Acute-phase proteins and other systemic responses to inflammation. N. Engl. J. Med. 340, 448–54
33. Kushner, I., and Elyan, M. (2008) Why does C-reactive protein predict coronary events? Am. J. Med. 121(7), e11.

34. Agrawal, A., Hammond, D. J., and Singh, S. K. (2010) Atherosclerosis-related functions of C- reactive protein. Cardiovasc. Hematol. Disord. drug targets. 10, 235–240

35. Moore, K. J., and Tabas, I. (2011) Macrophages in the pathogenesis of atherosclerosis. *Cell* **145**, 341–55.

36. Leake, D. S. (1997) Does an acidic pH explain why low density lipoprotein is oxidised in atherosclerotic lesions? *Atherosclerosis* **129**, 149–57

37. Björnheden, T., Levin, M., Evaldsson, M., and Wiklund, O. (1999) Evidence of hypoxic areas within the arterial wall in vivo. *Arteriosclerosis Thrombosis and Vascular Biology* **19**, 870–76

38. Sneck, M., Kovanen, P. T., and Oörni, K. (2005) Decrease in pH strongly enhances binding of native, proteolyzed, lipolyzed, and oxidized low density lipoprotein particles to human aortic proteoglycans. *The Journal of Biological Chemistry* **280**, 37449–54

39. Haka, A. S., Grosheva, I., Chiang, E., Buxbaum, A. R., Baird, B. A., Pierini, L. M., and Maxfield, F. R. (2009) Macrophages create an acidic extracellular hydrolytic compartment to digest aggregated lipoproteins. *Molecular Biology of the Cell* **20**, 4932–40

40. Naghavi, M., John, R., Naguib, S., Siadaty, M. S., Grasu, R., Kurian, K. C., Van Winkle, W. B., Soller, B., Litovsky, S., Madjid, M., Willerson, J. T., and Casscells, W. (2002) pH Heterogeneity of human and rabbit atherosclerotic plaques; a new insight into detection of vulnerable plaque. *Atherosclerosis* **164**, 27–35

41. Silver, I. A., Murrills, R. J., and Etherington, D. J. (1988) Microelectrode studies on the acid microenvironment beneath adherent macrophages and osteoclasts. *Experimental Cell Research* **175**, 266–76

42. Bhakdi, S., Torzewski, M., Klouche, M., and Hemmes, M. (1999) Complement and atherogenesis: binding of CRP to degraded, nonoxidized LDL enhances complement activation. Arterioscler. Thromb. Vasc. Biol. 19, 2348–54.

43. Sun, H., Koike, T., Ichikawa, T., Hatakeyama, K., Shiomi, M., Zhang, B., Kitajima, S., Morimoto, M., Watanabe, T., Asada, Y., Chen, Y. E., and Fan, J. (2005) C-reactive protein in atherosclerotic lesions: its origin and pathophysiological significance. Am. J. Pathol. 167, 1139–48.

44. Reynolds, G. D., and Vance, R. P. (1987) C-reactive protein immune-histochemical localization in normal and atherosclerotic human aortas. Arch. Pathol. Lab. Med. 111, 265–269.

45. Hatanaka, K., Li, X. A., Masuda, K., Yutani, C., and Yamamoto, A. (1995) Immuno-histochemical localization of C-reactive protein-binding sites in human atherosclerotic aortic lesions by a modified streptavidin-biotin-staining method. Pathol. Int. 45, 635–41

46. Hammond, D. J., Singh, S. K., Thompson, J. A, Beeler, B. W., Rusiñol, A. E., Pangburn, M. K., Potempa, L. A, and Agrawal, A. (2010) Identification of acidic pH-dependent ligands of pentameric C-reactive protein. *The Journal of Biological Chemistry* 285, 36235–44

47. Hirschfield, G. M., Gallimore, J. R., Kahan, M. C., Hutchinson, W. L., Sabin, C. A., Benson, G. M., Dhillon, A. P., Tennent, G. A., and Pepys, M. B. (2005) Transgenic human C- reactive protein is not pro-atherogenic in apolipoprotein E-deficient mice. Proc. Natl. Acad. Sci. U. S. A. 102, 8309–8314.

48. Ortiz, M. A., Campana, G. L., Woods, J. R., Boguslawski, G., Sosa, M. J., Walker, C. L., and Labarrere, C. A. (2009) Continuously-infused human C-reactive protein is neither

proatherosclerotic nor proinflammatory in apolipoprotein E-deficient mice. Exp. Biol. Med. 234, 624–631

49. Tennent, G. A., Hutchinson, W. L., Kahan, M. C., Hirschfield, G. M., Gallimore, J. R., Lewin, J., Sabin, C. A., Dhillon, A. P., and Pepys, M. B. (2008) Transgenic human CRP is not pro- atherogenic, pro-atherothrombotic or pro-inflammatory in apoE-/- mice. Atherosclerosis 196, 248–55.
50. Torzewski, M., Reifenberg, K., Cheng, F., Wiese, E., Küpper, I., Crain, J., Lackner, K. J., and Bhakdi, S. (2008) No effect of C-reactive protein on early atherosclerosis in LDLR-/-/human C-reactive protein transgenic mice. Thromb. Haemost. 99, 196–201.
51. Daugherty, A. (2002) Mouse models of atherosclerosis. *The American Journal of the Medical Sciences* **323**, 3–10
52. Pathak, A., Agrawal, A. Evolution of C-reactive protein. Front Immunol, 2019. 10:943.
53. Armstrong, P.B. Comparative biology of the pentraxin protein family: evolutionarily conserved component of the innate immune system. Int Rev Cell Mol Biol, 2015. 316: 1-47.
54. Nguyen, N.Y., Suzuki, A., Boykins, R.A., and Liu, T.Y. (1986) The Amino acid sequence of Limulus C-reactive protein. *The Journal of Biological Chemistry* **261**, 10456-65
55. Liu, T.Y., Syin, C., Nguyen, N.Y., Suzuki, A., Boykins, R.A., Lei, K.J., and Goldman, N. (1986) Comparison of Protein Structure and Genomic Structure of Human, Rabbit and Limulus C-Reactive Proteins: Possible Implications for Function and Evolution. *Journal of Protein Chemistry* **6**, 262-71

56. Agrawal, A., Gang, T.B., and Rusiñol, A. (2014) Recognition Functions of Pentameric C-Reactive Protein in Cardiovascular Disease. *Mediators of inflammation*. **2014**

57. Shrive, A.K., Burns, I., Chou, H., Stahlberg, H., Armstrong P.B., and Greenhough T.J. (2009) C-reactive protein and SAP-like pentraxin are both present in Limulus Polyphemus hemolymph - crystal structure of Limulus SAP *Journal of Molecular Biology* **386**, 1240-54.

58. Tharia, H.A., Shrive, A.K., Mills, J.D., Williams, C., and Greenhough, T.J. (2002) Complete cDNA sequence of SAP-like pentraxin from limulus Polyphemus: Implications for pentraxin evolution. *Journal of Molecular Biology* **316,** 583-97.

59. Lee PT, Bird S, Zou J and Martin SAM. (2017) Phylogeny and expression analysis of C-reactive protein (CRP) and serum amyloid-P (SAP) like genes reveal two distinct groups in fish. *Fish and Shellfish Immunology* **65**, 42-51

60. Ceciliani, F., Giordano, A., and Spagnolo, V. (2002) The systemic reaction during inflammation: the acute-phase proteins. *Protein and Peptide Letters* **9**, 211–23.

61. Castell, J. V, Gómez-Lechón, M. J., David, M., Fabra, R., Trullenque, R., and Heinrich, P. C. (1990) Acute-phase response of human hepatocytes: regulation of acute-phase protein synthesis by interleukin-6. *Hepatology* **12**, 1179–86

62. Hurlimann, J., G.J. Thorbecke, and G.M. Hochwald, The liver as the site of C-reactive protein formation. J Exp Med, 1966. 123(2): p. 365-78.

63. Ganapathi, M.K., et al., Effect of combinations of cytokines and hormones on synthesis of serum amyloid A and C-reactive protein in Hep 3B cells. J Immunol, 1991. 147(4): p.1261-5

64. Zhang, D., et al., The effect of interleukin-1 on C-reactive protein expression in Hep3B cells is exerted at the transcriptional level. Biochem J, 1995. 310 (Pt 1): p. 143-8.

65. Taylor, A.W., N.O. Ku, and R.F. Mortensen. Regulation of cytokine-induced human C-reactive protein production by transforming growth factor-beta. J Immunol, 1990. 145(8): p. 2507-13.

66. Yap, S.H., et al., Tumor necrosis factor (TNF) inhibits interleukin (IL)-1 and/or IL-6 stimulated synthesis of C-reactive protein (CRP) and serum amyloid A (SAA) in primary cultures of human hepatocytes. Biochim Biophys Acta, 1991. 1091(3): p. 405-8.

67. Patel, D.N., et al., Interleukin-17 stimulates C-reactive protein expression in hepatocytes and smooth muscle cells via p38 MAPK and ERK1/2-dependent NF-kappaB and C/EBPbeta activation. J Biol Chem, 2007. 282(37): p. 27229-38.

68. Ganter, U., et al., Dual control of C-reactive protein gene expression by interleukin-1 and interleukin-6. Embo J, 1989. 8(12): p. 3773-9.

69. Ochrietor, J. D., Harrison, K. A., Zahedi, K., and Mortensen, R. F. (2000) Role of STAT3 and C/EBP in cytokine-dependent expression of the mouse serum amyloid P-component (SAP) and C-reactive protein (CRP) genes. *Cytokine* **12**, 888–99

70. Poli, V., and Cortese, R. (1989) Interleukin 6 induces a liver-specific nuclear protein that binds to the promoter of acute-phase genes. *Proceedings of the National Academy of Sciences of the United States of America* **86**, 8202–06

71. Ramji, D. P., Vitelli, A., Tronche, F., Cortese, R., and Ciliberto, G. (1993) The two C/EBP isoforms, IL-6DBP/NF-IL6 and C/EBP delta/NF-IL6 beta, are induced by IL-6 to promote acute phase gene transcription via different mechanisms. *Nucleic Acids Research* **21**, 289–94

72. Wang, Y., Ripperger, J., Fey, G. H., Samols, D., Kordula, T., Wetzler, M., Van Etten, R. A., and Baumann, H. (1999) Modulation of hepatic acute phase gene expression by epidermal growth factor and Src protein tyrosine kinases in murine and human hepatic cells. *Hepatology* **30**, 682–97

73. Ganapathi, M. K., Schultz, D., Mackiewicz, A., Samols, D., Hu, S. I., Brabenec, A., Macintyre, S. S., and Kushner, I. (1988) Heterogeneous nature of the acute phase response. Differential regulation of human serum amyloid A, C-reactive protein, and other acute phase proteins by cytokines in Hep 3B cells. *The Journal of Immunology* **141**, 564–69

74. Darlington, G. J., Wilson, D. R., and Lachman, L. B. (1986) Monocyte-conditioned medium, interleukin-1, and tumor necrosis factor stimulate the acute phase response in human hepatoma cells in vitro. *The Journal of Cell Biology* **103**, 787–93

75. Agrawal, A., Cha-Molstad, H., Samols, D., and Kushner, I. (2003) Overexpressed nuclear factor-kB can participate in endogenous C-reactive protein induction, and enhances the effects of C/EBPb and signal transducer and activator of transcription-3. *Immunology* **108**, 539–47

76. Toniatti, C., Demartis, A., Monaci, P., Nicosia, A., and Ciliberto, G. (1990) Synergistic trans- activation of the human C-reactive protein promoter by transcription factor HNF-1 binding at two distinct sites. EMBO J. 9, 4467–75

77. Voleti, B., and Agrawal, A. (2005) Regulation of basal and induced expression of C-reactive protein through an overlapping element for OCT-1 and NF-kappaB on the proximal promoter. J. Immunol. 175, 3386–90

78. Nishikawa, T., Hagihara, K., Serada, S., Isobe, T., Matsumura, A., Song, J., Tanaka, T., Kawase, I., Naka, T., and Yoshizaki, K. (2008) Transcriptional complex formation of c-Fos, STAT3, and hepatocyte NF-1 alpha is essential for cytokine-driven C-reactive protein gene expression. J. Immunol. 180, 3492–501

79. Blaschke, F., Takata, Y., Caglayan, E., Collins, A., Tontonoz, P., Hsueh, W. A., and Tangirala, R. K. (2006) A nuclear receptor corepressor-dependent pathway mediates suppression of cytokine-induced C-reactive protein gene expression by liver X receptor. Circ. Res. 99(12), e88–99.

80. Singh, P.P., Voleti, B., Agrawal, A. A novel RBP-Jκ-dependent switch from C/EBPβ to C/EBPδ at the C/EBP binding site on the C-reactive protein promoter. J Immunol, 2007. 178:7302-09.

81. Voleti, B., Hammond, D.J. Jr, Thirumalai, A., Agrawal, A. Oct-1 acts as a transcriptional repressor on the C-reactive protein promoter. Mol Immunol, 2012. 52:242-248.

82. Cha-Molstad, H., Young, D. P., Kushner, I., and Samols, D. (2007) The interaction of c-Rel with C/EBPb enhances C/EBPb binding to the C-reactive protein gene promoter.*Molecular Immunology* 44, 2933–42

83. Zhang, D., Sun, M., Samols, I., and Kushner, I. (1996) STAT3 Participates in Transcriptional Activation of the C-reactive Protein Gene by Interleukin-6. *The Journal of Biological Chemistry* 271, 9503-09. 271.

84. Kovacs A, Tornvall P, Nilsson R, Tegnér J, Hamsten A, and Björkegren J. Human C-reactive protein slows atherosclerotic development in a mouse model with human-like hypercholesterolemia*. Proc Natl Acad Sci USA*. 2007; 104: 13768-13773.

85. Murphy C, Beckers J, and Rüther U. Regulation of the human C-reactive protein gene in transgenic mice. *J Biol Chem*. 1995; 270: 704-708.

86. Zhang, D., Sun, M., Samols, D., Kushner, I. 1996. STAT3 participates in transcriptional activation of the C-reactive protein gene by interleukin-6. *J Biol Chem*. **271**: 9503–9509.

87. Smith, C.L., Hager, G.L. 1997. Transcriptional regulation of mammalian genes in vivo. A tale of two templates. *J Biol Chem.* 272(44): 27493-27496.

88. Singh, S.K., Suresh, M.V., Praythe r, D.C., Moorman, J.P., Rusiñol, A.E, Agrwal, A. 2008. C-reactive protein bound- enzymatically modified low-density lipoprotein does not transform macrophage into foam cells. *J. Immunol*. **180 (6)**: 4312-66.

APPENDIX

Supplemental data for Chapter 2

CRP is an atheroprotective molecule

Methods

Atherosclerotic lesion measurement in the aorta (*en face*)

Formalin-fixed aortae were cut open longitudinally (*en face*) and pinned flat on a standard black wax dissection pan using 0.15 mm black anodized pins. Pinned aortae were stained with Sudan IV for lipid rich deposits in atherosclerotic lesions. Briefly, aortae were first washed with 1X PBS and then with 70% ethanol for 5 minutes. Aortae were stained with Sudan IV solution [0.5% Sudan IV in an acetone-absolute ethanol solution (1:1)] for 15 minutes and then washed with 80% ethanol for 3 minutes in order to remove background stain. Aortae were then washed with running water followed by 1X PBS. Pinned aortae were digitally photographed. Thus, a total of 120 aortae (60 for untreated group and 60 for mutant-CRP treated group) were processed and stained. The atherosclerotic lesion area (red colored deposits) was determined and measured using ImageJ software.

Aortic root atherosclerotic lesion measurement

For aortic root atherosclerotic lesion measurement, OCT-embedded heart tissue along with aortic root was mounted in a Leica CM1850 cryostat. 8-µm cross-sections were collected starting at the first appearance of the aortic valve leaflets, on a Superfrosted plus microscope slide (Fisher, cat# 12-550-15). Cross-sections were collected until the of the aortic valve leaflets disappearance and alternating cryosections from each mouse were stained with oil-red O for

lipids and counterstained with hematoxylin. Briefly, cryosections were air dried at RT for 30-40 minutes and then incubated in ice-cold neutral-buffered 10% formalin for 10 minutes followed by rinsing using tap water first and then with distilled water (DI). Cryosections were then incubated in 60% isopropanol (diluted with water) for 45 seconds and stained with fresh Oil Red O solution (ORO: Stock ORO - 0.5g ORO powder in 100 ml isopropanol; working ORO- 60 ml stock ORO + 40 ml DI) for 15 minutes under constant, low agitation. Following staining, cryosections were rinsed with 60% isopropanol for 30 seconds first and then twice with DI. Cryosections were counterstained with hematoxylin for 30 seconds and rinsed in running tap water for 3 minutes. Cryosections were then mounted with a water-soluble mounting medium (glycerol gelatin) at 55 ^{o}C. Images were digitally captured with an Olympus BX41 microscope equipped with a MicroPublisher 5.0 RTV CCD color camera (QImaging). Thus, a total of 120 hearts (60 for untreated group and 60 for mutant-CRP treated group) were processed. Approximately 48-72 cross-sections were collected per heart and every alternate cross-section were stained for lipids. Lesions in the aortic root (red colored areas) were measured using the Image-J software. Measurements were performed in a blind fashion.

CRP immunostaining

Cryosections were thawed, air dried for 1 hour and, fixed in ice-cold acetone for 10 minutes. Sections were then washed with 1X PBS for 5 minutes, air dried and circled using a hydrophobic barrier (ImmEdge, Vector laboratories, cat # H-4000). Immunostaining was performed with Vectastain ABC Elite kit (Vector laboratories, cat # PK-6100) and manufacturer's instructions were followed. CRP was detected with Rabbit anti-CRP (Millipore, 10 μg/ml/section). Color was developed using DAB as substrate (Vector laboratories, ImmPACT

DAB, cat # SK-4105). Macrophages were detected with Rabbit anti-CD68 for pan macrophages (ThermoFisher Scientific, cat# PA5-78996; diluted 1:100) and Rabbit anti-CD163 for M2 macrophages (abcam, cat# ab213612; diluted 1:100). Sections were counterstained with methyl green. Images were digitally captured with an Olympus BX41 microscope equipped with a MicroPublisher 5.0 RTV CCD color camera (QImaging).

Measurement of circulating cytokines and CRP in the plasma of LDLR$^{-/-}$ mice

Plasma was collected from whole blood via cardiac puncture at the time of sacrifice using EDTA as an anti-coagulant. Cytokines were measured in the pooled plasma samples, at every given week point, with Bio-plex mouse cytokine group I 8-plex assay kit (Lot # 64140214). Cytokine measured were IL-1β, IL-6, TNF-α, IL-4, IL-10, IL-12, and IFN-γ. Manufacturer's instructions were followed. Mutant CRP levels were measured by ELISA in the plasma samples of five out of twelve randomly selected mice at every given week point. Briefly, microtiter wells were coated with anti-CRP IgG (diluted 1:1000 in 1X TBS) and incubated overnight at 4^0 C. Wells were blocked with TBS containing 0.5% gelatin for 45 minutes followed by addition of pooled plasma samples, diluted in buffer containing 1X TBS, 0.1% gelatin, 0.02% Tween 20 (ELISA buffer, pH 7.2). Wells were incubated with plasma samples for 2 h at 37 °C. After the CRP incubation step, the wells were washed with ELISA buffer and rabbit anti-CRP antibody (Sigma, diluted 1/1000 in ELISA buffer), was used (100 µl/well, 1 h at 37 °C) to detect bound CRP. HRP-conjugated donkey anti-rabbit IgG (GE Healthcare), diluted in ELISA buffer, was used (100 µl/well, 1 h at 37 °C) as the secondary antibody. Color was developed using ABTS as the substrate, and the absorbance was read at 405 nm in a microtiter plate reader (Molecular Devices).

Data Analysis

For atherosclerotic lesion measurement in the whole aorta and aortic root, median total lesion was reported and medians were compared. Data was analyzed using non-parametric test (Mann-Whitney test) using Graphpad Prism software. $p \leq 0.05$ was considered statistically significant. For analysis of circulating cytokines and CRP in the plasma, data is represented as mean $\pm$ standard deviation and unpaired student t-test was used to analyze statistically significant differences. $p \leq 0.05$ was considered statistically significant.

Results

F66A/T76Y/E81A mutant CRP significantly decreased atherosclerotic lesion in the aortae (*en face*) of LDLR$^{-/-}$ mice

To investigate the effect of mutant CRP on the early stages of development of atherosclerosis in LDLR$^{-/-}$ mice, *en face* atherosclerotic lesion area was analyzed. The experiment was performed twice with n=6 mice in each group at every given data collection time point. The data are presented as a combination of two independently performed experiments. Administration of mutant CRP had no effect on the *en face* atherosclerotic lesion at 1, 3, and 5 weeks but, at 7th and 9th week (7 weeks: 8 weeks on high fat diet and 7 weeks of mutant CRP injections, 9 weeks: 10 weeks on high fat diet and 9 weeks of mutant CRP injections), the size of atherosclerotic lesion area in mutant CRP treated mice was significantly lower when compared to the lesion area in untreated mice (Fig A.1). In comparison to the untreated mice, the lesion area was 39% less in mutant CRP treated mice at 7th week ($p = 0.007$) and 42% less in mutant CRP treated mice at 9th week ($p = 0.002$). Also, in untreated group the disease progressed in an incremental manner from week 1 through week 7 and stayed constant until week 9 but similar disease progression was not observed in mutant CRP treated group where the disease progressed from week 1 through week 5 and stayed almost constant until week 9. This data suggest that mutant CRP decreased the atherosclerotic lesion area in the aortae of LDLR$^{-/-}$ mice between 8 and 10 weeks of high fat diet and 7 and 9 weeks of mutant CRP administration and prevented the progression of atherosclerosis after 6 weeks of high fat diet and 5 weeks of mutant CRP administration.

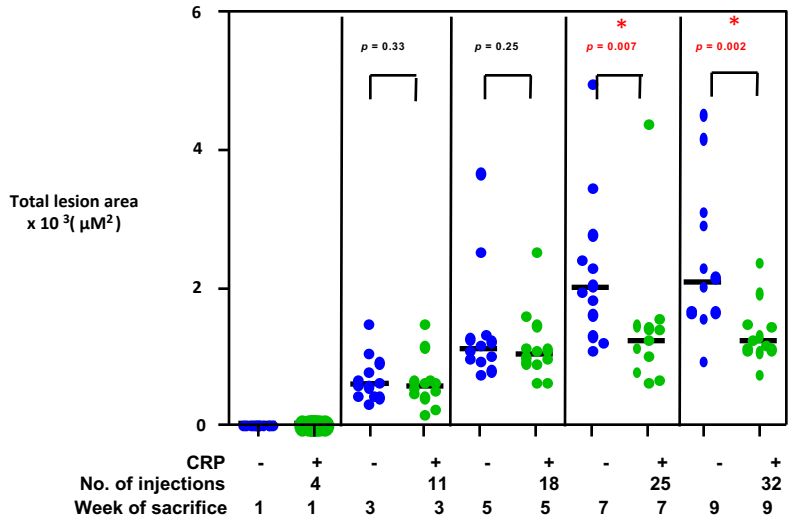

Figure A.1: F66A/T76Y/E81A mutant CRP reduces atherosclerosis in the whole aorta of LDLR$^{-/-}$mice. Quantification of total atherosclerotic plaque or lesion coverage in *en face* aorta specimens from untreated and mutant CRP treated LDLR$^{-/-}$ mice maintained on a high fat diet is shown. The scatterplot represents the quantification of total atherosclerotic lesion coverage in *en face* aorta specimens from untreated and mutant CRP treated LDLR$^{-/-}$ mice. Data were collected at 5 different time points, i.e, 1, 3, 5, 7, and 9 weeks of mutant CRP administration at alternate days (TBS was injected for untreated group). A scatterplot of total atherosclerotic lesion coverage is shown. Each symbol represents the total area of the whole aorta that stained positively for Sudan IV in individual untreated (blue) or mutant CRP treated (green) LDLR$^{-/-}$ mice. Horizontal black lines indicate median total lesion area in the whole aorta for each group of animals. Asterisks (red) denote statistically significant differences between groups (*$p \leq 0.05$).

Statistically significant differences in total lesion coverage is determined by Mann Whitney test.

The aortic root atherosclerotic lesion area of LDLR$^{-/-}$ mice was unaffected by F66A/T76Y/E81A mutant CRP.

Another parameter to investigate effect of mutant CRP on the early stages of atherosclerosis development in LDLR$^{-/-}$ mice was cross-sectional analysis of ORO stained aortic root sections. The experiment was performed twice with n=6 mice in each group at every given week time point. The data are presented as a combination of two independently performed experiments. Mutant CRP did not affect the atherosclerotic lesion area in the aortic root at any given time point specifically. It neither decreased the lesion area nor delayed the progression of the disease, as observed in the first set of experiment (Fig A.2). Hence data suggests that mutant CRP had no effect on the atherosclerotic lesion area in the aortic root of LDLR$^{-/-}$ mice.

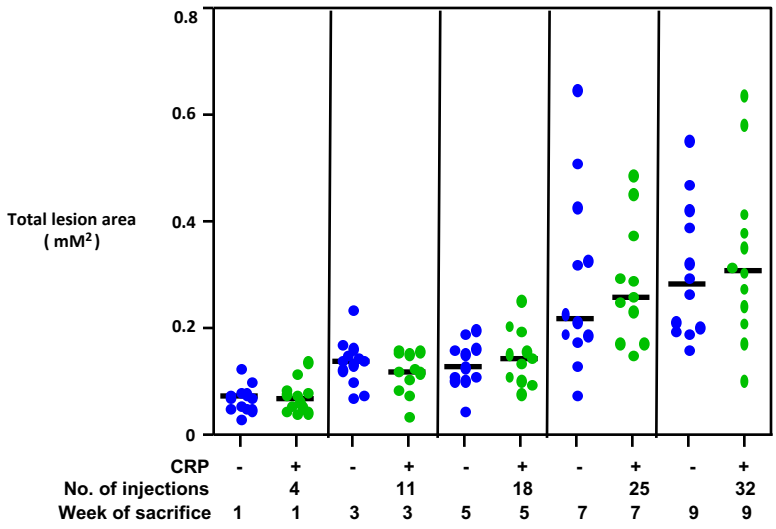

Figure A.2: F66A/T76Y/E81A mutant CRP did not affect the lesion progression in the aortic root of LDLR$^{-/-}$mice. Quantification of total lesion area in 8 μm thick aortic root sections covering the length of the aortic root (from the beginning of the appearance of aortic valves until the disappearance of valves) from untreated and mutant CRP treated LDLR$^{-/-}$ mice maintained on a high fat diet is shown. Data was collected at 5 different time points, i.e, 1, 3, 5, 7, and 9 weeks of mutant CRP administration at alternate days (TBS was injected for untreated group). A scatterplot of total atherosclerotic lesion coverage in the aortic root is shown. Each symbol represents the total area of the aortic root that stained positively for ORO in individual untreated (blue) or mutant CRP treated (green) LDLR$^{-/-}$ mice. Horizontal black lines indicate the median of total aortic root lesion area for each group of animals.

The levels of circulatory cytokines were sparsely detectable in the plasma of LDLR$^{-/-}$ mice

In order to analyze the effect of mutant CRP administration in systemic circulation, circulating levels of pro-inflammatory and anti-inflammatory cytokines were measured in both untreated and mutant CRP-treated mice (Table A.1). Unfortunately, the cytokines were either sparsely detectable or not detectable at all. Anti-inflammatory cytokines IL-4 and IL-10 were undetectable while pro-inflammatory cytokines IL-6, IL-1α, and TNF-α were sparsely detectable. Therefore, the effect of mutant CRP on the cytokine profiling in the plasma of LDLR$^{-/-}$ mice, could not be evaluated.

Week of sacrifice	IL-6 (ng/ml)		IL-1β (ng/ml)		TNF-α (ng/ml)	
	Untreated	CRP- treated	Untreated	CRP-treated	Untreated	CRP-treated
1	2.41 ± 1.92	2.49 ± 0.73	9.48 ± 10.9	4.33 ± 6.12	118.19 ± 90.07	41.49 ± 1.93
3	1.39 ± 0.73	2.57 ± 0.27	1.72 ± 0.69	0.99 ± 1.33	26.32 ± 1.93	25.2 ± 0.33
5	1.22 ± 0.28	1.92 ± 0.96	ND	ND	21.36 ± 1.28	91.3 ± 7.23
7	2.11 ± 0.24	2.5 ± 1.15	ND	ND	31.34 ± 1.29	33.73 ± 18.83
9	2.12 ± 1.55	1.32 ± 0.33	0.84 ± 0.91	0.86 ± 0.18	40.48 ± 13.08	9.34 ± 6.8

Table A.1: Levels of circulating pro-inflammatory cytokines were analyzed in pooled plasma samples from experiment 1 and experiment 2 respectively and results are expressed as mean ± SE. Samples were collected at five different time points, i.e, 1, 3, 5, 7, and 9 weeks of mutant CRP administration at alternate days (TBS was injected for control group). No statistically significant differences were found between the untreated and mutant CRP treated groups at any time point (ND: not detectable).

Mutant CRP levels in the plasma of LDLR$^{-/-}$ mice

To further evaluate the presence of administered mutant CRP in the plasma of LDLR$^{-/-}$ mice, CRP ELISA was performed. CRP levels observed in untreated mice are considered baseline levels, as these mice did not receive mutant CRP. Amongst all week points, mutant CRP was detected only after 1st week of mutant CRP administration (Table A.2). This could be explained in light of the half-life of this mutant CRP. Because mutant CRP was injected every 48 hours and the half-life of this CRP is approximately 15-20 hours, there is a possibility that the mutant CRP was cleared from the system by the time plasma was collected. The detection of mutant CRP at certain time points above baseline levels can also be explained in part of the

sample collection time since, we injected mutant CRP every 48 hours and the sample collection time varied between 24 hours post mutant CRP administration and 48 hours post mutant CRP administration. Also, no CRP antibodies were detected in the mouse plasma samples (data not shown).

Week of sacrifice	CRP concentration (ng/ml)	
	Untreated	CRP- treated
1	19.4 ± 2.61	341.6 ± 220.7
3	25.8 ± 5.81	27.6 ± 11.89
5	54.4 ± 17.01	78 ± 38.9
7	64.6 ± 47.34	171.8 ± 105.1
9	87 ± 31.32	79 ± 17.73

Table A.2: Circulating levels of mutant CRP were analyzed in pooled plasma samples from experiment 1 and experiment 2 respectively and results are expressed as mean $\pm$ SE. Samples were collected at five different time points, i.e, 1, 3, 5, 7, and 9, weeks of mutant CRP administration at alternate days (TBS was injected for control group.

Mutant CRP did not alter the MΦ1/ MΦ2 macrophage ratio at the atherosclerotic lesion area of LDLR$^{-/-}$ mice

To evaluate the effect of mutant CRP on the inflammatory environment, immunostaining for pro-inflammatory macrophage (MΦ1) and anti-inflammatory macrophage (MΦ2), in the aortic root atherosclerotic lesions of both untreated and mutant CRP treated mice was performed using CD 68 as the pan macrophage marker and CD 163 as the MΦ2 macrophage marker. As

expected, atherosclerotic lesions stained CD 68-positive for macrophages whereas, the lesion area stained CD 163-negative suggesting that there were no anti-inflammatory MΦ2 macrophages present (Fig A.3A, A.3B). This implies that the macrophages present at the atherosclerotic lesions were pro-inflammatory MΦ1 macrophages and these data were consistent for both untreated and mutant CRP treated lesions that further suggests that mutant CRP administration did affect the macrophage phenotype at the aortic root atherosclerotic lesion area.

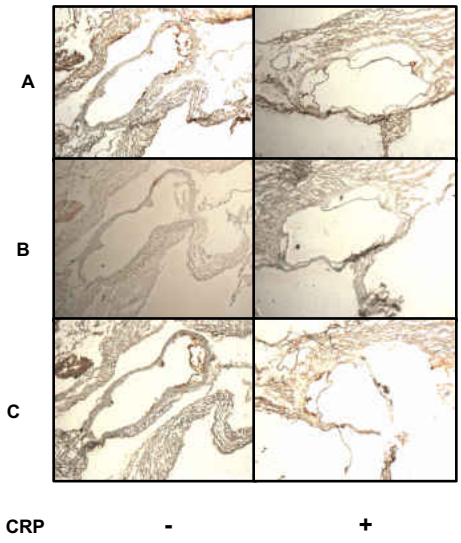

Figure A.3: Macrophage and CRP immunostaining in aortic root lesions. Representative aortic root sections from untreated and mutant CRP treated $LDLR^{-/-}$ mice fed on a high fat diet, stained for pan macrophages using CD 68 as the pan macrophage marker, is shown (A). CD 68-positive areas are stained brown. For MΦ2 (anti-inflammatory macrophages) staining, CD 163 was used as a marker (B). Positive CRP stained lesion areas are indicated in brown (C).

Mutant CRP was not present at the atherosclerotic lesion in the aortic root area

In order to test the presence of administered mutant CRP at the atherosclerotic lesion in the aortic root area, CRP immunostaining was performed in the aortic root lesions of both untreated and mutant CRP treated mice at every given data collection week point. Anti-CRP gave false-positive staining in the aortic root atherosclerotic lesion of untreated and mutant CRP treated mice (Fig A.3C). This suggests that anti-CRP (both polyclonal anti-CRP and (Fab)-fragmented anti-CRP) was cross reacting with immune complexes present in the atherosclerotic lesion such as ox-LDL-IgG immune complexes. Due to the false-positive CRP staining, the presence and absence of mutant CRP at the aortic root atherosclerotic lesion could not be evaluated.

Discussion

In this study we investigated the effect of a non-native pentameric CRP created by site-directed mutagenesis, F66A/T76Y/E81A mutant CRP, that does not bind to PCh since the PCh binding site of this mutant CRP is abolished due to mutations of critical amino acids forming the PCh-binding pocket, i.e, Glu^{81}, Phe^{66} and Thr^{76}, on the development of atherosclerosis employing LDL receptor knockout mouse model of atherosclerosis. Our major findings were as follows: 1) F66A/T76Y/E81A mutant CRP, in the whole aorta, had an effect on the progression and development of atherosclerosis wherein administration of this protein significantly reduced the size of *en face* atherosclerotic lesion in $LDLR^{-/-}$ mice at 8-10 weeks of high fat diet and halted the progression of the disease post 6 weeks of high fat diet. 3) Mutant CRP showed no effect on the progression and development of atherosclerosis in the aortic root. 4) The effect of mutant CRP administration on the levels of circulating cytokines in the plasma could not be evaluated. 5) Mutant CRP administration did not alter the macrophage phenotype at the atherosclerotic lesion area. 6) The presence of administered mutant CRP could not be evaluated at the atherosclerotic lesion area in the aortic root.

In the current study, we could not analyze the presence of administered F66A/T76Y/E81A mutant CRP at atherosclerotic lesion in the aortic root because anti-CRP (both polyclonal anti-CRP and (Fab)-fragmented anti-CRP) provided false-positive staining as mutant CRP was detected in the aortic root atherosclerotic lesion of both untreated and mutant CRP treated mice. Since, the lesion area in the aortic root is extremely complex, one of the possible reasons can be that anti-CRP was recognizing and cross reacting with immune complexes present in the atherosclerotic lesion such as ox-LDL-IgG immune complexes (1-2).

Macrophages are heterogeneous cell populations that have been shown to be present in the developing lesion during pathogenesis of atherosclerosis. Macrophages have the ability to switch from their "classically activated" pro-inflammatory (MΦ1) phenotype to an "alternative" anti-inflammatory (MΦ2) phenotype and *vice versa*, depending on the microenvironment or specific signals sensed by them (3-4). In order to further understand the atheroprotective effect of F66A/T76Y/E81A mutant CRP in lieu of its ability to alter the macrophage phenotype from anti-inflammatory (MΦ2) to pro-inflammatory (MΦ1), we stained the aortic root atherosclerotic lesion for macrophages. The lesion areas were found to be macrophage-rich as they identified as CD68-positive while, in contrast, the lesion area stained negative for MΦ2 phenotype in both untreated and mutant CRP treated mice suggesting that the atherosclerotic lesion had a greater concentration of macrophages specifically M1 macrophages and F66A/T76Y/E81A mutant CRP did not affect or alter macrophage phenotype.

Since, atherosclerosis is considered as a chronic inflammatory condition with concomitant increase in pro-inflammatory cytokines such as IL-6, IL-1β, TNF-α and also, it has been shown that native CRP can interact with modified LDL and reduce the proinflammatory effects produced by modified LDL and foam cells. Therefore, in order to observe the effect of F66A/T76Y/E81A mutant CRP on the levels of circulating cytokines in the plasma, a Bio-plex multi cytokine assay was performed. Unfortunately, the cytokines could not be detected as they were either sparsely detectable or not detectable at all. Anti-inflammatory cytokines IL-4 and IL-10 were undetectable while pro-inflammatory cytokines IL-6, IL-1α, and TNF-α were sparsely detectable and hence, the effect of mutant CRP on the cytokine profiling in the plasma of $LDLR^{-/-}$ mice could not be evaluated. Along with it, there were no antibodies produced against administered mutant CRP.

References

1. Oksjoki R, Kovanen PT, Lindstedt KA, Janssoon B, and Pentikäinen MO. OxLDL-IgG immune complexes induce survival of human monocytes. *Arterioscler Thromb Vasc Biol*. 2006; 26: 576-583.
2. Wu R, Huang YH, Elinder LS, and Frostegård J. Lysophosphatidylcholine is involved in the antigenicity of oxidized LDL. *Arterioscler Thromb Vasc Biol*. 1998; 18: 626-630.
3. Gaetano de M, Crean D, Barry M, and Belton O. M1- and M2-type macrophage responses are predictive of adverse outcomes in human atherosclerosis. *Front Immunol.* 2016; 7: 275.
4. Zhang X, Xia S, and Li Q. Pravastatin polarizes the phenotype of macrophages towards M2 and elevates serum cholesterol levels in apolipoprotein E knockout mice. *J Int Med Res.* 2018; 46(8): 3365-3373.

VITA

ASMITA PATHAK

Education: Ph.D. Biochemistry, East Tennessee State University, Johnson City, TN, 2020

M.Sc. Biochemistry, Jamia Millia Islamia, Delhi, India, 2015

B.Sc. Biochemistry, Delhi University, Delhi, India, 2013

Professional Experience: Graduate Research Assistant, James H. Quillen College of Medicine, East Tennessee State University, Department of Biomedical Science, 2015-2020

Research Student, CSIR-IGIB, Delhi, India, 2015

Publications: Thirumalai, A., S. K. Singh, D. J. Hammond Jr., T.B. Gang, D.N. Ngwa, **A. Pathak**, and A. Agrawal. Purification of recombinant C-reactive protein mutants. *J. Immunol. Methods* 443: 26-32, 2017.

Singh, S. K., A. Thirumalai, **A. Pathak**, D. N. Ngwa, and A. Agrawal. Functional transformation of C-reactive protein by hydrogen peroxide. *J. Biol. Chem*. 292: 3129-3136, 2017.

Pathak A, Agrawal A. Evolution of C-reactive protein. *Front. Immunol*. 10:943. doi:10.3389/fimmu.2019.00943.

Presentations and Awards:

Pathak, A., S. K. Singh, A. Thirumalai, P. B. Armstrong, and Agrawal A. Evolution of a host-defense function of C-reactive protein from horseshoe crab to humans. Appalachian student research forum, ETSU, April, 2016.

Pathak, A., S. K. Singh, A. Thirumalai, P. B. Armstrong, and Agrawal A. Evolution of a host-defense function of C-reactive protein from horseshoe crab to humans. Immunology meeting 2016, Seattle, WA. J. Immunol. 196: 132.5

Pathak, A., S. K. Singh, and A. Agrawal. C-reactive protein is an atheroprotective molecule. Appalachian student research forum ETSU, April, 2018. **(*won 1st place award*)**

Pathak, A., S. K. Singh, and A. Agrawal. C-reactive protein is an atheroprotective molecule. Immunology meeting 2018, Austin, TX. J. Immunol. 200:170.16, 2018.